Dynamical Systems Theory

Björn Birnir
Center for Complex and Nonlinear Dynamics
and Department of Mathematics
University of California
Santa Barbara[1]

Contents

List of Figures

Chapter 1

Introduction

1.1 The 3 Body Problem

In the 16th and 17th century major progress was made in celestial mechanics that at the time constituted the theoretical part of astronomy. It started with the careful observation made by Tycho Brahe which were then formulated into Kepler's laws by Kepler and thereafter lead to the solution of the two-body problem in astronomy. This was the integration of the equations of motions of two large celestial bodies such as the Sun and Jupiter in our planetary system that can be formulated as the rotation around a common center of gravity, see Figure 1.1. These developments lead to the great hope of the 18th century that the equations of motion for our planetary system could be integrated and a great deal of effort was expended trying to integrate the three-body problem. This was the model problem for the motion of two bodies such as the Earth and Jupiter around the Sun, ignoring all the other planets. In spite of a great effort of most of the best mathematicians of the time no progress was made for most of the 18th century.

The methods that most of the mathematicians used to try to solve the problem was to find additional integrals of the motion. Since the three-body problem is a Hamiltonian system it was known that if enough integrals of the motion could be found then the equations of the motion could be integrated.

In 1898 Poincaré dropped a bombshell that shook the mathematical world. He proved that for a three-body problem consisting of the Sun and Jupiter and a comet moving perpendicular to the planetary plane, see Figure 1.1, *there exist no analytic integrals*. In proving this he set the stage for mathematics of the latter half of the 19th century and discovered *Nonlinear Dynamics*!

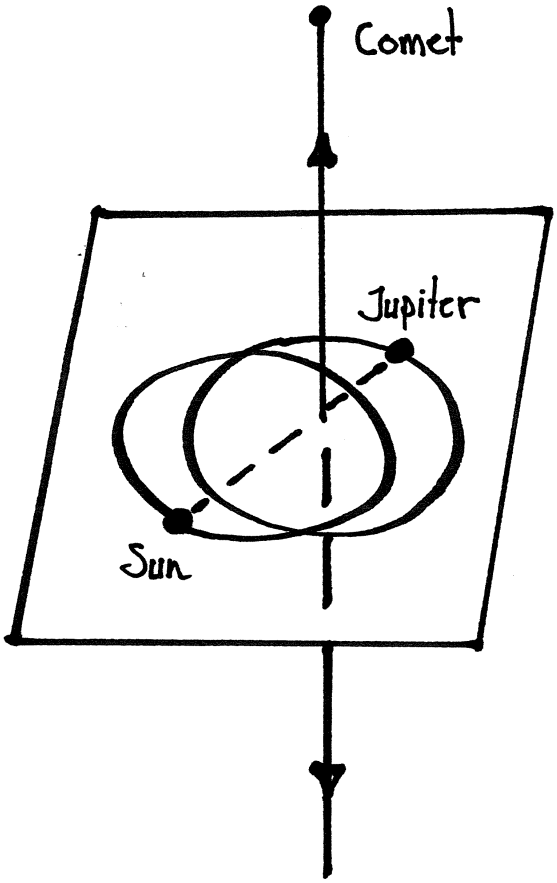

Figure 1.1: The rotation of the Sun and Jupiter in a plane around a common center of mass and the motion of a comet perpendicular to the plane.

1.2 Nonlinear Dynamical Systems Theory

Nonlinear dynamics has profoundly changed how scientist view the world. It had been assumed for a long time that *determinism* implied *predictability* or if the behavior of a system was completely determined, for example by differential equation, then the behavior of the solutions of that system could be predicted forever after. Nonlinear dynamics showed that this assumption was *false*. Namely, one could have a solution that was completely determined by an ordinary differential equation (ODE) and an initial condition and still its trajectory could not be predicted. The reason is that the nonlinearity leads to an instability which in turn implies a loss of predictability. This effect is best described by:

The Butterfly Effect: *A monarch butterfly fluttering its wings in Santa Barbara, California, today may cause a storm in the town of Akureyri, on the north coast of Iceland, in two weeks time.*

What happens is that the instability leads to a loss of information and this is the perfect nightmare of someone who is trying to use a computer to obtain his answers. The tiny round-off errors that one finds in any numerical computation by a computer are being magnified exponentially in time. This means that after a short time the error in the computation is overwhelming the answer and the result of the computation is numerical junk.

We will in later chapters associated chaotic behavior with positive Lyapunov exponents and another way of saying the above is that positive Lyapunov exponents lead to limits on predictability.

1.3 The Nonlinear Pendulum

The motion of the nonlinear pendulum, see Figure 1.3 is determined by Newton's law

$$F = ma$$

where m is the mass and a the acceleration. Now the arclength that the pendulum travels is $\ell\theta$, where ℓ is the length of the arm of the pendulum and θ is the angle from the vertical directions. From Figure 1.3 we can tell using basic trigometry that $F = -mg\sin(\theta)$ where the gravitational force is $F_1 = mg$ where g is the gravitational acceleration. The negative sign in F comes from the fact that θ is measured in the counterclockwise direction, whereas F points in the clockwise

direction. The force F_2 in Figure 1.3 is balanced by the tension in the arm of the pendulum. Thus the above equation becomes

$$m\ell\ddot{\theta} = -mg\sin(\theta)$$

Dividing by $m\ell$ we get that

$$\ddot{\theta} + \frac{g}{\ell}\sin(\theta) = 0$$

where

$$\omega = \sqrt{\frac{g}{\ell}}$$

is the frequency of the nonlinear pendulum. The energy of the nonlinear pendulum is obtained by multiplying the equation by $\dot{\theta}$

$$\dot{\theta}\ddot{\theta} + \omega^2\sin(\theta)\dot{\theta} = 0$$

and integrating with respect to t

$$\frac{\dot{\theta}^2}{2} + \omega^2(1-\cos(\theta)) = C$$

where C is a constant. If we damp and drive the nonlinear pendulum its motion is described by the equation

$$\ddot{\theta} + \delta\dot{\theta} + \omega^2\sin(\theta) = \varepsilon\cos(\Omega t)$$

Now we let $x = \theta$ and set $\omega = 1$, then the nonlinear pendulum (without damping and driving) is described by the equation

$$\ddot{x} + \sin(x) = 0 \tag{1.1}$$
$$x(0) = x_0,\ \dot{x}(0) = \dot{x}_0.$$

x_0 and $\dot{x}_0$ are the initial position (angle) and initial (angular) velocity of the pendulum. With these initial conditions specified, the initial value problem (IVP) (1.1) determines the solution $x(t)$ for all time. We will now give a complete *qualitative analysis* of the solutions of the Equation 1.1. This is done by the following steps.

1. Write the equations as a first order system.

   We let $y = \dot{x}$ and rewrite the equation as a first order system

$$\frac{d}{dt}\begin{pmatrix} x \\ y \end{pmatrix} = \begin{pmatrix} y \\ -\sin(x) \end{pmatrix}.$$

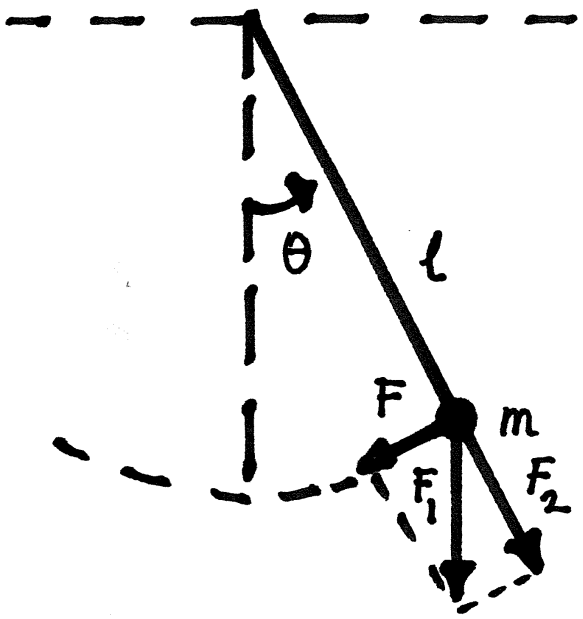

Figure 1.2: The nonlinear pendulum is your typical grandfather's clock, where the pendulum makes the angle θ with the vertical line. The distance that the pendulum travels is the arc length $\ell\theta$ where ℓ is the length of the arm and gravity pulls on the pendulum with the force $F_1 = mg$ where m is the mass of the pendulum and g the gravitational acceleration.

2. Find the *stationary solutions*.

   If we set the right hand side of last equation equal to zero, we get two equations

   $$y = 0,\ \sin(x) = 0,$$

   that imply that the origin $(x,y) = (0 \pmod{2\pi}, 0)$ is a stationary solution and so is $(x,y) = (\pi \pmod{2\pi}, 0)$. The straight-down position of the pendulum $(x,y) = (0,0)$ is clearly a stationary solution. It should be stable. The straight-up position of the pendulum $(x,y) = (\pm\pi, 0)$ is also a stationary solution. It ought to be unstable. The phase plane has the period 2π in the x direction so it is really a cylinder.

3. Determine the *stability* of the stationary solutions

   Consider the nonlinear pendulum

   $$\ddot{x} + \sin(x) = 0.$$

   We linearize the system and let $z = \frac{\partial x}{\partial x_o}$, the derivative of x with respect to the initial condition x_o. Then the linearized system becomes

   $$\dot{z} = D_{(x,y)} f(x) z$$

   where $f(x,y)$ is the vector field

   $$f(x,y) = \begin{pmatrix} y \\ -\sin(x) \end{pmatrix}$$

   Now $D_{(x,y)} f$ is simply the Jacobian of f

   $$D_{(x,y)} \begin{pmatrix} y \\ -\sin(x) \end{pmatrix} = \begin{pmatrix} 0 & 1 \\ -\cos(x) & 0 \end{pmatrix}$$

   We first evaluate Jacobian at the stationary solution

   $$D_{(x,y)} f \begin{pmatrix} 0 \\ 0 \end{pmatrix} = \begin{pmatrix} 0 & 1 \\ -1 & 0 \end{pmatrix}$$

   The eigenvalues of this matrix are $\lambda = \pm i$, with no real eigenvectors. This says that the stationary solution $(x,y) = (0,0)$ is *marginally stable*. Next we

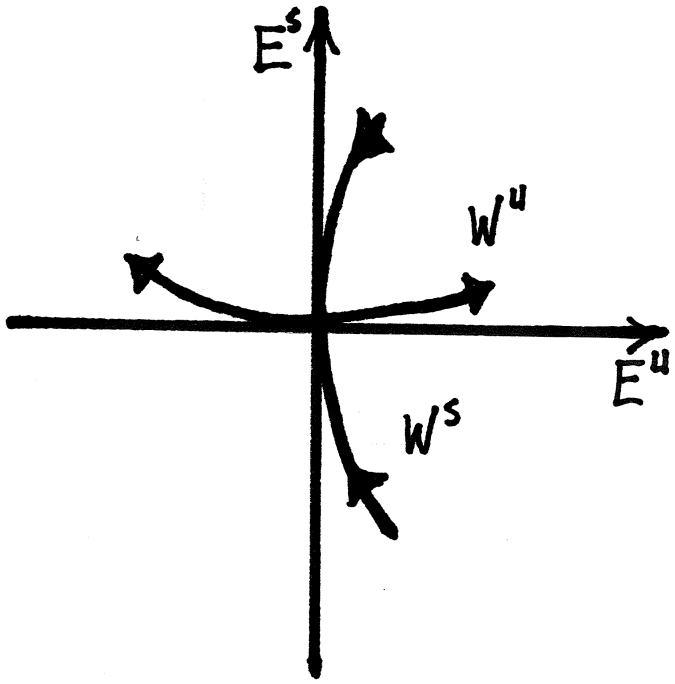

Figure 1.3: W^u denotes the unstable and W^s the stable manifolds, E_u is the (linear) unstable subspace and E_s the (linear) stable subspace.

evaluate the Jacobian at the stationary solution $(x,y) = (\pi \pmod{2\pi}, 0)$ to get the matrix

$$\begin{pmatrix} 0 & 1 \\ 1 & 0 \end{pmatrix}.$$

The eigenvalues of this matrix are $\lambda = \pm 1$, with eigenvectors $(1/\sqrt{2})(1,+1)$ and $(1/\sqrt{2})(1,-1)$ respectively. That one of the eigenvalues has a positive real part implies that the stationary solution $(x,y) = (\pi \pmod{2\pi}, 0)$ is *unstable*. The eigenvectors determine the linear unstable and stable manifolds E_u and E_s, see Figure 3, and Theorem 2.2 give the existence of the nonlinear unstable $W^u_{loc}(\pi,0)$ and stable $W^s_{loc}(\pi,0)$ manifolds, which are tangent to E_u and E_s respectively, see Figure 3.

4. Draw the *phase portrait*

   The phase portrait is shown in Figure 4.

5. Describe the different types of solutions.

   (a) The first type are the above *stationary solutions*.

   (b) The circles and ellipses around the origin represent small oscillations of the pendulum around the straight-down stationary solution. These types of solutions are called *librations*.

   (c) The *homoclinic connections* connecting the straight up $(\pi,0)$ stationary solution with itself are the third type of solutions.

   (d) The *rotation* above the homoclinic connections represent solutions that rotate around the circle in two possible directions.

   (e) There are only these *four types* of solutions.

If we multiply the equation (1.1) by $\dot{x}$ and integrate with respect to t we get the *energy* of the pendulum

$$E(x,y) = \frac{y^2}{2} + 1 - \cos(x) = constant.$$

This is obviously the same expression as we obtained above with $\theta = x$, $\dot{\theta} = y$ and $\omega = 1$. The first part of this expression is the *kinetic energy* and the second part the *potential energy*. E is constant for each solution (orbit) of the IVP, and it can be used to prove the existence of the elliptical orbits around the origin in Figure 4. In this case, since the ODE is two-dimensional and has an integral, we can

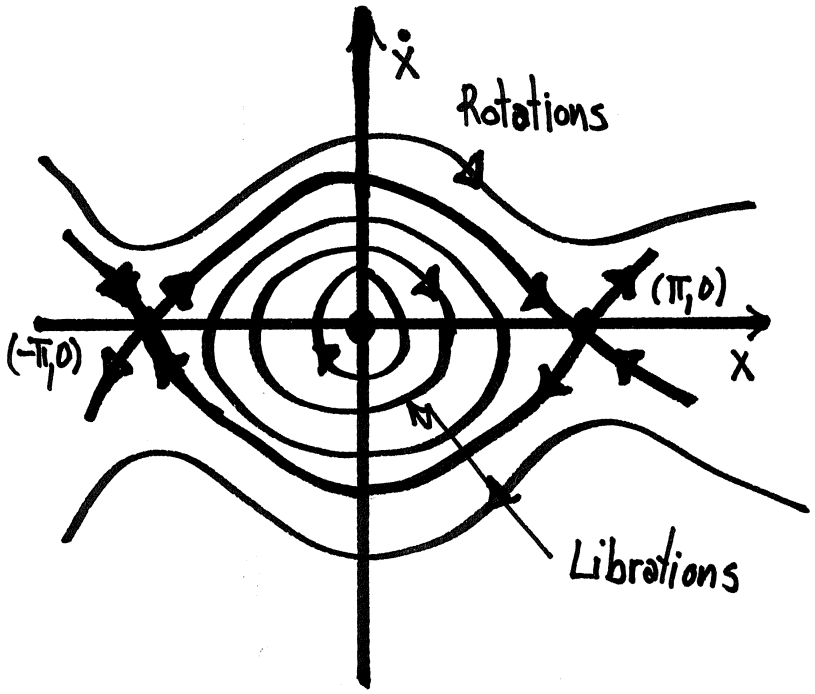

Figure 1.4: The phase portrait for the nonlinear pendulum shows four different type of solutions. The first type are the stationary solutions at the origin, that is a center and the one at $(\pm\pi, 0)$ that is a saddle. Around the origin there are periodic orbits corresponding to small oscillations of the pendulum that are called librations. Then there are two homoclinic connections connecting the saddle to itself, because $(\pm\pi, 0)$ are really the same point corresponding to the vertical position of the pendulum. The fourth type of solutions are rotations, above and below the homoclinic connections. They correspond to rotations of the pendulum around the circle with increasing velocity as the distance from the origin increases.

find W^u and W^s explicitly. The homoclinic orbits approach the stationary solution $(x,y) = (\pi \pmod{2\pi}, 0)$ as $t \to \infty$ so by continuity they must have the same energy as this stationary solution. We therefore set the energy equal to the energy of the stationary solution

$$\frac{y^2}{2} + 1 - \cos(x) = E(\pi, 0) = 2.$$

This gives a first order equation for x that is solved, see Appendix A, to give

$$(x,y) = \pm 2(\tan^{-1}[\sinh(t)],\ \mathrm{sech}(t)),$$

the $-$ sign gives $W^u(\pi,0)$ and the $+$ sign gives $W^s(\pi,0)$. Notice that both of these manifolds are globally defined.

Adding damping the pendulum equation (1.1) gives the initial value problem:

$$\ddot{x} + \delta\dot{x} + \sin(x) = 0 \tag{1.2}$$

$$x(0) = x_0,\ \dot{x}(0) = \dot{x}_0. \tag{1.3}$$

The phase portrait of its solutions is shown in Figure 1.3. The stability of the stationary solution $(x,y) = (\pi \pmod{2\pi}, 0)$ remains the same, this is because it is *hyperbolic* and therefore *structurally stable*. The stationary solution $(x,y) = (0,0)$ on the other hand turns into a sink. The homoclinic connections are not structurally stable and break under the perturbation but one rotation from each direction connects with the stable manifolds of the stationary solution $(x,y) = (\pi \pmod{2\pi}, 0)$. Every other solution eventually spirals into the sink, see Figure 1.3.

1.4 The Homoclinic Tangle

The analysis of the damped and driven nonlinear pendulum

$$\ddot{x} + \delta\dot{x} + \sin(x) = \varepsilon\cos(\omega t) \tag{1.4}$$

$$x(0) = x_0,\ \dot{x}(0) = \dot{x}_0. \tag{1.5}$$

is more involved. The first problem is that the equation is non-autonomous and one must analyze the extended phase space, which is three-dimensional, instead of the two-dimensional phase space above. This is harder but more interesting things can happen in three dimensions. Poincaré got around this problem by inventing the Poincaré map, see Figure 1.4. This allowed him to reduce the analysis

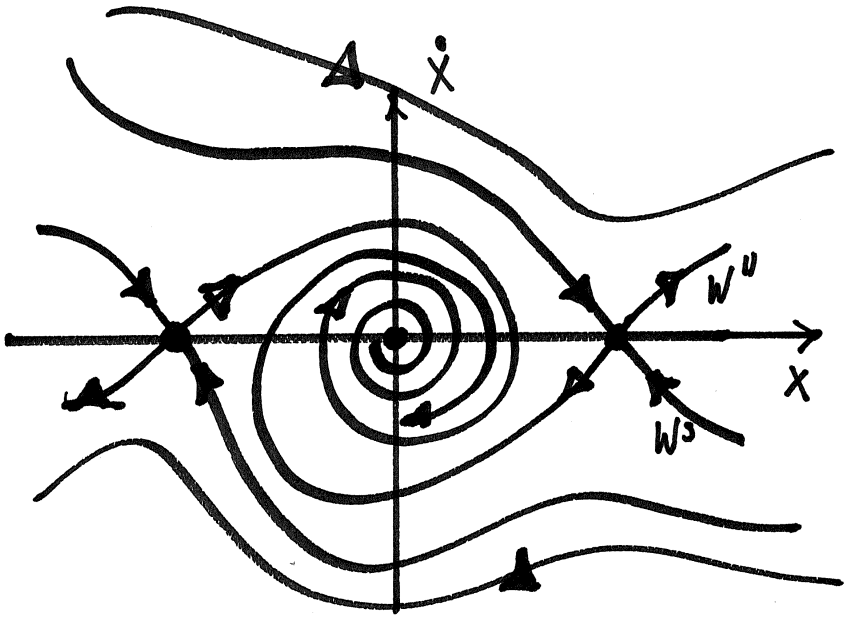

Figure 1.5: The phase portrait of the damped pendulum is similar to the undamped one except that the origin has changed to a sink and all solutions, except the saddle and the two rotations that connect to the stable manifolds of the saddle, spiral into the sink.

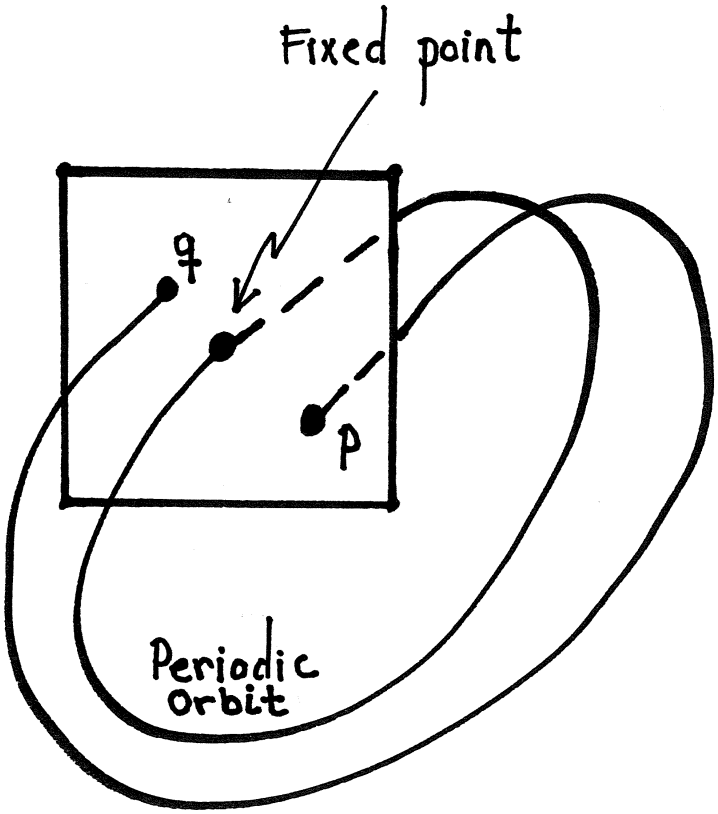

Figure 1.6: The plane perpendicular to the periodic orbit is called a transversal. The Poincaré map is the return map to the transversal. Thus the Poincaré map of the point q is the point p. The periodic orbit itself gives a fixed point of the Poincaré map.

of a three-dimensional vector field to the analysis of the two-dimensional map. It will be our main tool in the analysis of chaotic dynamics. When ε is turned on in the equation (1.4) the sink at the origin turns into a stable periodic orbit. The hyperbolic point at $(\pi(\mathrm{mod}\, 2\pi), 0)$ turns into a hyperbolic (*unstable*) periodic orbit. The orbits (they are now a sequence of points) in at neighborhood of the origin still spiral into it, but something strange can happen in a neighborhood of the hyperbolic fixed point, corresponding to the hyperbolic periodic orbit. The hyperbolic fixed point still has stable W^s and unstable W^u manifolds. But if the balance of the damping and the driving (ε and δ) is right the unstable manifold can come into a neighborhood of the hyperbolic fixed point and cross its stable manifold transversely,

$$W^u(\pi, 0) \perp W^s(\pi, 0)$$

see Figure 1.4. This could not happen in a flow because it would violate the uniqueness of the solution starting at the intersection point. But it can happen in a map because then the intersection point just corresponds to a particular orbit of the flow. If these manifolds cross once they must cross infinitely often and we get a *homoclinic tangle* close to the hyperbolic fixed point, see Figure 1.4. This is what Poincaré discovered in the three-body problem and he showed that the existence of the homoclinic orbit implies that no analytic integrals of the motion can exist. We will go through his argument when we study the Smale horseshoe in Chapter 5.

Exercise 1.1

Perform the qualitative analysis of the Duffing's equation,

$$\ddot{x} - x + x^3 = 0,$$

1. Find the stationary solutions.

2. Determine the stability of the stationary solutions.

3. Draw the phase portrait of the Duffings equation.

4. Use the phase portrait and (1) - (3) to identify four different types of solutions of the Duffing's equation and describe their qualitative behaviour.

5. Find the energy of the Duffing's equation and use it to compute the homoclinic orbits, compare Appendix A.

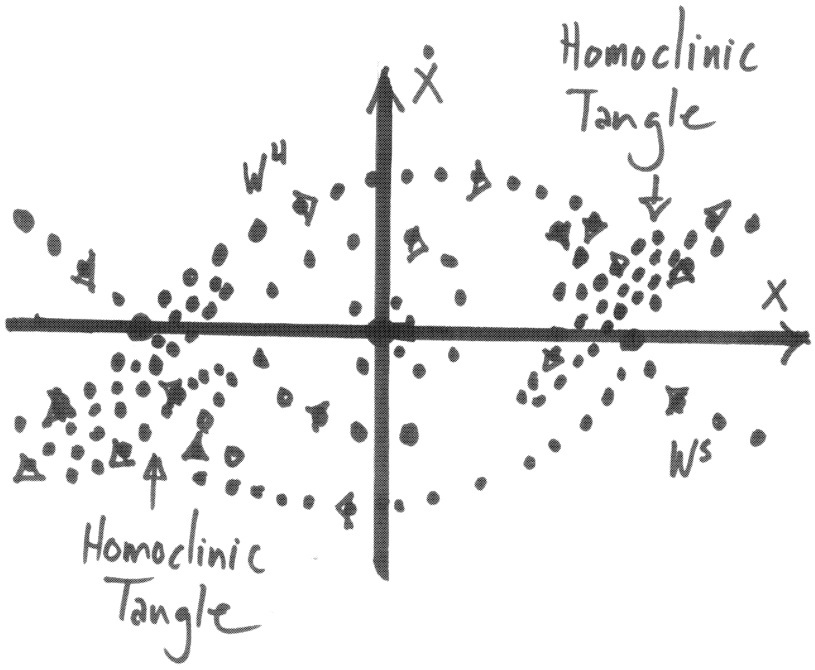

Figure 1.7: The phase space of the Poincaré map of the damped and driven nonlinear pendulum.

6. Add damping to the equation

$$\ddot{x} = \delta x - x + x^3 = 0,$$

and describe how this changes the analysis (1) - (3) above when δ is small.

7. Add forcing to the equation

$$\ddot{x} = \delta x - x + x^3 = \varepsilon \cos(\omega t),$$

and describe what it's Poincaré map looks like for small ε.

Chapter 2

Existence, Uniqueness and Invariance

2.1 The Picard Existence Theorem

The fundamental theorem in ordinary (and partial) differential equations is the Picard existence theorem. We start with the definition of Lipschitz continuous functions.

Definition 2.1 *A function $f : U \times [t_0, t_0+T] \to \mathbb{R}^n$, $U \subset \mathbb{R}^n$, is Lipschitz continuous in U if there exists a constant L such that*

$$\|f(y,t) - f(x,t)\| \leq L\|y - x\|$$

for all $x, y \in U$ and $t \in [t_0, t_0+T]$. If $U = \mathbb{R}^n$, f is called globally Lipschitz.

Theorem 2.1 *Consider the initial value problem*

$$\dot{x} = f(x,t), \quad x(t_0) = x_0, \quad x \in \mathbb{R}^n, t \in \mathbb{R}, \tag{2.1}$$

in the time interval $|t - t_0| \leq a$, and the box $x \in D$, $D = \{x | \|x - x_0\| \leq d\}$, here a and d are positive constants. Suppose that the function (vector field) $f(x,t)$ satisfies the two conditions

(i) $f(x,t)$ is continous in $G = I \times D = [t_0 - a,\ t_0 + a] \times D$,

(ii) $f(x,t)$ is Lipschitz continous in G,

then there exists a unique solution of (2.1) for the time interval $|t-t_0| \leq \max(a, \frac{d}{M})$*, where*

$$M = \max_G \|f(x,t)\|.$$

Proof: We write the ODE and the initial condition (2.1) as the integral equation

$$x(t) = x_0 + \int_{t_0}^{t} f(x(s),s)ds. \tag{2.2}$$

It is easy to see that (2.1) and (2.2) are actually equivalent. Picard's idea was to iterate this equation and define the sequence

$$\begin{aligned} x_1(t) &= x_0 + \int_{t_0}^{t} f(x_0,s)ds \\ x_2(t) &= x_0 + \int_{t_0}^{t} f(x_1(s),s)ds \\ &\vdots \\ x_{n+1}(t) &= x_0 + \int_{t_0}^{t} f(x_n(s),s)ds \\ &\vdots \end{aligned}$$

If the sequence of iterates $\{x_n(t)\}$ converges it will converge to the solution of (2.2). The first thing we must check is that the iterates actually lie in D, see Figure 2.1,

$$\begin{aligned} \|x_1(t) - x_0\| &= \|\int_{t_0}^{t} f(x_0,s)ds\| \\ &\leq \int_{t_0}^{t} \|f(x_0,s)\|ds \\ &\leq M|t-t_0| \leq d \end{aligned}$$

for $|t-t_0| \leq \min(a, \frac{d}{M})$. This was the reason for the choice of the length of the time interval, as this minimum. Now the computation is the same for all the iterates so the whole sequence lies in D.

Next we use induction to show that successive iterates satisfy the inequality

$$\|x_n(t) - x_{n-1}(t)\| \leq \frac{ML^{n-1}|t-t_0|^n}{n!}.$$

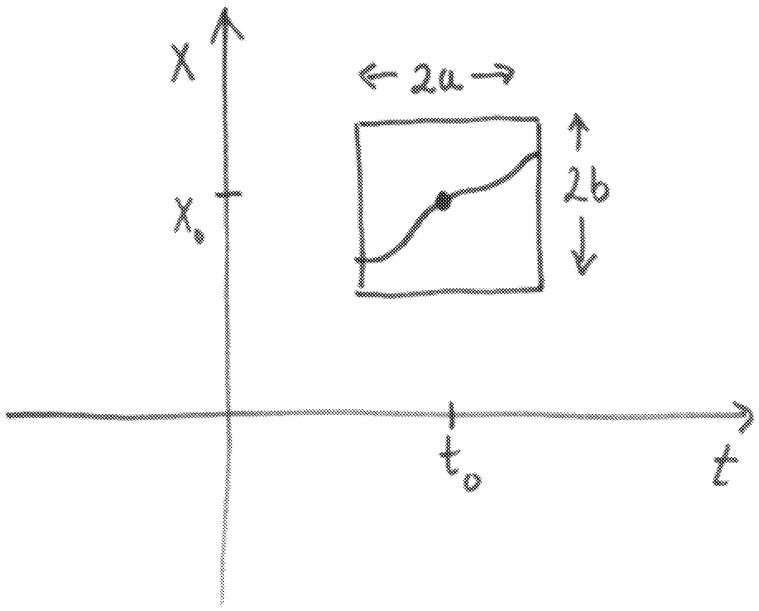

Figure 2.1: The square $|t - t_o| \leq a$, $\|x - x_o\| \leq b$, where the solution of the initial value problem (2.1) exists.

When $n = 1$ this is the estimate above

$$\|x_1(t) - x_0\| \leq M|t - t_0|.$$

We assume

$$\|x_{n-1}(t) - x_{n-2}(t)\| \leq \frac{ML^{n-2}|t - t_0|^{n-1}}{(n-1)!}$$

and consider the difference of

$$x_n(t) = x_0 + \int_{t_0}^{t} f(x_{n-1}(s), s)ds$$

and

$$x_{n-1}(t) = x_0 + \int_{t_0}^{t} f(x_{n-2}(s), s)ds,$$

$$x_n(t) - x_{n-1}(t) = \int_{t_0}^{t} [f(x_{n-1}(s), s) - f(x_{n-2}(s), s)]\, ds$$

so

$$\begin{aligned} \|x_n(t) - x_{n-1}(t)\| &\leq \int_{t_0}^{t} \|f(x_{n-1}(s), s) - f(x_{n-2}(s), s)\|ds \\ &\leq L\int_{t_0}^{t} \|x_{n-1}(s) - x_{n-2}(s)\|ds \end{aligned}$$

by the Lipschitz condition

$$\begin{aligned} &\leq ML^{n-1}\int_{t_0}^{t} \frac{|s - t_0|^{n-2}}{(n-1)!}ds = ML^{n-1}\frac{|s - t_0|^n}{n!}\Big|_{t_0}^{t} \\ &= ML^{n-1}\frac{|t - t_0|^n}{n!} \end{aligned}$$

This completes the induction.

Now the space of continous funtions on the interval I is a complete metric space with the metric

$$\|x(t)\|_{sup} = \max_I |x(t)|$$

and to show that the sequence $\{x(t)\}$ converges we just have to show that it is *Cauchy*, i.e. given $\varepsilon > 0$, $\exists N$ such that

$$\|x_n(t) - x_m(t)\| < \varepsilon, \text{ for } \forall\, n, m \geq N.$$

But this is straight-forward

$$\begin{aligned}\|x_n(t)-x_m(t)\| &\leq \sum_{j=m+1}^{n}\|x_j(t)-x_{j-1}(t)\| \\ &\leq M\sum_{j=m+1}^{n}\frac{L^{j-1}|t-t_0|^j}{j!}\end{aligned}$$

by the estimate above

$$\leq \frac{M}{L}\sum_{j=1}^{\infty}\frac{L^j|t-t_0|^j}{j!} = \frac{M}{L}\left(e^{L|t-t_0|}-1\right).$$

If we choose $|t-t_0|$ sufficiently small then

$$\|x_n(t)-x_m(t)\| \leq \frac{M}{L}\left(e^{L|t-t_0|}-1\right) < \varepsilon,$$

for $\forall\, n,m$. This means that $\{x_n(t)\}$ is a Cauchy sequence and converges to a continous function on I, $x_n(t) \longrightarrow x(t)$ as $n \longrightarrow \infty$. Moreover, taking the limit as $n \longrightarrow \infty$ in

$$x_n(t) = x_0 + \int_{t_0}^{t} f(x_{n-1}(s),s)ds,$$

we get

$$x(t) = x_0 + \int_{t_0}^{t} f(x(s),s)ds$$

by uniform convergence, so $x(t)$ satisfies (2.2). This in turn implies that $x(t)$ is continously differentiable since f is continous so $x(t)$ satisfies (2.1). **QED**

Example 2.1 *Consider the IVP*

$$\begin{aligned}\dot{x} &= x^{1/2} \\ x(0) &= 0.\end{aligned}$$

$x \equiv 0$ *is a solution but so is*

$$x(t) = \begin{cases} (t-c)^2/4, & t \geq c > 0 \\ 0, & t < c. \end{cases}$$

We have infinitely many solutions one for each value of c, see Figure 2.1.

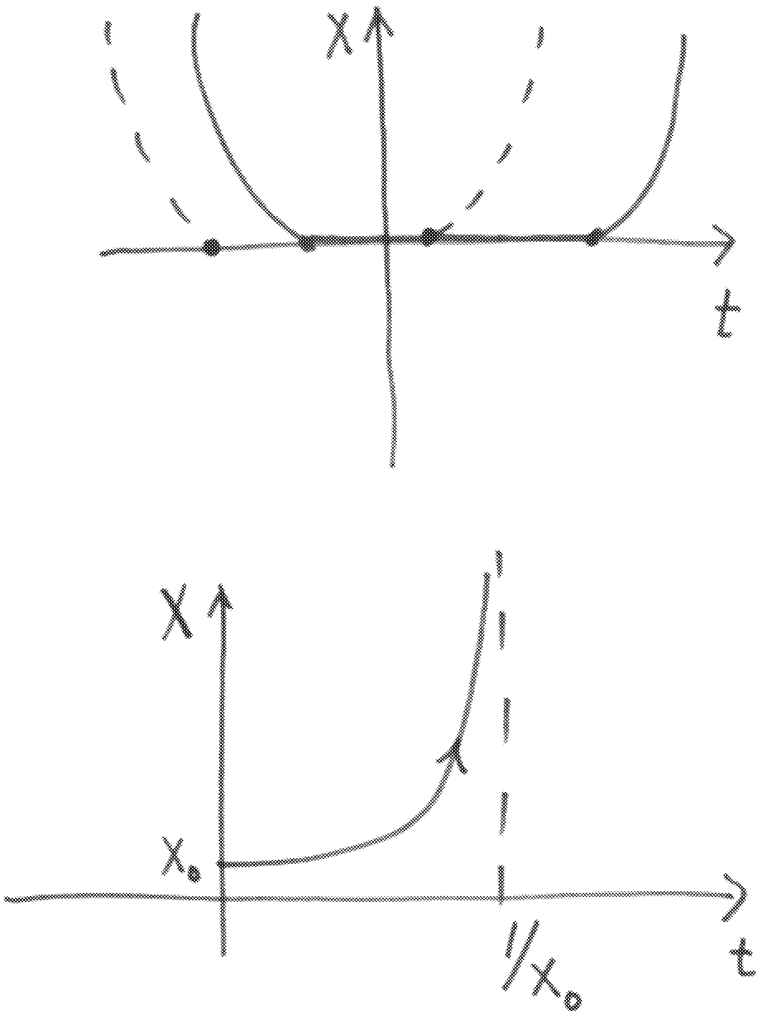

Figure 2.2: The top figure show the graphs of two of the many solutions that satisfy the ODE in Example 2.1. The bottom figure show the solution in Example 2.2, that is blowing up in a finite time.

Example 2.2 Finite-time Blow-up

Consider the IVP

$$\begin{aligned} \dot{x} &= x^2 \\ x(0) &= x_0. \end{aligned}$$

The solution is

$$x(t) = \frac{x_0}{(1 - x_0 t)}.$$

It exists for $t < 1/x_0$*, but*

$$\lim_{t \to 1/x_0} x(t) = +\infty,$$

see Figure 2.1.

Exercise 2.1

1. Show that the IVP

$$\begin{aligned} \dot{x} &= \sqrt{1 - x^2} \\ x(0) &= x_0 \end{aligned}$$

has infinitely many continuous solutions in the region $|x| \leq 1$. Show also that there are only two solutions that have a continuous second derivative $\ddot{x}$.

2. Find the solution to the IVP

$$\begin{aligned} \dot{x} &= 1 + x^2 \\ x(0) &= x_0 \end{aligned}$$

and the finite time when it blows up.

The following (more general) form of Grönwall's inequality is an important technical tool.

Theorem 2.2 *Let* $u(t)$ *and* $v(t)$ *be non-negative continuous functions on* $[\alpha, \beta]$*,* $C \geq 0$ *a constant, and suppose*

$$v(t) \leq C + \int_\alpha^t v(s)u(s)ds, \quad \text{for } \alpha \leq t \leq \beta. \tag{2.3}$$

Then

$$v(t) \leq C \exp\left[\int_\alpha^t u(s)ds\right], \quad \textit{for } \alpha \leq t \leq \beta \tag{2.4}$$

and if $C = 0$, $v(t) \equiv 0$.

Proof: We let

$$C + \int_\alpha^t v(s)u(s)ds = V(t).$$

Then

$$v(t) \leq V(t)$$

by the hypothesis and we assume in addition that

$$v(t) > 0, \quad \text{for } (t-\alpha) \text{ small},$$

then

$$V'(t) = v(t)u(t) \leq V(t)u(t).$$

We can solve this differential inequality, because

$$v(t) > 0, \quad \text{for } (t-\alpha) \text{ small } \Rightarrow V(t) > 0.$$

The solution is

$$V(t) \leq V(0) \exp\left(\int_\alpha^t u(s)ds\right) = C \exp\left(\int_\alpha^t u(s)ds\right).$$

This implies that

$$v(t) \leq C \exp\left(\int_\alpha^t u(s)ds\right)$$

and

$$C = 0 \Rightarrow v(t) \equiv 0 \quad \text{for } (t-\alpha) \text{ small}.$$

But then $v(t) \equiv 0$, for all $t \in [\alpha, \beta]$ because we can make the same argument with any $\alpha_1 \in [\alpha, \beta]$ instead of α. **QED**

The first application shows that a solution to an ODE depends continuously on its initial data, for finite time.

Corollary 2.1 *Let $y(t)$ and $x(t)$ be two solutions of the ODE (2.1), with a Lipschitz continuous vector field f and assume that the solution exists for $|t-t_0| < T_0$. Then for $\varepsilon > 0$ and $T < T_0$, there exists a $\delta > 0$ such that*

$$\|y_0 - x_0\| < \delta \Rightarrow \|y(t) - x(t)\| < \varepsilon$$

for $|t-t_0| \leq T$.

Proof: We use the integral equation (2.2),

$$y(t) - x(t) = y_0 - x_0 + \int_{t_0}^{t} (f(y(s),s) - f(x(s),s))ds$$

and the Lipschitz continuity to get the inequality

$$\|y(t) - x(t)\| \leq \|y_0 - x_0\| + K \int_{t_0}^{t} \|y - x\|(s)d|s|.$$

Then Theorem 2.2 states that

$$\|y(t) - x(t)\| \leq \|y_0 - x_0\| e^{K|t-t_0|}.$$

Now

$$\|y_0 - x_0\| < \varepsilon e^{-Kt} = \delta$$

implies that

$$\|y(t) - x(t)\| < \varepsilon, \quad \text{for } |t-t_0| < T.$$

QED

The next application of the Grönwall's inequality is to show that if the derivative of the vector field is globally bounded, then the solution is bounded by an exponential function. First we must discuss:

Theorem 2.3 The Mean-Value Theorem in $\mathbb{R}^n$

If $f(x,t)$ is C^1 in $\mathbb{R}^n$, that is the Jacobian derivative $D_x f$ exists and is continuous, then

$$f(y,t) - f(x,t) = \int_0^1 D_x f(x + s(y-x), t) \cdot (y-x)ds. \tag{2.5}$$

Proof: We apply the fundamental theorem of calculus

$$\begin{aligned} f(y,t)-f(x,t) &= f(x+s(y-x),t)|_{s=0}^{s=1} \\ &= \int_0^1 \frac{d}{ds} f(x+s(y-x),t)ds \\ &= \int_0^1 D_x f(x+s(y-x),t)\cdot(y-x)ds \end{aligned}$$

where s is a parameter and $\cdot$ denotes the multiplication of an $n\times n$ matrix by a vector in $\mathbb{R}^n$. **QED**

Corollary 2.2 *Suppose the derivative $D_x f$ of the vector field in the IVP (2.1) and (2.2) is bounded in a strip $U=\{(x,t)\mid x\in\mathbb{R}^n,\ |t-t_0|\le d\}$. Let $N=\max_U \|D_x f(x,t)\|$ and $M=\sup_{|t-t_0|\le d}\|f(x_0,t)\|$. Then the solution is bounded*

$$\|x(t)-x_0\| \le \frac{M}{N}(e^{N|t-t_0|}-1),$$

by an exponential function in U.

Proof: We use the integral equation (2.2)

$$\begin{aligned} x-x_0 &= \int_{t_0}^t f(x(s),s)ds \\ &= \int_{t_0}^t \left[f(x_0,s)+\int_0^1 D_x f(x+r(x-x_0),s)\cdot(x-x_0)dr \right] ds, \end{aligned}$$

by the mean-value theorem. Therefore

$$\begin{aligned} \|x-x_0\| &\le \int_{t_0}^t \left[\int_0^1 \|D_x f(x+r(x-x_0))\|dr\cdot\|x-x_0\|+\|f(x_0,s)\| \right] ds \\ &\le N\int_{t_0}^t \left(\|x-x_0\|(s)+\frac{M}{N} \right) ds \end{aligned}$$

Thus

$$\|x-x_0\|+\frac{M}{N} \le \frac{M}{N}+N\int_{t_0}^t \left(\|x-x_0\|(s)+\frac{M}{N} \right) ds$$

and by Theorem 2.2

$$\|x-x_0\|+\frac{M}{N} \le \frac{M}{N}\exp\left(N|t-t_0|\right).$$

This proves the assertion. **QED**

If the vector field is only assumed to be continuous the solution of the Initial Value Problem (2.1), but it may not be unique. The proof requires the classical Arzela-Ascoli Theorem: A uniformly bounded and equicontinuous sequence of functions on a compact set $G \subset \mathbb{R}^{n+1}$ has a uniformly convergent subsequence.

Theorem 2.4 The Peano Existence Theorem
Let $U \subset \mathbb{R}^n \times \mathbb{R}$ be an open set and $f(x,t)$ a continuous function on U. Then there exists a constant $c > 0$ and a continuous function $x(t)$, such that for every $(x_0,t_0) \in U$, $(x(t),t) \in U$ for $|t-t_0| < c$ and $x(t)$ satisfies the IVP

$$\dot{x} = f(x,t), \quad x(t_0) = x.$$

2.2 Global Solutions

We saw in Corollary 2.2 that if the derivative $D_x f(x,t)$ of the vector field f is bounded for all x and t then the solution of the IVP has exists globally. It is very restrictive to require $D_x f$ to be globally bounded and a less restrictive method is to seek an *a priori* bound on x.

Example 2.3

The motion of a spring with a stiffening (nonlinear) restoring force is described by the equation

$$\ddot{x} = -x - x^3$$

We move the two terms on the right hand side left and multiply by $\dot{x}$. Then integration in t yields the energy

$$\frac{\dot{x}^2}{2} + \frac{x^2}{2} + \frac{x^4}{4} = \text{constant} = K$$

This implies that

$$|x| \leq 2K^{1/2}, \text{ and } |\dot{x}| \leq (2K)^{1/2}$$

for all time, so the solution exist globally, see Corollary 2.3 below.

Exercise 2.2 *Show that the solutions of the nonlinear pendulum*

$$\ddot{x} + sin(x) = 0$$

have global existence.

Exercise 2.3 *What can you say about the interval of existence of the solution to*

$$\ddot{x} + x^2 = c$$

where c is a constant?

Global solutions are obtained by piecing together *local solutions*. In fact it follows from the Local Existence Theorem 2.1 that

1. Every point (t_o, x_o) lies on some solution $(t, x(t))$.
2. If (t_o, x_o) lies on two solutions $(t, x(t))$ and $(t, y(t))$, then these solutions must be the same in an interval $|t - t_o| < a$, around t_o.

The second statement above is strengthen considerably by the follwing Lemma

Lemma 2.1 *If two solutions of the same ODE agree at a point then they must be the same in their whole interval of existence.*

Proof: Suppose that the solution $(t, x(t))$ is defined on the interval $[a, b)$ and the other solution $(t, y(t))$ is defined on the interval $[a, c)$ with $b < c$. Let

$$d = inf\{t | x(t) \neq y(t)\}$$

and consider the interval $[a, d]$. $x(t)$ and $y(t)$ both exist on $[a, d)$ and since they are continuous, their limits at d must be equal

$$\lim_{t \to d} x(t) = \lim_{t \to d} y(t)$$

This means that $d > b$ and consequently $b = c$ because otherwise $x(t)$ exists beyond b contradicting the statement above. **QED**

We define the solution *in the large* $(t, z(t))$ to be the union of the local solutions $(t, x(t))$. It exists on the union of the local intervals and is uniquely defined by any initial point (t_o, x_o) by above discussion.

Next we prove in two steps that if solution only exist for a finite time interval then they must blow-up.

Theorem 2.5 *Let $\bar{D}$ be a closed and bounded subset of a region U where solution $(t, x(t))$ is defined. If the solution is only defined on the time interval $[a, b)$ with $b < \infty$, then $(t, x(t))$ must leave $\bar{D}$ for all t sufficiently close to b.*

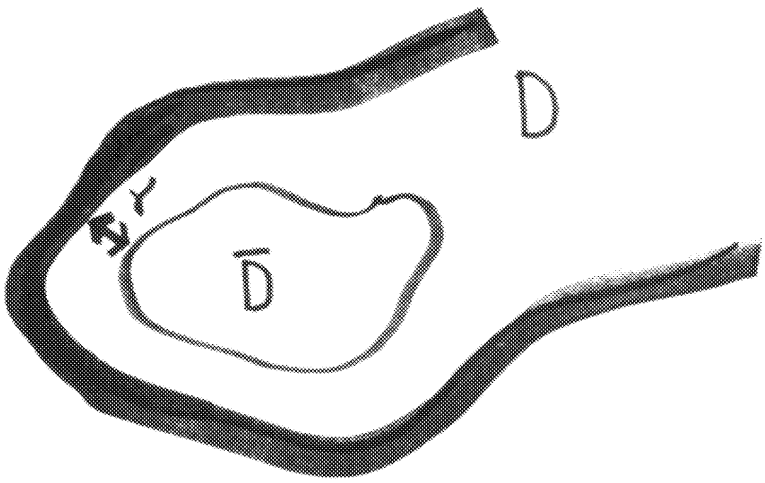

Figure 2.3: The compact set $\bar{D}$ has the distance γ to the compliment of the region U.

Proof: We assume there exists a solution $(t,x(t))$ defined for $0 \leq |t-t_0| < \beta$ and passing through some point (t_0,x_0) of $\bar{D}$. We have to prove that there exists an α such that the solution lies outside $\bar{D}$, for $\beta - \alpha < t - t_0 < \beta$. Now consider the region $\mathbb{R}^{n+1} \setminus U$, see Figure 2.2. Let

$$\gamma = \inf_{\{(x,t)\in\bar{D},(y,\tau)\in\mathbb{R}^{n+1}\setminus U\}}(|t-\tau| + \|x-y\|)$$

be the distance between $\bar{D}$ and $\mathbb{R}^{n+1} \setminus U$, and consider the rectangles

$$R(\tau,y) = \{(t,x)||t-\tau| \leq \delta, \|x-y\| \leq \delta\}$$

where $\delta < \gamma$. Then

$$D^* = \cup_{(\tau,y)\in\bar{D}} R(\tau,y)$$

is also a closed and bounded set. Now let

$$\alpha = \min(\delta, \delta/M),\ M = \max_{(t,x)\in D^*}\|f\|.$$

Then by the Picard Existence Theorem 2.1 $(t,x(t))$ exists in the interval $|t-t_0| < \alpha$. Now if $\beta - \alpha < t_1 < \beta$ and $(t_1,x(t_1)) \in D^*$ then the solution would exist beyond $t - t_0 = \beta$ which is a contradiction. **QED**

Corollary 2.3 *If the solution $x(t)$ of the IVP only exists for time less than $b < \infty$, then*

$$\lim_{t\to b}\|x(t)\| = \infty$$

Proof: We let U in Theorem 2.5 be the strip

$$U = \{(t,x)||t| < b\}$$

and D be the rectangle

$$D = \{(t,x)||t| < b, \|x\| \leq d\}$$

Then $(t,x(t))$ must leave $\bar{D}$ for t approaching b, but since it cannot leave the side $t = b$ of D, it must leave the sides $\|x\| = d$. However, d is arbitrary. **QED**

2.3 Lyapunov Stability

A first order system

$$\dot{x} = f(x) \tag{2.6}$$
$$x(t_0) = x_0$$

is said to be autonomous if the vector field $f(x)$ is independent of time. If $\dot{x} = 0$, x is called a stationary solution of (2.6). Then x must be a singular point $f(x) = 0$ of the vector field. A solution is said to be Lyapunov stable if solutions that start close to it stay close for all time.

Definition 2.2 *A solution of the first order system (2.6) is Lyapunov stable if for* $\varepsilon > 0$*, there exists* $\delta > 0$*, such that*

$$\|y_0 - x_0\| < \delta \Rightarrow \|y(t) - x(t)\| < \varepsilon,$$

for $t \geq t_o$*.* $x(t)$ *is asymptotically Lyapunov stable if*

$$\lim_{t\to\infty} y(t) = x(t).$$

The tool that allows us to prove Lyapunov stability is a Lyapunov function.

Definition 2.3 *A function* $V : \mathbb{R}^n \to \mathbb{R}$ *is called a Lyapunov function if it has continuous partial derivatives*

1. V *is non-negative,* $V(x) \geq 0$
2. $V(x) = 0$ *if and only if* $x = \bar{x}$*, a stationary solution*
3. V *is non-increasing*
$$\frac{dV}{dt} \leq 0$$

Theorem 2.6 *Suppose the vector field* $f(x)$ *is continuous in a neighborhood of a stationary solution* $\bar{x}$ *and that there exists a Lyapunov function for (2.6) in this neighborhood. Then* $\bar{x}$ *is stable. Morover, if*

$$\frac{dV}{dt} < 0$$

then $\bar{x}$ *is asymptotically stable.*

We define exit points and prove a technical lemma before proving the theorem.

Definition 2.4 *Let $f(x,t)$ be continuous on an open set U and $D \subset U$ be an open subset. $(t,x_0) \in \partial D \cap U$ is an exit point of D if $(t,x(t)) \in D$ for $t-\varepsilon < t < t_0$ and ε small. If, moreover, $(t,x(t)) \notin \bar{D}$, for $t_0 < t < t_0+\varepsilon$, then (t_0,x_0) is called a strict exit point of D.*

Lemma 2.2 *Let f be continuous on an open subset U and $D \subset U$ open such that $\partial D \cap U$ is either empty or consists of points which are not exit points. Then the solution of (2.6), with $(t_0,x_0) \in D$, stays in D as long as it exists.*

Proof: Suppose that the solution $(t,x(t))$ leaves D at some time t_1, then

$$(t_1,x(t_1)) \in \partial D \cap U$$

and $(t_1,x(t_1))$ is an exit point contrary to hypothesis. **QED**

We now proof Theorem 2.6.

Proof: Choose $\varepsilon > 0$ and let $\gamma < \min_{\|x-x_0\|=\varepsilon} V(x)$. We can then choose δ such that the ball $\|x-x_0\| \leq \delta$ lies inside the region $V(x) = \gamma$, see Figure 2.3. We define the sets

$$U = \{x|\ \|x-\bar{x}\| < \varepsilon\},\ \ D = \{x|\ V(x) < \gamma\},\ \ \partial D = \{x|\ V(x) = \gamma\}$$

and consider the function $v(x) = V(x) - \gamma$. Then

$$\dot{v} = \dot{V} \leq 0$$

since V is a Lyapunov function. Therefore no point on ∂D is an exit point. Consequently by Lemma 2.2, if $(t_0,x_0) \in D$, then $(t,x(t))$ must stay inside D as long as the solution exists. However, $D \subset U$ so that $\|x(t)-\bar{x}\| < \varepsilon$ as long as the solution exists, but this implies the $x(t)$ must exist for all t, by Theorem 2.5, because $x(t)$ is prevented from running to the boundary of U.

Now suppose $\dot{V} < 0$, then $V(x(t)) \to 0$ as $t \to \infty$ and this implies that $x(t) \to \bar{x}$. **QED**

Example 2.4

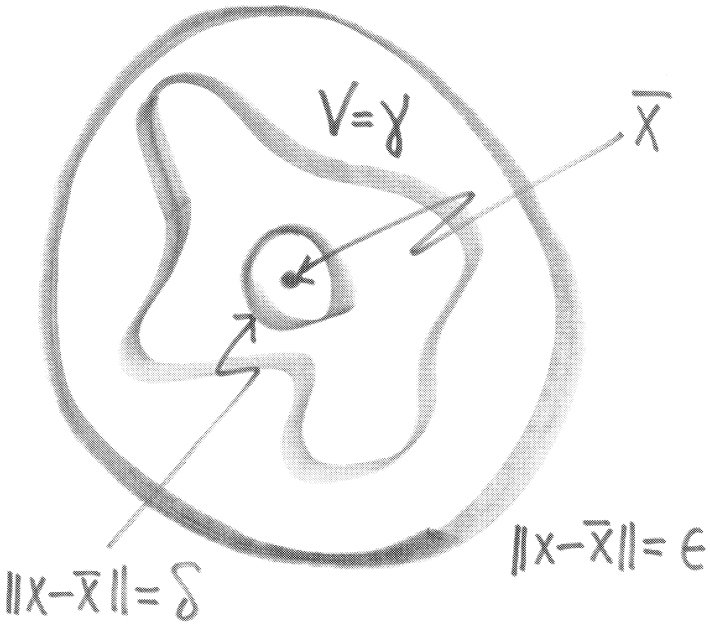

Figure 2.4: The set defined by $V(x) = \gamma$ lies outside the δ ball and inside the ε ball.

The Lorenz equation

$$\begin{aligned} \dot{x} &= \sigma(y-x) \\ \dot{y} &= \rho x - y - xz \\ \dot{z} &= xy - \beta z \end{aligned}$$

where σ, ρ and β are positive constants, describe Rayleigh-Bénard convection in the atmosphere, see Lorenz [15]. This heating of air by the earth's surface during the day and cooling by the upper layers in the atmosphere is the basis mechanism in the daily weather cycle. The x and y variables are two components of the velocity of air and z is temperature. We show that the function

$$V(x,y,z) = \frac{1}{2}(x^2 + \sigma(y^2+z^2))$$

is a Lyapunov function for the Lorenz equations. First $V \geq 0$ is positive definite since $\sigma > 0$, $V(x,y,z) = 0$ implies $(x,y,z) = (0,0,0)$ and the origin is a stationary solution of the Lorenz equations. This verifies the first two conditions of Definition 2.2. By use of the Lorenz equations

$$\begin{aligned} \frac{dV}{dt} &= x\dot{x} + \sigma(y\dot{y} + z\dot{z}) \\ &= \sigma(xy - x^2) + \sigma(\rho xy - y^2 - xyz) + \sigma(-\beta z^2 + xyz) \end{aligned}$$

Thus

$$\begin{aligned} \dot{V} &= -\sigma(x^2 - (1+\rho)xy + y^2) - \sigma\beta z^2 \\ &= -\frac{\sigma(1+\rho)}{2}(x^2+y^2) - \frac{\sigma(1-\rho)}{2}(x^2-y^2) - \sigma\beta z^2 \end{aligned}$$

We conclude that V is a Lyapunov function if and only if $\rho \leq 0$. This implies that the origin is stable if $\rho \leq 0$ and asymptotically stable if $\rho < 0$.

2.4 Absorbing Sets, Omega-Limit Sets and Attractors

If an ODE is dissipative then all orbits of solutions will end up in a bounded set and one can make strong statements about the phase portrait.

Definition 2.5 *The ODE, $\dot{x} = f(x)$, has an absorbing set D; if for every bounded set $U \subset \mathbb{R}^n$, there exists a time $T(U)$ such that $x(0) = x_o \in U$ and $t \geq T(U)$ implies that $x(t) \in D$.*

This means that all orbits are eventually absorbed by D see Figure 2.4.

Example 2.5

Consider and ODE

$$\dot{x} + \delta x = f(x,t),$$

where $\|f(x,t)\| \leq K$. We can integrate this equation to get

$$\frac{d}{dt} e^{\delta t} x = e^{\delta t} f(x,t)$$

or

$$x(t) = x_o e^{-\delta t} + \int_0^t e^{-\delta(t-s)} f(x(s),s) ds$$

and

$$\|x(t)\| \leq \|x_o\| e^{-\delta t} + \frac{K}{\delta}(1 - e^{-\delta t}). \tag{2.7}$$

The last inequality implies that

$$\|x(t)\| \leq \frac{K}{\delta} + \kappa$$

where κ is an arbitrarily small number, defines an absorbing set for the ODE. Namely, if we solve the inequality (2.7) for t, we get

$$\|x_o\| e^{-\delta t} + \frac{K}{\delta}(1 - e^{-\delta t}) \leq \frac{K}{\delta} + \kappa$$

and

$$(\|x_o\| - \frac{K}{\delta}) e^{-\delta t} \leq \kappa$$

so

$$-\delta t \leq log[\frac{\kappa}{(\|x_o\| - \frac{K}{\delta})}]$$

and

$$t \geq -\frac{1}{\delta} log[\frac{\kappa}{(\|x_o\| - \frac{K}{\delta})}].$$

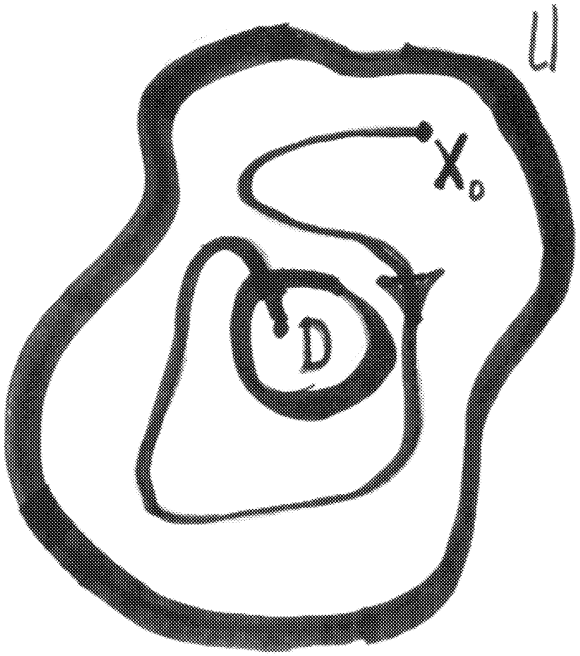

Figure 2.5: Every orbit starting in U is eventually absorbed by the absorbing set D.

This means that if the initial data lies in a bounded set defined by $\|x_o\| \leq M$, then $x(t) \in D$ for

$$t \geq T(M) = -\frac{1}{\delta} log[\frac{\kappa}{(\|x_o\| - \frac{K}{\delta})}].$$

Stationary solutions are the simplest structure that one can encounter in phase space the ω and α limit sets are more general structures. Stationary solutions are clearly *invariant* under the flow and the union of orbits tending towards them in positive time is called their *basin* of attraction. We will now generalize these notions to more complicated attracting sets.

Definition 2.6 *The ω limit set of a solution to an ODE, $x(t),\ x(0) = x_o$ consists of all points y such that there exists a sequence $t_n \to \infty$ as $n \to \infty$ and*

$$\lim_{n\to\infty} x(t_n) = y.$$

The α limit set of $x(t)$ consists of all points y such that there exists a sequence $t_n \to -\infty$ as $n \to \infty$ and

$$\lim_{n\to\infty} x(t_n) = y.$$

The ω limit set consists of all points that points sampled from the solutions converge to in positive time, whereas the α limit set consists of the points that points sampled from the solution converge to in negative time.

Theorem 2.7 *The α and ω sets are* closed *sets, if the solution $x(t)$ is also compact then these sets are* compact, non-empty *and* connected *sets.*

Proof: We first show that the ω limit set is closed. Suppose that

$$\lim_{n\to\infty} y_n = y$$

where $y_n \in \omega\{x(t)\}$. Then by definition of ω there exist sequences $\{t_m^n\}$ such that

$$\lim_{n\to\infty} x(t_m^n) \to y_n.$$

We can choose a (diagonal) sequence $\{t_n^n\}$ from the sequences $\{t_m^n\}$ such that

$$\lim_{n\to\infty} x(t_n^n) \to y.$$

Thus $y \in \omega\{x(t)\}$.

Next we prove the (sequential) compactness of $\omega\{x(t)\}$. Let $\{y_n\}$ be a sequence in $\omega\{x(t)\}$. Then there exist sequences $\{t_k^n\}$, such that $\{x(t_k^n)\}$ converge to y_n as $k \to \infty$. Since the orbit $x(t)$ is compact the diagonal sequence $\{x(t_n^n)\}$ has a convergent subsequence $\{x(t_j^j)\}$, that converge to $y \in \omega\{x(t)\}$ as $j \to \infty$. This implies that the corresponding subsequence $y_j = \lim_{k\to\infty} x(t_k^j)$ also converges to y as $j \to \infty$. We have shown that $\{y_n\}$ has a convergent subsequence.

Now $\omega\{x(t)\}$ is not empty if it is compact because we can find a convergent subsequence of $x(t_n)$ converging to a point

$$\lim_{k\to\infty} x(t_k) = y$$

and then $y \in \omega\{x(t)\}$. Thus $\omega\{x(t)\}$ contains at least one point y.

We now prove that $\omega\{x(t)\}$ is a connected set. Suppose that ω consists of two disjoint sets X and Y. Then both X and Y must be compact and the distance between them is a positive number

$$d(X,Y) = d.$$

However since both X and Y consist of limit points of $x(t)$, $x(t)$ visits both X and Y infinitely often for arbitrarily large t. Moreover, since $x(t)$ is a continuous function of t and $x(t)$ is covering the distance between X and Y infinitely often, there exists a sequence $\{x(t_n) = x_n\}$ such that

$$d(Y,x_n) = \frac{d}{2}.$$

The sequence $\{x(t_n)\}$ has a convergent subsequence

$$\lim_{k\to\infty} x_k = z$$

and thus

$$\lim_{k\to\infty} x(t_k) = z,$$

so $z \in \omega\{x(t)\}$. The distance

$$d(X,z) \geq d(X,Y) - d(Y,z) = \frac{d}{2},$$

so z is neither in X nor Y, but this contradicts the decomposition

$$\omega = X \cup Y.$$

The proof for the α limit set is similar. **QED**

Definition 2.7 *The time-τ map of an ODE $\dot{x} = f(x)$, $x(0) = x_o$, is defined to be*

$$T_\tau x(t) = x(t+\tau).$$

This is also called the time-advance map.

Definition 2.8 *A set D is invariant under a map T if $TD \subset D$, it is negatively invariant if $D \subset TD$. In particular, D is invariant if it is both positively and negatively invariant.*

Exercise 2.4 *Show that $\omega(x_o)$ and $\alpha(x_o)$ are both invariant.*

Definition 2.9 *If D and A are both subsets of $\mathbb{R}^n$ and $\|T^n D - A\| \to 0$ as $n \to \infty$, then we say that A attracts D. If A attracts a neighborhood of itself and is invariant, it is called an* attractor*; if it is also compact and attracts $\mathbb{R}^n$, it is called a* global attractor.

Theorem 2.8 *If an ODE, $\dot{x} = f(x)$, has an absorbing set D, then the ω-limit set of D*

$$\omega(D) = \cap_n \overline{\cup_{m \geq n} T^m D}$$

is a global attractor.

Proof: We first observe that $\omega(D)$ is compact and non-empty because it is a nested intersection of closed and bounded sets. Then we show that it is invariant. Let $K_n = \overline{\cup_{m \geq n} T^m D}$ and $K = \omega(D)$. Then K is positively invariant because if $y \in K$, there exists a sequence $z_n = T^n y_n \to y$ and $T^m z_n = T^{m+n} y_n \in K^{m+n}$, thus

$$T^m y = lim_{n\to\infty} T^{m+n} y_n \in K.$$

K is also negatively invariant. If $T^n y_n \to y \in K$ then $\{T^{n-m} y_m\}$ has a convergent subsequence, by the compactness of K, and if $z = lim_{n\to\infty} T^{n-m} y_m$, then

$$y = T^m z \in T^m K.$$

This shows that $K \subset T^m K$. Now K attracts a neighborhood, because if it does not, then there exists a sequence y_n in a neighborhood of K such that

$$\|T^n y_n - K\| \geq \varepsilon > 0.$$

But $\{T^n y_n\}$ has a convergent subsequence

$$y = lim_{m\to\infty} T^m y_m \in K,$$

which is a contradiction. Moreover, K attracts D which attracts $\mathbb{R}^n$ so K attracts $\mathbb{R}^n$. **QED**

Exercise 2.5 *Show that the global attractor is unique.*

Theorem 2.9 *If an ODE, $\dot{x} = f(x)$, has a Lyapunov function; then its global attractor is connected and can be expressed as*

$$A = W^u(S),$$

the unstable set of the stationary solutions $\bar{x} \in S$,

$$W^u(S) = \{x \in \mathbb{R}^n : x(-t), x(0) = x, \text{ is defined for } t \geq 0 \text{ and } x(-t) \to S, \text{ as } t \to \infty\}.$$

Moreover, if each stationary solution is isolated, then S if finite and

$$A = \cup_{\bar{x}_j \in S}^{N} W^u(\bar{x}_j).$$

We first proof the following Lemma,

Lemma 2.3 *If the ODE, $\dot{x} = f(x)$, $x(0) = x_o$, has a Lyapunov function and $x_o \in \mathbb{R}^n$, then $\omega(x_o) \in S$ and if $x(t)$, is a compact orbit then $\alpha(x_o) \in S$, also.*

Proof: Since the Lyapunov function $V(x(t))$ is non-increasing, $V(x(t)) \to c$, a constant, as $t \to \infty$. Now $v = V - c$ is also a Lyapunov function and this means that if $x(t_n) \to y \in \omega(x_o)$, as $t_n \to \infty$, $y = \bar{x} \in S$ is a stationary solution. Now let $t_n \to -\infty$ such that $t_{n-1} - t_n \geq 1$, T be the time-τ map, and consider

$$V(x(t_{n-1} + t)) \leq V(x(t_n + t))$$

where the inequality follow from the properties of V. If

$$x(t_n + t) \to y,$$

then by the compactness of $x(t)$

$$V(x(t_n + t)) \to c.$$

Then

$$v = V - c$$

is also a Lyapunov function and $v(y) = 0$. This means that $y = \bar{x} \in S$. **QED**

We can now proof Theorem 2.9.

Proof: By Lemma 2.3 $\alpha(x) \subset S$, for each $x \in A$. Thus $A \subset W^u(S)$. Clearly, $S \subset A$ and since A attracts a neighboorhood of itself $W^u(S) \subset A$ also.

If all stationary solutions $\bar{x} \in S$ are isolated then S is a finite set, by the compactness of A, and

$$A = \cup_{\bar{x}_j \in S}^{N} W^u(\bar{x}_j).$$

QED

The Picard Theorem 2.1 is an example (the first in history) of a fixed point or contraction mapping theorem.

Theorem 2.10 *The Contraction Mapping Principle A contraction mapping*

$$d(Tx,Ty) \leq \theta d(x,y), \quad 0 < \theta < 1,$$

on a complete metric space has a unique fixed point

$$T\bar{x} = \bar{x}.$$

Proof: We first prove the uniqueness. Suppose x and y are both fixed points $Tx = x$, $Ty = y$. Then

$$d(x,y) = d(Tx,Ty) \leq \theta d(x,y)$$

since $0 < \theta < 1$,

$$(1-\theta)d(x,y) \leq 0 \Longrightarrow d(x,y) = 0$$

so $x = y$. Next we prove the estimate

$$d(T^m x, T^n x) \leq \frac{\theta^n}{(1-\theta)} d(Tx,x), \quad m > n$$

for the sequence of (Picard) iterates $\{T^n x\}$.

$$\begin{aligned} d(T^m x, T^n x) &\leq d(T^m x, T^{m-1} x) + d(T^{m-1} x, T^{m-2} x) \\ &\quad + \cdots + d(T^{n+1} x, T^n x), \end{aligned}$$

by the triangle inequality,

$$\leq (\theta^{m-1} + \theta^{m-2} + \cdots + \theta^n) d(Tx,x)$$

by the contraction inequality

$$\leq \frac{\theta^n}{(1-\theta)} d(Tx,x).$$

Now sending $n \to \infty$ we see that the sequence is Cauchy and since the metric space is complete, there exists an $\bar{x}$ in the space such that

$$\lim_{n\to\infty} T^n x = \bar{x}.$$

Finally, $\bar{x}$ is a fixed point because

$$\begin{aligned} d(T\bar{x},\bar{x}) &= \lim_{n\to\infty} d(T^{n+1}x, T^n x) \\ &= \lim_{n\to\infty} \theta^n d(Tx,x) = 0. \end{aligned}$$

QED

Chapter 3

The Geometry of Flows

3.1 Vector Fields and Flows

In this chapter we will tackle ODEs from a geometrical point of view. This is a natural vantage point because an ODE is really a statement about the tangent space to a manifold. The structure of the tangent space governs the geometry of the manifold. First we define the objects that we will work with.

Definition 3.1 *A function $f : U \to V$, where $U \subset \mathbb{R}^n$ and $V \subset \mathbb{R}^m$, is a C^k function, or k-times differentiable, if its component functions y_j are k-times differentiable*

$$(y_1, y_2, \ldots, y_m) = f(x_1, x_2, \ldots, x_n)$$

and the derivative $\partial^k y_j / \partial x_l^k$, $j,l \leq k$ is continous. If $k = \infty$ then we say that f is smooth.

Definition 3.2 *A one to one map $f : U \to V$, $U \subset \mathbb{R}^n$, $V \subset \mathbb{R}^n$, is a diffeomorphism if both f and f^{-1} are C^k, $k \geq 1$, functions.*

Definition 3.3 *A differentiable structure on a locally Euclidian space M is a collection of open sets U_j and coordinate maps $\varphi_j : U_j \to \mathbb{R}^n$, such that $j \in J$, J a set of indicies,*

1. $\cup_{j \in J} U_j = M$
2. $\varphi_j \; o \; \varphi_k^{-1}$ *is C^k, for $j,k \in J$*

3. *The collection is maximal or if* (U,φ) *is any coordinate system then* $(U,\varphi) \subset \{(U_j,\varphi_j), j \in J\} = \mathcal{F}$

Definition 3.4 *An n-dimensional manifold of class k is a n-dimensional locally Euclidian space M with a* C^k *differentiable structure* $\mathcal{F}$.

Example 3.1

The n-sphere is a n-dimensional manifold.

$$S^n = \{x \in \mathbb{R}^{n+1} | \sum_{j=1}^{n} x_j^2 + (x_{n+1}-1)^2 = 1\}$$

The differentiable structure consists of two open sets

$$U_1 = S^n - (0,0,\cdots,2), \;\; U_2 = S^n - (0,0,\cdots,0)$$

or the sphere with the two poles removed. The corresponding coordinate functions are the stereographic projections from each punctured sphere $\varphi_1 = p_1$, $\varphi_2 = p_2$, see Figure 3.1. In physics the manifold M is the phase space of the physical system and the motion on M is described by the ODE.

Definition 3.5 *An* **orbit** *of a point* $x \in M$ *is a map of a connected subset I of* $\mathbb{R}^n$ *into M,* $\phi_t(x) \in M$*, where* $t \in I$.

We now specialize to autonomous systems to introduce some concepts that do not always exist for non-autonomous systems.

Definition 3.6 g_t *is called a one-parameter group of transformation if it has the following properties, for* $t,s \in I \subset \mathbb{R}$*, and I is symmetric* $-I = I$,

1. $g_t : M \to M$
2. $g_t g_s = g_{t+s}$
3. $g_0 = identity$

These properties imply that $g_t^{-1} = g_{-t}$. For $t = T$ fixed, g_T is nothing but the time-T map, see Definition 2.7.

Definition 3.7 *The one parameter group along with its manifold* $(M,\{g_t\})$ *is called the (phase)* **flow**.

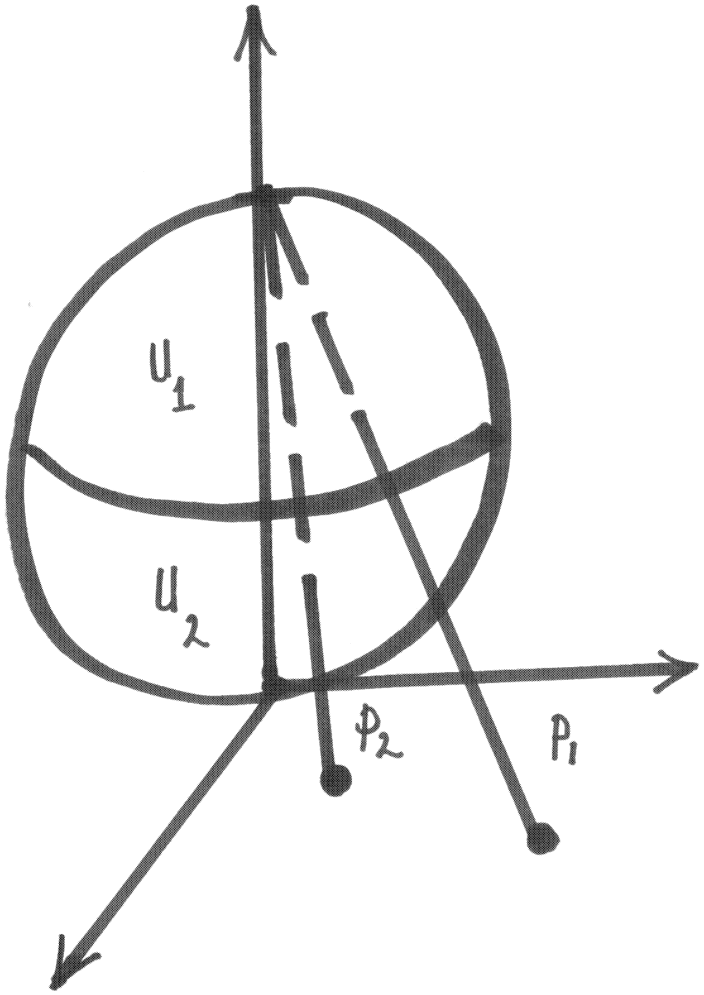

Figure 3.1: The two sphere with the two covering sets U_1 and U_2 and corresponding steriographic projection p_1 and p_2 to $\mathbb{R}^2$.

Lemma 3.1 *g_t is a one parameter group of* **diffeomorphism**, *if $(M,\{g_t\})$ is a flow and g_t is differentiable.*

Proof: That g_t is a one parameter group of diffeomorphism implies that $g_t^{-1} = g_{-t}$, now this in turn implies that g_t^{-1} is differentiable since g_{-t} is. Therefore, g_t is at least a C^1 diffeomorphism. **QED**

Suppose that we start with some initial condition $x \in M$. x will move under the flow and the solution to the initial value problem is its trajectory under the one parameter group g_t. The orbit of x becomes,

$$\phi_t(x) = g_t x, \;\; t \in I.$$

Thus it is the map of any connected time interval $I \subset \mathbb{R}$ into M, by g_t. If $I = \mathbb{R}$, then the orbit is called a *phase curve*.

The above definitions are easily modified if we add the time axis to the phase space to get the extended phase space $M \times \mathbb{R}$. Then $(M \times \mathbb{R}, \{g_t\})$ is the extended phase flow and the graph of the orbit $(t, \phi_t(x))$ is called an *integral curve*. Notice however that g_t only acts on M not on $M \times \mathbb{R}$.

Exercise 3.1

1. Find the phase space of the harmonic oscillator

   $$\ddot{x} + \omega^2 x = 0$$

   and the one parameter group of diffeomorphisms g_t. Also find two different type of orbits. Are these orbits phase curves?

2. Consider the nonlinear pendulum

   $$\ddot{x} + sin(x) = 0$$

   Describe four different types of phase curves for the nonlinear pendulum.

We differentiate the orbit with respect to time to get the phase velocity

$$\dot{\phi}_t(x) = v(x)$$

Since the orbit $\phi_t(x) = x(t)$ is just the solution the ODE, $\dot{x} = f(x)$, with initial condition $x(0) = x$, we conclude that the phase velocity is just the vector field

$$v(x) = f(x)$$

This is where the name vector field originates, v is the vector field on the phase space M that determines the flow.

Definition 3.8 *The (phase) velocity of a flow*

$$\dot{x} = \dot{\phi}_t(x) = v(x) = f(x)$$

is the vector determining the flow at the point $x \in M$. A point $\bar{x}$ where

$$v(\bar{x}) = 0$$

is called a **singular point** *of the vector field.*

It is clear from the definition that if $\phi_t(x)$ is C^k then $v(x)$ is C^{k-1}. By the Picard Existence Theorem 2.1, we know that if $v(x)$ is C^{k-1} then $\phi_t(x)$ is C^k. In the extended phase space v defines a direction field and a curve is an integral curve if and only if it is always tangent to the direction field, see Figure 3.1.

Example 3.2

1. $\dot{x} = kx$
2. $\dot{x} = sin(x)$

1. The phase space is $M = \mathbb{R}$, the one-parameter group of diffeomorphism is,

   $$g_t = e^{kt}$$

   and the orbit is

   $$\phi_t(x) = e^{kt}x$$

   $\bar{x} = 0$ is the single stationary solution and singular point of the vector field. The flow is away from 0, so 0 is a unstable stationary solution, see Figure 3.1.

2. The phase space is $M = \mathbb{R}$, but g_t is not a simple function, see the Exercise 3.2. However, g_t and $\phi_t(x)$ exist and can be worked out. The stationary solutions and singular point of the vector field are $x = n\pi$, $n \in \mathbb{Z}$. The even multiples of π are unstable and the odd multiples are stable, see Figure 3.1.

Exercise 3.2

1. Find the second semi-group in Example 3.2
2. Find g_t and $\phi_t(x)$ for Example 2.
3. Show that a one parameter group of transformation may not always exist or only exists for a finite time.

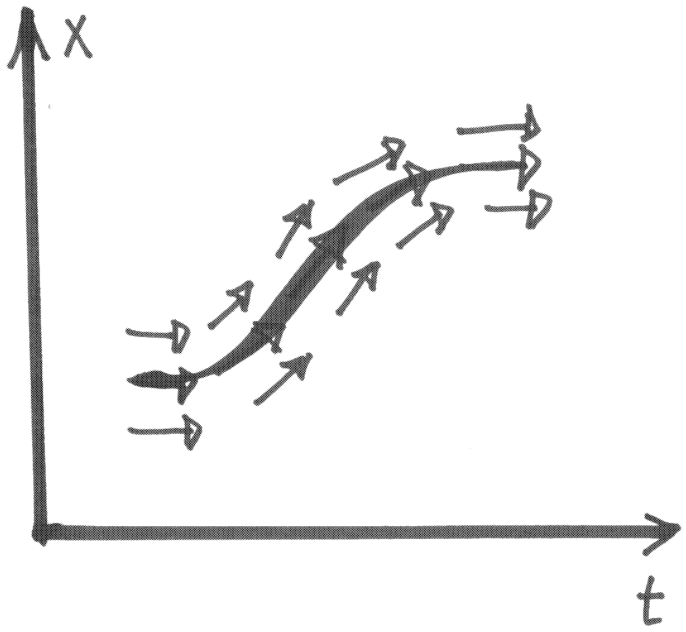

Figure 3.2: The direction vector field tangent to the integral curve of the orbit.

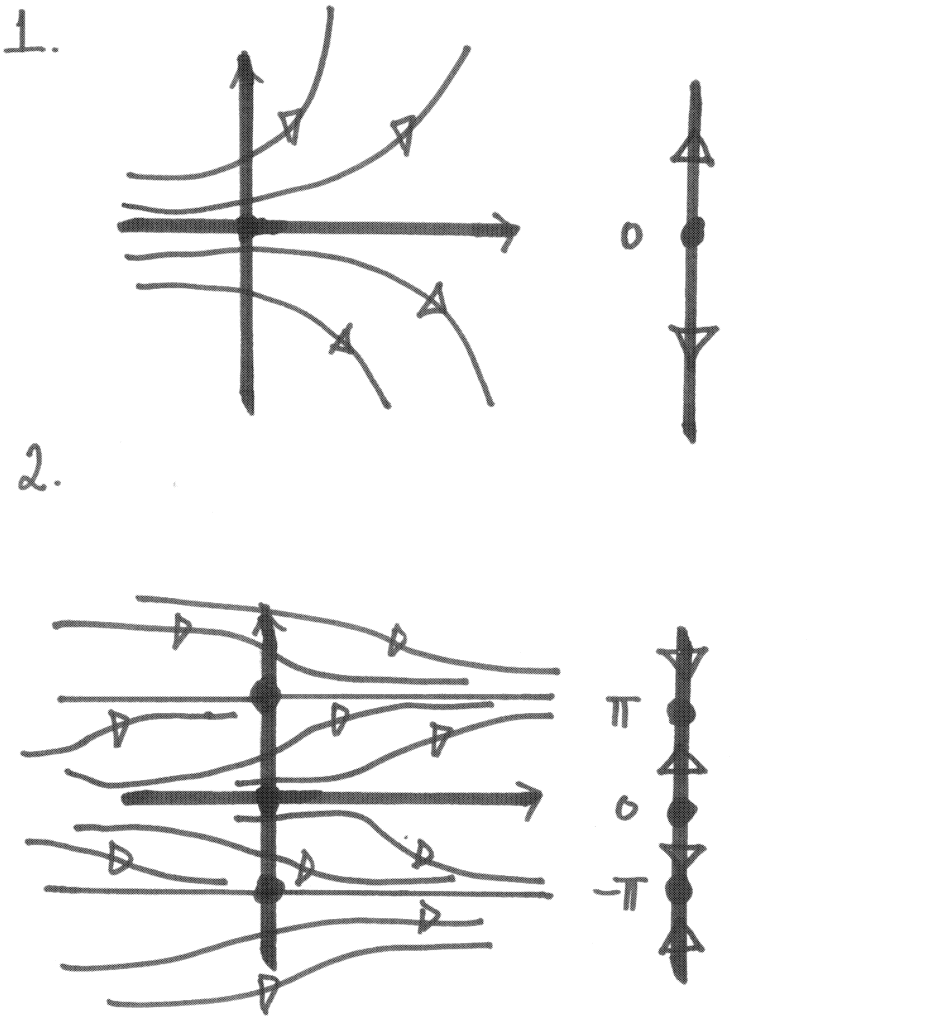

Figure 3.3: The extended phase space and the phase space of the ODEs 1 and 2, in Example 3.2, respectively.

3.2 The Tangent Space

We now consider the phase velocity from a slightly different point of view, namely as represented by its coordinates in Euclidian space. Let (U, φ) be a member of the differentiable structure on the manifold M, such that

$$x \in U \quad \text{and} \quad \varphi = (x_1, x_2, \ldots, x_n)$$

the x_js being coordinate functions. $v = (v_1, v_2, \ldots, v_n)$ where

$$v_j(x) = \frac{d}{dt} x_j \; o \; \phi_t(x)|_{t=0}, \quad j = 1, \ldots, n \tag{3.1}$$

Moreover, we define two orbits (or just curves) to be tangent at x if their difference is order t^2

$$\|\phi_t^1(x) - \phi_t^2(x)\| = O(t^2)$$

A change of coordinates is called *admissible* if it is a diffeomorphism. This notion of a class of admissible changes of coordinates permits us to define a tangent vector without a reference to a coordinate system.

Definition 3.9 *The velocity vector to an orbit at a point $x \in M$*

$$\dot{\phi}_t(x) = v(x)$$

is the equivalence class of tangents to the equivalence class of orbits at x. The tangent space at $x : TM_x$ is the equivalence class of all tangent vectors to orbits starting at x.

It is clear that two orbits are equivalent if there is a diffeomorphism taking one into the other, also if

$$y : U \to V$$

is a diffeomorpishm, then the Jacobian

$$D_x \, y : TU_x \to TV_y$$

is the corresponding map of the tangent spaces and this map is *linear*. We simply differentiate

$$\phi_t^2(y(x)) = y(\phi_t^1(x))$$

with respect to t, to get that

$$v_2(y(x)) = \dot{\phi}_t^2 = D_x y \; \dot{\phi}_t^1 = D_x y \; v_1(x)$$

by the chain rule. Moreover, it is easy to prove that the coordinate map (3.1) of v is one to one.

Lemma 3.2 *The coordinate map*

$$v : TM_x \to \mathbb{R}^n$$

is an isomorphism.

Proof: We have to show that if two tangent vectors $v_1 = v_2$ are the same then the corresponding orbits are tangent. Since

$$v_1 - v_2 = 0$$

$$D_x y\ (\dot{\phi}_t^1 - \dot{\phi}_t^2) = 0.$$

However, since $D_x y$ is invertible it follows that

$$\dot{\phi}_t^1 - \dot{\phi}_t^2 = 0.$$

This implies that

$$\|\phi_t^1(x) - \phi_t^2(x)\| = O(t^2).$$

QED

A sufficient condition for a differentiable map to be a diffeomorphism is given by the next theorem.

Theorem 3.1 *The Inverse Function Theorem Let $g : U \to V$ be a C^1 map from $\mathbb{R}^n$ to $\mathbb{R}^n$ and suppose that $detD_x g \neq 0$, at $x \in U$. This implies that*

$$D_x g : TU_x \to TV_y$$

is an isomorphism and then there exists a neighborhood $W \subset U$ of x, such that

$$g : W \to g(W)$$

and g restricted to W is a diffeomorphism.

Proof: Since $D_x g$ is an isomorphism $dimU = dimV$. Let x and y be coordinates on U and V respectively. Define

$$F(x,y) = y - g(x)$$

such that

$$F(x_0,y_0) = y_0 - g(x_0) = 0.$$

Then

$$detD_xF = -detD_xg \neq 0,$$

at $x = x_0$, and by the implicit function theorem there exists a small neighborhood $E \subset V$ of y_0 and a function

$$h : E \to h(E) = W$$

such that

$$F(h(y), y) = 0$$

for $y \in E$. Moreover, h is unique and differentiable as often as g. Clearly

$$h = g^{-1} \in C^1,$$

therefore g is a diffeomorphism. **QED**

3.3 Flow Equivalance

The nonautonomous ODE

$$\dot{x} = f(x,t)$$

can be made autonomous by introducing a new variable $\theta = t$, then $\dot{\theta} = 1$ and the above system is equivalent to the autonomous system

$$\begin{aligned} \dot{x} &= f(x,\theta) \\ \dot{\theta} &= 1 \end{aligned}$$

Thus our definition of the tangent vector and tangent space hold in the extended phase space $M \times \mathbb{R}$ with coordinates (x,θ). However, frequently this is not the most desirable result, we would like objects such as the semi-group to be defined for the phase space M itself and this is not always possible to do. But the addition of θ as above can be a very useful tool and it is just what we need for the next theorem. It is called the Rectification Theorem and it says that in a neighborhood of a nonsingular point any flow can be mapped onto straight linear flow.

Theorem 3.2 *The Rectification Theorem.*
Let (x_0, θ_0) be a nonsingular point of the vector field

$$\begin{aligned} \dot{x} &= f(x,\theta) \\ \dot{\theta} &= 1 \end{aligned}$$

then there exists a neighboorhood U of x and a diffeomorphism $g : U \to V \subset \mathbb{R}^{n+1}$ such that the ODE becomes

$$\dot{y} = 0$$
$$\dot{z} = 1$$

where $(y,z) = g(x,\theta)$. Moreover, if f is C^k then g is also C^k.

Proof: We define a map h from the line (y,z) to the orbit $(\phi_t(x),\theta)$. If we can show that h is a diffeomorphism, then $g = h^{-1}$ is the desired map. Define

$$(\phi_t(x),\theta) = h(y,z)$$

where $y = \phi_t(x)$, a constant in local coordinates, and $z = \theta$. h is clearly differentiable with respect to y and z and

$$D_{(y,z)}h = \begin{pmatrix} I & \dot{\phi}_t \\ 0 & 1 \end{pmatrix}$$

at $x = \phi_{t_0}$, $\theta = \theta_0$. It is easy to see that $D_{(y,z)}h$ does what it is supposed to do. It maps the vector field $(0,1)$ onto $(v,1)$, where $v = \dot{\phi}_t$,

$$\begin{pmatrix} I & v \\ 0 & 1 \end{pmatrix} \begin{pmatrix} 0 \\ 1 \end{pmatrix} = \begin{pmatrix} v \\ 1 \end{pmatrix}$$

Moreover

$$\det D_{(y,z)}h = 1 \neq 0$$

and by the inverse function theorem 3.1 h is a diffeomorphism. If $v = f$ is C^{k-1}, then h is C^k and g is also C^k by the inverse function theorem. **QED**

It is helpful to view the proof of the Rectification Theorem geometrically. $D_{(y,z)}h$ maps $\mathbb{R}^n \times \mathbb{R}$ onto $\mathbb{R}^n \times V$, where $V = \text{span}(v,1)$. However, $(v,1)$ is transverse to $\mathbb{R}^n$, see Figure 3.3, so both spaces are $n+1$ dimensional. Now kernal$D_{(y,z)}h$ is empty so the map is an isomorphism. The inverse of $D_{(y,z)}h$ is $D_{(x,\theta)}g$, the derivative of g.

Exercise 3.3 *Prove the Picard Theorem 2.1 (away from a singular point) using the Rectification Theorem.*

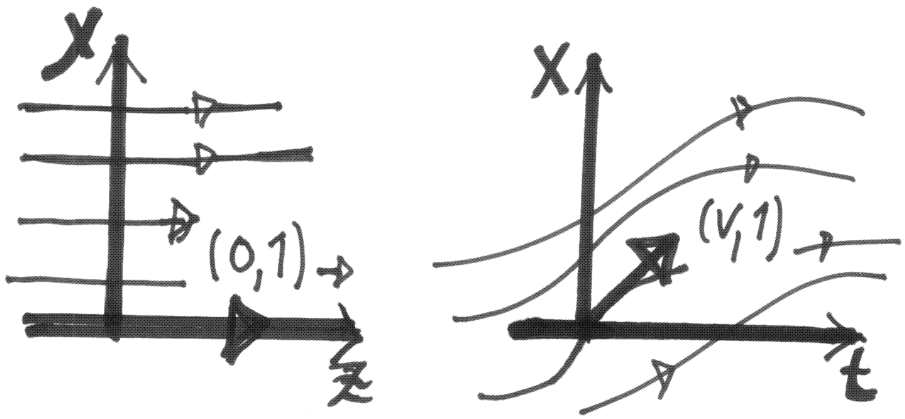

Figure 3.4: The two vector fields in the Rectification Theorem and the map between them.

Definition 3.10 Flow Equivalence

Two flows are conjugate (equivalent) if there exists a one to one map g between corresponding orbits or

$$\phi_t^2 \; o \; g = g \; o \; \phi_t^1$$

The flows are

1. **linearly conjugate** *if g is a linear map, then* $g \in C^\infty$,
2. **differentiably conjugate** *if g is a diffeomorphism,* $g \in C^k, \; k \geq 1$,
3. **topologically conjugate** *if g is a homoeomorphism* $g \in C^0$.

Lemma 3.3 *Two linear systems are linearly conjugate if and only if they have the same eigenvalues with the same algebraic and geometric multiplicity.*

Proof: Consider the systems

$$\dot{x} = Ax \;\text{ and }\; \dot{y} = By$$

they are linearly conjugate if

$$\phi_t^2(h(x)) = h\phi_t^1(x)$$

where h is an $n \times n$ invertible matrix. Now

$$\begin{aligned} \dot{\phi}_t^2 = h\dot{\phi}_t^1 = hA\phi_t^1 \\ = hAh^{-1}h\phi_t^1 = hAh^{-1}\phi_t^2 \end{aligned}$$

Comparing

$$\dot{\phi}_t^2 = hAh^{-1}\phi_t^2 \;\text{ and }\; \dot{y} = By$$

we conclude that A and B are similar matricies

$$B = hAh^{-1}$$

Conversely, if A and B are similar matricies then the equations

$$\dot{\phi}_t^2 = hAh^{-1}\phi_t^2 \;\text{ and }\; \dot{y} = By$$

can both be solved with the same initial data to give the solution

$$\phi_t^2(hx) = h\phi_t^1(x)$$

by the uniqueness of the solution to the initial value problem. This shows that the two orbits are linearly conjugate. **QED**

Theorem 3.3 *Two linear systems are differentiably conjugate if and only if they are linearly conjugate.*

Proof: Consider the systems

$$\dot{x} = Ax \quad \text{and} \quad \dot{y} = By$$

If the orbits are differentiably conjugate by Lemma 3.3 is suffices to show that A and B are similar matricies. Suppose that

$$\phi_t^2(g(x)) = g(\phi_t^1(x)) \tag{3.2}$$

where g is at least in C^1. We expand the orbits in t:

$$\phi_t^1(x) = \phi_{t=0}^1(x) + \dot{\phi}_{t=0}^1(x)t + O(t^2) = x + Axt + O(t^2)$$

Similarly,

$$\phi_t^2(x) = y + Byt + O(t^2)$$

We substitute these expansions into Equation 3.2 and differentiate with respect to the initial data x. This can be done because g is a diffeormophism and the orbits depend continuously on their initial data. The differentiation of

$$g(x) + Bg(x)t + O(t^2) = g(x + Axt + O(t^2))$$

gives

$$(I + Bt + O(t^2))g' = g'(I + At + O(t^2))$$

where g' is the Jacobian of g. This shows that

$$Bg' = g'A$$

and the matricies are similar. The converse is immediate because a linear conjugacy is a C^∞ diffeomorphism. **QED**

Remark 3.1 *Theorem 3.3 shows that differentiable conjugacy is too strict an equivalence relation at a singular point of a vector field. We must settle for* **topological conjugacy**.

We will show below that generically a nonlinear flow is topologically conjugate to its linearization. The topological conjugacy classes are given by the invariant manifold theorems. Namely, the stable and unstable manifold theorem and the center manifold theorem.

Chapter 4

Invariant Manifolds

The linear stable and unstable manifolds E_s and E_u of a hyperbolic stationary solution, consisting of the eigenvectors of the stable and unstable eigenvalues respectively, are the tangent spaces of their nonlinear counterparts, at the origin. The existence of the nonlinear stable and unstable manifolds, see Figure 4 is given by the following theorem.

Theorem 4.1 *The Invariant Manifold Theorem*
Consider the equation

$$\dot{x} = Ax + g(x), \quad x \in \mathbb{R}^n$$

where A has n eigenvalues λ_j*, and* $Re\lambda_j \neq 0$*;* $g(x)$ *is* C^k *in a neighborhood of* $x = 0$ *and*

$$\lim_{\|x\| \to 0} \frac{\|g(x)\|}{\|x\|} = 0,$$

then there exists a neighborhood U of the origin, a C^k *manifold* W^s *and a* C^k *function* $h^s : \Pi^s(U) \to E_u$*, where* $\Pi^s(U)$ *is the projection of U onto* E_s*, such that*

1. $h^s(0) = 0$ *and* $\frac{\partial h^s}{\partial x_s}(0) = 0$*,* W^s *is the graph of* h^s
2. $x(t_0) \in W^s \Longrightarrow x(t) \in W^s, \forall\, t \geq t_0$
3. $x(t_0) \neq W^s \Longrightarrow \exists\, \delta > 0,\ t_1 \geq t_0,\ \|x(t)\| > \delta,\ \forall\, t \geq t_1$

There also exists a C^k *manifold* W^u *and a* C^k *function* $h^u : \Pi^u(U) \longrightarrow E_s$*, where* $\Pi^u(U)$ *is the projection of U onto* E_u*, such that,*

1. $h^u(0) = 0$ *and* $\frac{\partial h^u}{\partial x_u}(0) = 0$*, and* W^u *is the graph of* h^u

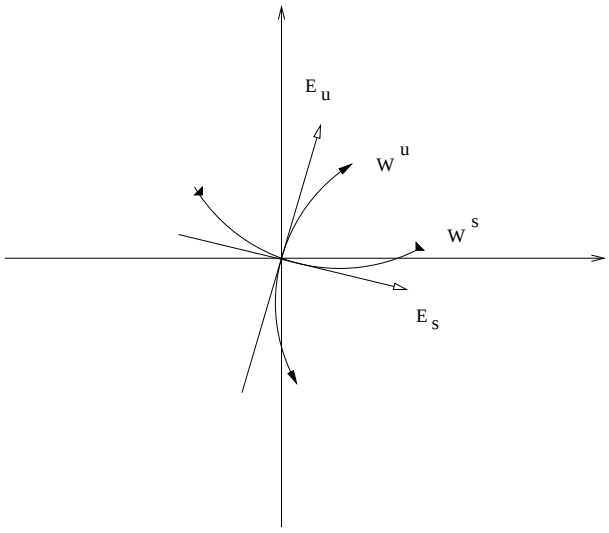

Figure 4.1: The Invariant Manifolds around a Hyperbolic Stationary Orbit.

2. $x(t_0) \in W^u \Longrightarrow x(t) \in W^u, \forall\, t \leq t_0$

3. $x(t_0) \neq W^u \Longrightarrow \exists\, \delta > 0,\ t_1 \leq t_0,\ \|x(t)\| > \delta,\ \forall\, t \leq t_1$

Proof: By the statement of the theorem we both have to prove the existence of the functions h_s and h_u whose graphs are the manifolds W^s and W^u and the existence of the solutions to the ODE $x_s(t) \in W^s$ and $x_u(t) \in W^u$.

If E_s is the linear stable manifold of the linearized system $\dot{y} = Ay$ then A leaves E_s invariant, $AE_s \subset E_s$, and if we define the exponential of a matrix to be the power series

$$e^{tA} = I + At + \frac{A^2t^2}{2} + \cdots + \frac{A^nt^n}{n} + \cdots,$$

then the exponential also leaves E_s invariant, $e^{tA}E_s \subset E_s$. Moreover, we have an estimate

$$\|e^{tA}y_s\| \leq C_s e^{-\rho t}\|y_s\|, \quad t \geq 0 \tag{4.1}$$

and the same remarks apply to E_u so $e^{tA}E_u \subset E_u$ and

$$\|e^{tA}y_u\| \leq C_u e^{\sigma t}\|y_u\|, \quad t \leq 0 \tag{4.2}$$

C_s, and C_u are constants. $-\rho$ and σ are respectively the smallest (in absolute value) negative and positive real parts of the eigenvalues of A.

We now express the ODE as an integral equation

$$x(t) = e^{(t-t_0)A}x(t_0) + \int_{t_0}^{t} e^{(t-\tau)A}g(x(\tau))d\tau.$$

Since $\mathbb{R}^n$ is a direct sum $\mathbb{R}^n = E_s \oplus E_u$ we can split $x = x_s + x_u$ and write an integral equation for x_s and x_u separately

$$x_s(t) = e^{(t-t_0)A}x_s(t_0) + \int_{t_0}^{t} e^{(t-\tau)A}g(x(\tau))_s d\tau$$

and

$$x_u(t) = e^{(t-t_0)A}x_u(t_0) + \int_{t_0}^{t} e^{(t-\tau)A}g(x(\tau))_u d\tau.$$

We have used here that both E_s and E_u are invariant under the flow. Next we look for a solution that lies in W^s and therefore remains in a neighborhood of the origin for all $t \geq 0$. If we consider the second equation and notice that x_u picks up the positive eigenvalues of A, we realize that the only way we are going to get a solution that stays in a neighborhood of the origin is to send $t_0 \to \infty$. Then

$$\lim_{t_0\to\infty} \|e^{-t_0A}x_u(t_0)\| \leq \lim_{t_0\to\infty} C_u' e^{-\sigma' t_0} = 0,$$

assuming $x_u(t)$ stays bounded, where σ' is now the smallest positive real part of the eigenvalues of A. This gives

$$x_u(t) = \int_{\infty}^{t} e^{(t-\tau)A}g(x(\tau))_u d\tau$$

and adding this to the equation for x_s above, with $t_0 = 0$, gives

$$x(t) = e^{tA}x_s(0) + \int_0^t e^{(t-\tau)A}g(x(\tau))_s d\tau - \int_t^{\infty} e^{(t-\tau)A}g(x(\tau))_u d\tau. \tag{4.3}$$

Now let $x_s(0) = x_s^0 \in E_s$ and recall some spaces that we already encountered in the proof of Picard's theorem. First let

$$C^0([0,\infty);\mathbb{R}^n)$$

be the space of continuous functions from the half-line $\mathbb{R}^+ = [0,\infty)$ into $\mathbb{R}^n$. Each point in $C^0([0,\infty);\mathbb{R}^n)$ is a n-vector valued function $x(t) \in \mathbb{R}^n$, for t fixed. However, $C^0([0,\infty);\mathbb{R}^n)$ is not a Banach space under the sup norm. It is a Fréchet

space or a complete metric space under a sequence of quasi-norms but this is not what we need. We have to introduce a weight $e^{\mu t}$ where $\mu = min(\rho, \sigma)$ to make $C^0_\mu([0,\infty);\mathbb{R}^n)$ into a complete normed linear space, or in other words a Banach space, under the norm

$$\|x(t)\|_\mu = \sup_{t\in[0,\infty)} e^{\mu t}\|x(t)\|.$$

We have forced the function in $C^0_\mu([0,\infty);\mathbb{R}^n)$ to decay exponentially in t by inserting the weight $e^{\mu t}$ and this makes the space a Banach space. We will restrict the space further by making the functions lie in a small ball in $\mathbb{R}^n$ and define the space on which we will prove the contraction to be

$$C^0_{\mu,\delta}([0,\infty);\mathbb{R}^n) = \{x(t) \in C^0_\mu |\ \|x(t)\| \le \delta\}.$$

This restriction partially destroys the Banach space structure because the sum of two vectors $x, y \in C^0_{\mu,\delta}$ in no longer lies in this ball, $x+y \in C^0_{\mu,\delta}$, so it is not a linear space. However, it is easy to check that this space is a complete metric space and this is all we need for an application of the Contraction Mapping Principle 2.10.

Now we use the integral equation (4.3) to define a map

$$F(x(t)) = e^{tA}x_s(0) + \int_0^t e^{(t-\tau)A}g(x(\tau))_s d\tau - \int_t^\infty e^{(t-\tau)A}g(x(\tau))_u d\tau. \qquad (4.4)$$

Then $F(x(t))$ is a contraction on $C^0_{\mu,\delta}$, if $\|x^0_s\| < \gamma$, γ small. This last inequality defines the small neighborhood U of the origin, in the statement of the theorem.

First we must show that F maps $C^0_{\mu,\delta}$ into itself. We multiply the equation (4.3) by $e^{\mu t}$ and apply the triangle inequality and the two inequalities (4.1) and (4.2) above, and the hypothesis on g, in the first step; since $\lim_{|x|\to 0}\frac{\|g(x)\|}{\|x\|} = 0$, so that there exists $\varepsilon > 0$ such that $\|Dg(x)\| \le \varepsilon\|x\|$,

$$\begin{aligned}
e^{\mu t}\|x(t)\| &\le C_s e^{-(\rho-\mu)t}\|x_s(0)\| + C_s\varepsilon\int_0^t e^{-(\rho-\mu)(t-\tau)}e^{\mu\tau}\|x(\tau)\|d\tau \\
&+ C_u\varepsilon\int_t^\infty e^{(\sigma+\mu)(t-\tau)}e^{\mu\tau}\|x(\tau)\|d\tau \\
&\le C_s\|x_s(0)\| + \varepsilon\left(\frac{C_s}{(\rho-\mu)} + \frac{C_u}{(\sigma+\mu)}\right)\|x(t)\|_\mu \\
&\le C_s\gamma + \varepsilon\left(\frac{C_s}{(\rho-\mu)} + \frac{C_u}{(\sigma+\mu)}\right)\delta \\
&\le \delta,
\end{aligned}$$

for $\|x_s(0)\| \leq \gamma$ and ε small enough.

Secondly we show the F is a contraction. We need to show that there exists $0 < \theta < 1$ such that

$$\|F(x_1(t)) - F(x_2(t))\| \leq \theta \|x_1(t) - x_2(t)\|,$$

where the map F is defined by the integral equation. Consider

$$\begin{aligned}
& e^{\mu t}[F(x_1(t)) - F(x_2(t))] = \\
& e^{\mu t} e^{tA}(x^0_{1,s} - x^0_{2,s}) + e^{\mu t} \int_0^t e^{(t-\tau)A}[g(x_1(\tau))_s - g(x_2(\tau))_s] d\tau \\
& - e^{\mu t} \int_t^\infty e^{(t-\tau)A}[g(x_1(\tau))_u - g(x_2(\tau))_u] d\tau \\
\leq \quad & e^{-(\rho-\mu)t}\|x^0_{1,s} - x^0_{2,s}\| + \varepsilon C_s \int_0^t e^{-(\rho-\mu)(t-\tau)} e^{\mu\tau}\|x_1(\tau) - x_2(\tau)\| d\tau \\
& + \varepsilon C_u \int_t^\infty e^{(\sigma+\mu)(t-\tau)} e^{\mu\tau}\|x_1(\tau) - x_2(\tau)\| d\tau,
\end{aligned}$$

by the estimates above and the hypothesis on g. Estimating as above, we get

$$\begin{aligned}
\leq \quad & e^{-(\rho-\mu)t}\|x^0_{1,s} - x^0_{2,s}\| \\
& + \left(\varepsilon \frac{C_s}{(\rho-\mu)} + \varepsilon \frac{C_u}{(\sigma+\mu)} \right) \sup_{[0,\infty)} e^{\mu t}\|x_1(t) - x_2(t)\|.
\end{aligned}$$

In particular, for $x^0_{1,s} = x^0_{2,s}$ we get a unique fixed point for

$$\varepsilon \left(\frac{C_s}{(\rho-\mu)} + \frac{C_u}{(\sigma+\mu)} \right) = \theta < 1.$$

We have shown that the integral equation (4.3) has a unique solution $x(t)$, but this gives us a function $h^s : E_s \to E_u$. Namely, $x(t) = (x_s, x_u)(t)$ where

$$x_s(t) = e^{(t-t_0)A} x_s(t_0) + \int_{t_0}^t e^{(t-\tau)} g_s(x(\tau)) d\tau$$

and

$$x_u(t) = -\int_t^\infty e^{(t-\tau)A} g_u(x(\tau)) d\tau.$$

At $t = t_0$, we get $x_s(t_0) = x_s$ and

$$h^s(x_s) = x_u(t_0) = -\int_{t_0}^{\infty} e^{(t-\tau)A} g_u(x(\tau))\, d\tau.$$

This is the desired function. The dependance of h^s on x_s enters throught the dependance on $x(\tau)$ that depends on the initial data $x_s(t_0) = x_s$.

We will now prove that the function h^s has the properties (1) - (3). To prove (1) we consider the integral equations above that $x^s(t)$ satisfies,

$$x_s(t) = e^{tA} x_s(0) + \int_0^t e^{(t-\tau)A} g(x(\tau))_s d\tau,$$

where we have chosen $t_0 = 0$ for convenience. We get using the triangle inequality for the norm and taking the limit as $t \to \infty$

$$\begin{aligned}
\lim_{t\to\infty} \|x_s(t)\| &\leq \lim_{t\to\infty} C_s e^{-\rho t} \|x_s(0)\| + \lim_{t\to\infty} C_s \varepsilon e^{-\mu t} \int_0^t e^{-(\rho-\mu)(t-\tau)} e^{\mu\tau} \|x(\tau)\| d\tau \\
&\leq C_s \lim_{t\to\infty} e^{-\rho t} \|x_s(0)\| + \frac{C_s \varepsilon}{(\rho-\mu)} \lim_{t\to\infty} e^{-\mu t} \|x(t)\|_\mu = 0.
\end{aligned}$$

This says that

$$\lim_{t\to\infty} x_s(t) = 0$$

and consequently

$$h^s(0) = 0$$

because

$$\begin{aligned}
\|h^s(0)\| = \lim_{t\to\infty} \|x_u(t)\| &\leq \lim_{t\to\infty} C_u \varepsilon e^{-\mu t} \int_t^{\infty} e^{(\sigma+\mu)(t-\tau)} e^{\mu\tau} \|x(\tau)\| d\tau \\
&\leq \frac{C_u \varepsilon}{(\sigma+\mu)} \lim_{t\to\infty} e^{-\mu t} \|x(t)\|_\mu = 0.
\end{aligned}$$

Then we differentiate the equation for h

$$D_{x_s} h^s = -\int_t^{\infty} e^{(t-\tau)A} D_x g(x(\tau))_u D_{x_s} x(\tau) d\tau$$

This integral converges uniformly, since $D_{x_s} x$ is bounded by the Continous Dependence on Parameters Theorem and

$$D_{x_s} h^s(0) = \lim_{t\to\infty} D_{x_s} x_u(t) = 0$$

by the estimate

$$\|D_{x_s}h^s(0)\| = \lim_{t\to\infty} D_{x_s}x_u(t) \le \lim_{t\to\infty} C_u e^{-\mu t}\int_t^\infty e^{(\sigma+\mu)(t-\tau)}e^{\mu\tau}\|x(\tau)\|\|D_{x_s}x(\tau)\|d\tau$$
$$\le \frac{C}{(\sigma+\mu)}\lim_{t\to\infty} e^{-\mu t}\|x(t)\|_\mu = 0.$$

To prove (2) we consider the integral equation (4.3). If $x(t_0)\in W^s$ then

$$x_u(t_0) = -\int_{t_0}^\infty e^{(t-\tau)A}g(x(\tau))_u d\tau,$$

and $x_s(t_0) = x_s$. Solving the equations for $x_u(t)$ and $x_s(t)$ with this initial data, we get

$$x_s(t) = e^{(t-t_0)A}x_s + \int_{t_0}^t e^{(t-\tau)A}g(x(\tau))_s d\tau \tag{4.5}$$

$$x_u(t) = -\int_t^\infty e^{(t-\tau)A}g(x(\tau))_u d\tau. \tag{4.6}$$

However, adding the two equations (4.5) and (4.6) and setting $t_0 = 0$, gives the equation (4.3) that characterizes W^s so $x(t)\in W^s$ for $t\ge 0$.

The property (3) is proven by an estimate. If we write the original ODE in integral form then

$$x(t) = e^{(t-t_0)A}x_u(t_0) + \int_{t_0}^t e^{(t-\tau)A}g(x(\tau))_u d\tau + e^{(t-t_0)A}x_s(t_0) + \int_{t_0}^t e^{(t-\tau)A}g(x(\tau))_s d\tau.$$

We let σ' be the smallest positive real part of the eigenvalues of A, σ is the largest positive real part of the eigenvalues of A as above. Now by the triangle inequality and the estimates (4.1) and (4.2)

$$\begin{aligned}
\|x(t)\| &\ge C_u e^{\sigma'(t-t_0)}\|x_u(t_0)\| - C_u\varepsilon e^{-\mu t}\int_{t_0}^t e^{(\sigma+\mu)(t-\tau)}e^{\mu\tau}\|x(\tau)\|)d\tau \\
&- C_s e^{-\rho(t-t_0)}\|x_s(t_0)\| - C_s\varepsilon e^{-\mu t}\int_{t_0}^t e^{-(\rho-\mu)(t-\tau)}e^{\mu\tau}\|x(\tau))\|d\tau \\
&\ge C_u(e^{\sigma'(t-t_0)}\|x_u(t_0)\| - e^{-\mu t}\frac{\varepsilon}{(\sigma+\mu)}\|x(t)\|_\mu) - C_s(e^{-\rho(t-t_0)}\|x_s(t_0)\| \\
&+ \frac{\varepsilon}{(\rho-\mu)}e^{-\mu t}\|x(t)\|_\mu) \ge \delta,
\end{aligned}$$

for $t-t_0$ sufficiently large. This shows that if $x_u(t_0)\neq 0$ so $x(t_0)\notin W^s$ then $x(t)$ must leave a neighborhood of the origin at some time $t_1\ge t_0$ and stay out for $t\ge t_1$. **QED**

How do we compute the stable and the unstable manifolds? We derive an equation for h^s (and h^u) and approximate these function by quadradic and higher Taylor polynomials. The equations can be written as

$$\begin{aligned} \dot{x} &= Ax + f(x,y), \quad x \in E^s \\ \dot{y} &= By + g(x,y), \quad y \in E^u. \end{aligned}$$

Now we substitute in $y = h^s$, by the chain rule

$$D_x h^s \dot{x} = By + g(x, h^s)$$

or

$$Dh(Ax + f(x,h)) = Bh(x) + g(x,h)$$

where we dropped the superscript and all functions are functions of x only. This is the equation satisfied by $h^s(x)$, similarly $h^u(y)$ satisfies the equation

$$Dh(By + g(h,y) = Ah + f(h,y).$$

Example 4.1

$$\frac{d}{dt}\begin{pmatrix} x_1 \\ x_2 \end{pmatrix} = \begin{pmatrix} -1 & 0 \\ 0 & 1 \end{pmatrix}\begin{pmatrix} x_1 \\ x_2 \end{pmatrix} + \begin{pmatrix} -x_2^2 \\ x_1^2 \end{pmatrix}$$

$$\begin{aligned} \dot{x} &= -x - y^2 \qquad A = -1 \\ \dot{y} &= y + x^2 \qquad B = 1 \end{aligned}$$

We want to find the function $h^s : E_s \to E_u$ whose graph is the stable manifold W^s. h^s satisfies the equation

$$Dh(Ax + f(x,h)) = Bh + g(x,h)$$

or in our case

$$h'(-x - h^2) = h + x^2.$$

We look for a solution that is a power series in x

$$h(x) = ax^2 + bx^3 + \cdots$$

where a and b are unknown coefficients to be determined,

$$h'(x) = 2ax + 3bx^2 + \cdots.$$

Substituting h and h' into the equation above we obtain

$$(2ax+3bx^2+\cdots)(-x-(ax^2+bx^3+\cdots)^2)=ax^2+bx^3+\cdots+x^2$$

or

$$-2ax^2-3bx^3+\cdots=(a+1)x^2+bx^3+\cdots.$$

Equating coefficients gives

$$\begin{aligned} -2a &= a+1, \qquad & a &= -1/3 \\ -3b &= b, \qquad & b &= 0. \end{aligned}$$

Thus

$$h^s(x)=\frac{-x^2}{3}+O(x^4).$$

Exercise 4.1

1. *Find the linear and nonlinear stable and unstable manifolds of the hyperbolic stationary solutions of the Duffing equations,*

$$\ddot{x}\pm(x-x^3)=0,$$

   and draw them. What difference do the $\pm$ signatures make?

2. *Find the stable and unstable manifolds of the hyperbolic stationary solution at the origin for the system*

$$\frac{d}{dt}\begin{pmatrix}x\\y\end{pmatrix}=\begin{pmatrix}1&0\\0&-1\end{pmatrix}\begin{pmatrix}x\\y\end{pmatrix}+\begin{pmatrix}-y^3\\x^3\end{pmatrix}$$

Chapter 5

Chaotic Dynamics

5.1 Maps and Diffeomorphisms

We have already discussed in Definition 2.7 the time-T map of a flow which is a C^{k+1} diffeomorphism if the flow is invertible and the vector field a C^k function. Now we consider general C^k diffeomorphisms and their connections to flows.

Definition 5.1 *A map*

$$x_{m+1} = f(x_m), \quad x_m \in \mathbb{R}^n,\ m \in \mathbb{Z} \tag{5.1}$$

is a C^k diffeomorphism if $f : \mathbb{R}^n \longrightarrow \mathbb{R}^n$ is a C^k diffeomorphism.

The orbit of the map $\{x_m\} \subset \mathbb{R}^n$ is now a sequence generated by composing the function f with itself. We will use the shorthand

$$f^m(x) = f \circ f \circ \cdots \circ f \quad (\text{m times}).$$

Maps have their local existence theory analogous to the ODE theory in Chapter I and a linear theory analogous to the theory of linear ODE's. We will not review this theory here. A nice account of the theory of linear ODE's can be found in Perko [17] Chapter 1.

We will use diffeomorphism as a tool to understand flows (one can also use flows as a tool to understand diffeomorphisms) and in particular, we are interested in the analog for maps of stationary solutions of ODE's and their stability.

Definition 5.2 *$\bar{x}$ is called a fixed point of a map (5.1) if $f(\bar{x}) = \bar{x}$. x^* is a periodic point of period m if $f^{m+1}(x^*) = x^*$.*

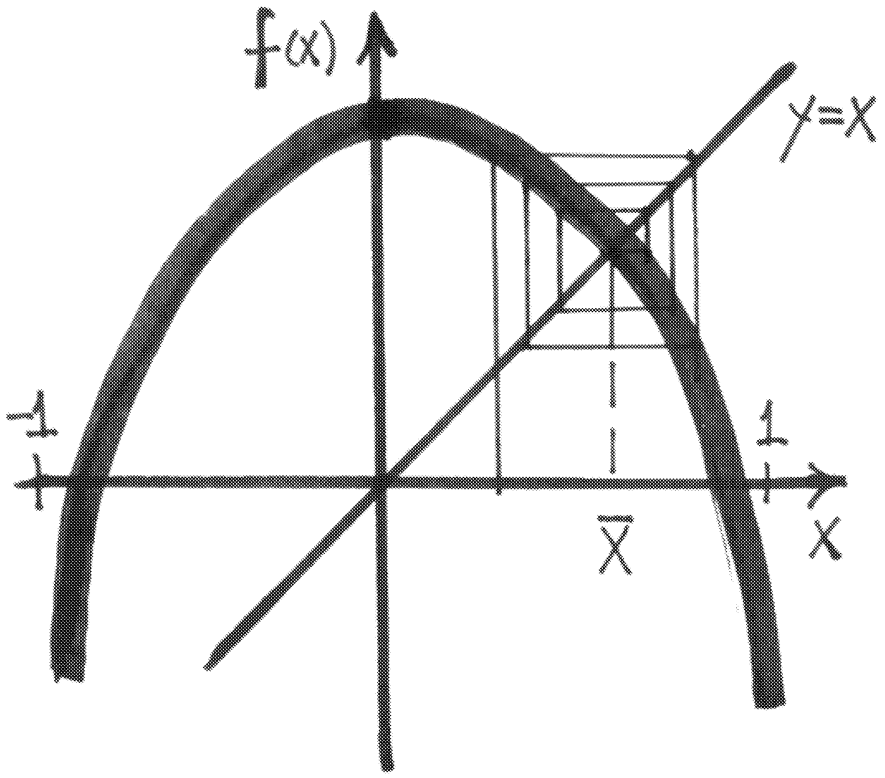

Figure 5.1: The Quadradic Map

Example 5.1 *Consider the quadratic map*

$$x_{m+1} = f(x_m)$$

where

$$f(x) = 1 - \mu x^2,$$

see Figure 5.1. This map has two fixed points where the graph of f meets the line $y = x$ and since one of these points has slope less than one, it is stable. The other has slope greater than one and is unstable, see below.

Definition 5.3 *An orbit $\{x_m\}$ of a map (5.1) is stable if for $\varepsilon > 0$, there exists $\delta > 0$, such that*

$$\|x_0 - y_0\| < \delta \Rightarrow \|x_m - y_m\| < \varepsilon, \quad m \geq 1.$$

$\{x_m\}$ is asymptotically stable if

$$\lim_{m\to\infty} y_m = x_m.$$

Stability can be proven by a Lyapunov function but we are mostly interested in fixed points and periodic orbits which are hyperbolic. Consider the map (5.1) linearized about a fixed point $\bar{x}$,

$$x_{m+1} - \bar{x} = Df(\bar{x})(x_m - \bar{x})$$

then the stability of $\bar{x}$ is given by the following lemma.

Lemma 5.1 *If $|\lambda| < 1$ for all $\lambda \in \sigma(Df(\bar{x}))$ then $\bar{x}$ is (asymptotically) stable. If $|\lambda| > 1$ for some $\lambda \in \sigma(Df(\bar{x}))$ then $\bar{x}$ is unstable.*

Here $\sigma(Df(\bar{x}))$ denotes the spectrum of f linearized about the fixed point $\bar{x}$.

Proof: By the Mean-Value Theorem

$$x_m - y_m = \int_0^1 Df\,(sx_{m-1} + (1-s)y_{m-1})\,ds \cdot (x_{m-1} - y_{m-1}).$$

Thus if $x_m = \bar{x}$ and $\|\bar{x} - y_m\| < \delta$, then $\|\bar{x} - y_m\| \leq (\max|\lambda| + \eta)\|\bar{x} - y_{m-1}\|$, where η can be made arbitrarily small by making δ sufficiently small. Now iteration gives $\|\bar{x} - y_m\| \leq (\max|\lambda| + \eta)^m \|x_0 - y_0\|$. If $\max|\lambda| < 1$ then

$$\lim_{m\to\infty} y_m = \bar{x}.$$

If there exists an eigenvalue $|\lambda| > 1$ then we can pick $\bar{x} - y_0$ to be the corresponding eigenvector. Then

$$\bar{x} - y_1 = \int_0^1 Df(s\bar{x} + (1-s)y_0)\, ds \cdot (\bar{x} - y_0),$$

by the mean value theorem and

$$\|\bar{x} - y_1\| \geq (|\lambda| - \eta)\|\bar{x} - y_0\|,$$

where η is small. An iteration gives

$$\|\bar{x} - y_m\| \geq (|\lambda| - \eta^*)^m \|\bar{x} - y_0\|,$$

where η^* is still small. This shows that $\{y_m\}$ diverges from $\bar{x}$. **QED**

If x^* is a periodic orbit of period m then we get the criteria,

Corollary 5.1 *If $|\lambda| < 1$ for all $\lambda \in \sigma(Df^m(x^*))$ then x^* is (asymptotically) stable. If $|\lambda| > 1$ for some $\lambda \in \sigma(Df^m(x^*))$ then x^* is unstable.*

Invariant sets for maps are defined in the same way as those for flows in Chapter 1. As for ODE's we are interested in conjugacy classes of maps.

Definition 5.4 *Two maps f and g are topologically conjugate if*

$$h \circ g = f \circ h$$

where h is a homeomorphism.

Lemma 5.2 *Suppose $f : \mathbb{R} \to \mathbb{R}$ is a diffeomorphism and $Df(x) > 0$ for some $x \in \mathbb{R}$. Then the map $x_{m+1} = f(x_m)$ is topologically conjugate to the time-1 ($T = 1$) map of the flow φ_t defined by $\dot{x} = f(x) - x$.*

Proof: Since f is a diffeomorphism and $Df(x) > 0$ for some x, it follows that $Df(x) > 0$ for all $x \in \mathbb{R}$. Consider the graph of f and its intersections with the line $y = x$ in Figure 5.1. The fixed points of the map $\bar{x}_i = f(\bar{x}_i)$ are clearly equal to the stationary solutions of the ODE

$$\dot{x}_i = f(\bar{x}_i) - \bar{x}_i = 0.$$

Moreover the orientation or the direction in which the points map or flow is the same for the map and the flow in each subinterval $[\bar{x}_i, \bar{x}_{i+1}]$. This is because sign

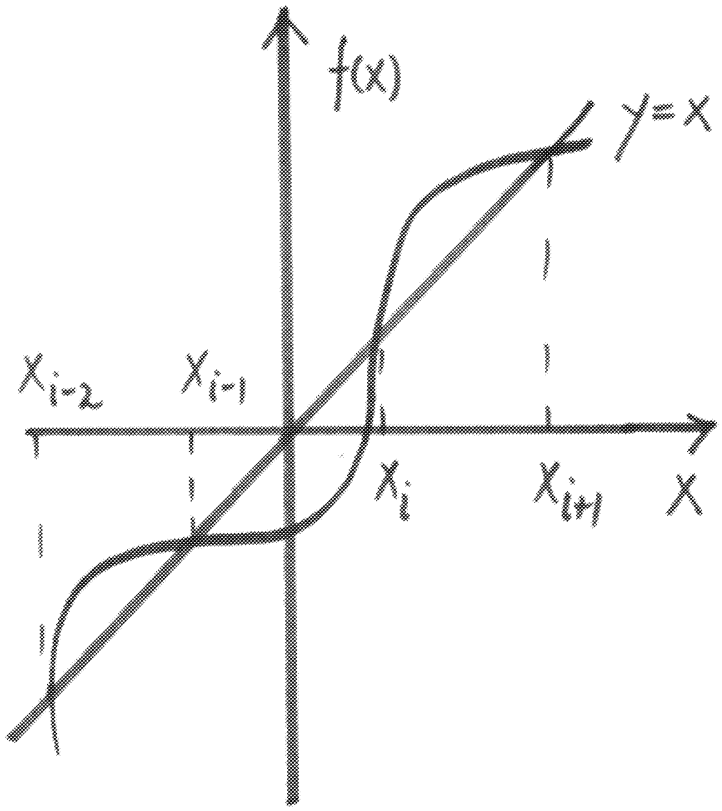

Figure 5.2: The graph of the function $f(x)$ and the line $y = x$.

$[x_{m+1}-x_m] = \text{sign}\,[f(x_m)-x_m] = \text{sign}\,\dot{x}$. Now let $x_0 \in (\overline{x}_i, \overline{x}_{i+1})$ be any point and define the intervals

$$f : [P_m, P_{m+1}] \longrightarrow [P_{m+1}, P_{m+2}]$$

where $P_n = f^n(x_0)$ and

$$\varphi_1 : [Q_m, Q_{m+1}] \longrightarrow [Q_{m+1}, Q_{m+2}]$$

where $Q_m = \varphi_m(x_0)$. Both f and φ_1 move the intervals in the same direction. We want to construct a homeomorphism taking the orbits of φ onto the orbits of f. First we construct a homeomorphism taking $[Q_0, Q_1]$ onto $[P_0, P_1]$. There are many ways of doing this but we will pick the simplest and let

$$h_0(y) = x_0 + \left[\frac{f(x_0)-x_0}{\varphi_1(y_0)-y_0}\right][y-y_0].$$

Now clearly $h(y_0) = P_0$ and $h(y_1) = h(\varphi(y_0)) = f(x_0) = P_1$, so $h[Q_0] = P_0$ and $h[Q_1] = P_1$. Moreover, h is monotone (linear) and thus maps $[Q_0, Q_1]$ onto $[P_0, P_1]$ in a one to one and invertible fashion. For the mth intervals we simply define

$$h_m(y) = f^m \circ h_0 \circ \varphi_{-m}(y).$$

In other words h_m pulls $[Q_m, Q_{m+1}]$ back to $[Q_0, Q_1]$ by φ_{-m}, maps it to $[P_0, P_1]$ by h_0 and h_m moves it forward to $[P_m, P_{m+1}]$ by f^m. The desired homeomorphism is then

$$h(y) = \begin{cases} \overline{x}_i & \text{for } y = \overline{x}_i \\ h_m(y) & \text{for } y \in (Q_m, Q_{m+1}) \\ \overline{x}_{i+1} & \text{for } y = \overline{x}_{i+1}. \end{cases}$$

Finally, we check that h has the right property,

$$\begin{aligned} h \circ \varphi_1 &= h_m \circ \varphi_1 = f^m \circ h_0 \circ \varphi_{-m} \circ \varphi_1 \\ &= f \circ f^{m-1} \circ h \circ \varphi_{-(m-1)} = f \circ h. \end{aligned}$$

QED

If two maps are topologically conjugate they are said to be of the same topological type. One has to construct a homeomorphism between them to show that two maps are conjugate. It is on the other hand frequently easier to show that two maps are not topologically conjugate for example if they have a different number of fixed point (and periodic orbits) then they must belong to different conjugacy classes. The argument is simply that otherwise a non-trivial orbit gets mapped onto a fixed point by a homeomorphism and this is impossible.

5.2 Classification of Flows and Maps

We can now give a complete local classification of flows and maps up to topological conjugacy. By the Hartmann-Grobmann Theorem, see Hartman [12], a nonlinear system

$$\dot{x} = f(x)$$

is topologically conjugate to its linearization

$$\dot{y} = Df(x)y, \quad y = x - \bar{x},$$

at a hyperbolic stationary solution $\bar{x}$. Then the Rectification Theorem 3.2, see Arnold [2], says that the flow on the linear unstable manifold E^u and the linear stable manifold E^s are topologically equivalent to the flows of

$$\dot{x}_u = x_u, \text{ and } \dot{x}_s = -x_s$$

respectively, where $x_u = p_u \circ x$ and $x_s = p_s \circ x$ denote the projections onto E^u and E^s. This proves the following theorem.

Theorem 5.1 *The flow of the system*

$$\dot{x} = f(x)$$

at a hyperbolic stationary solution $\bar{x}$ is topologically conjugate to the flow of

$$\dot{x} = \begin{pmatrix} I_u & 0 \\ 0 & -I_s \end{pmatrix} x$$

in a neighborhood of the origin, where rank $I_u = \dim E^u$ and rank $I_s = \dim E^s$.

This means that we only have to count the different configurations with respect to the imaginary axis that n eigenvalues can have, to make a complete list of the local topological conjugacy classes at a hyperbolic stationary solutions in n dimensions. This count is easy, just place all n eigenvalues in the right half plane and then move one at a time over to the left half plane to get $n+1$ configurations. Thus there are $n+1$ different local conjugacy classes of flows at a hyperbolic stationary solution.

The discussion is similar for maps. The map

$$x_{m+1} = f(x_m), \quad m \in \mathbb{Z},$$

is topologically conjugate to its linearization

$$y_{m+1} = Df(x)y_m, \quad y_m = x_m - \overline{x}$$

at a hyperbolic fixed point. Now if we decompose $Df(x)$ into two matricies, U with eigenvalues inside and S with eigenvalues outside the unit circle, then U (or S) is orientation-preserving if $\det U > 0$ and orientation-reversing if $\det U < 0$. Recall that the eigenvalues come in conjugate pairs because $f(x_m)$ is real. Then the Hartmann-Grobmann Theorem, see Hartman [12], proves the following theorem.

Theorem 5.2 *The nonlinear map*

$$x_{m+1} = f(x_m), \quad m \in \mathbb{Z}$$

is topologically conjugate at a hyperbolic fixed point to the map

$$y_{m+1} = \begin{pmatrix} U & 0 \\ 0 & S \end{pmatrix} y_m$$

where $\lambda \in \sigma(U) \Longrightarrow |\lambda| > 1$, $\lambda \in \sigma(S) \Longrightarrow |\lambda| < 1$, *rank* $U = \dim E^u$, *rank* $S = \dim E^s$ *and* U *and* S *are either orientation-preserving or orientation-reversing.*

Now we count how many local conjugacy classes there are for maps. Two maps are topologically conjugate at a hyperbolic fixed point if and only if rank $U_1 =$ rank U_2, rank $S_1 =$ rank S_2 and the orientation of U_1 and U_2 and respectively S_1 and S_2 are the same. This means that we just have to count in how many ways we can configure n eigenvalues with respect to the unit circle. That is $n+1$ configurations as above. However, only $n-1$ of those have 4 orientation namely $++$, $+-$, $-+$ and $--$, where the first signature refers to $\det U$ and the second to $\det S$. Two configurations have only two possible signature, the eigenvalues are all inside the unit circle, $U = 0$, and all outside $S = 0$. This gives

$$4(n-1) + 2 \cdot 2 = 4n$$

local equivalence classes for maps in n dimensions. We now consider the one-dimensional case to explain and then prove the converse of the statement above. There are four possible positions of the eigenvalues with respect to the unit circle and positive and negative real axis. These are illustrated in Figure 5.2, the first two corresponding maps, on Figure 5.2, are orientation preserving the last two are orientation reversing. Now if the signatures of $\det U_1$ and $\det U_2$ are different, then U_1 has a different number of (generalized) eigenvectors along which the map looks like case 1 (and case 4) and they are not topologically conjugate.

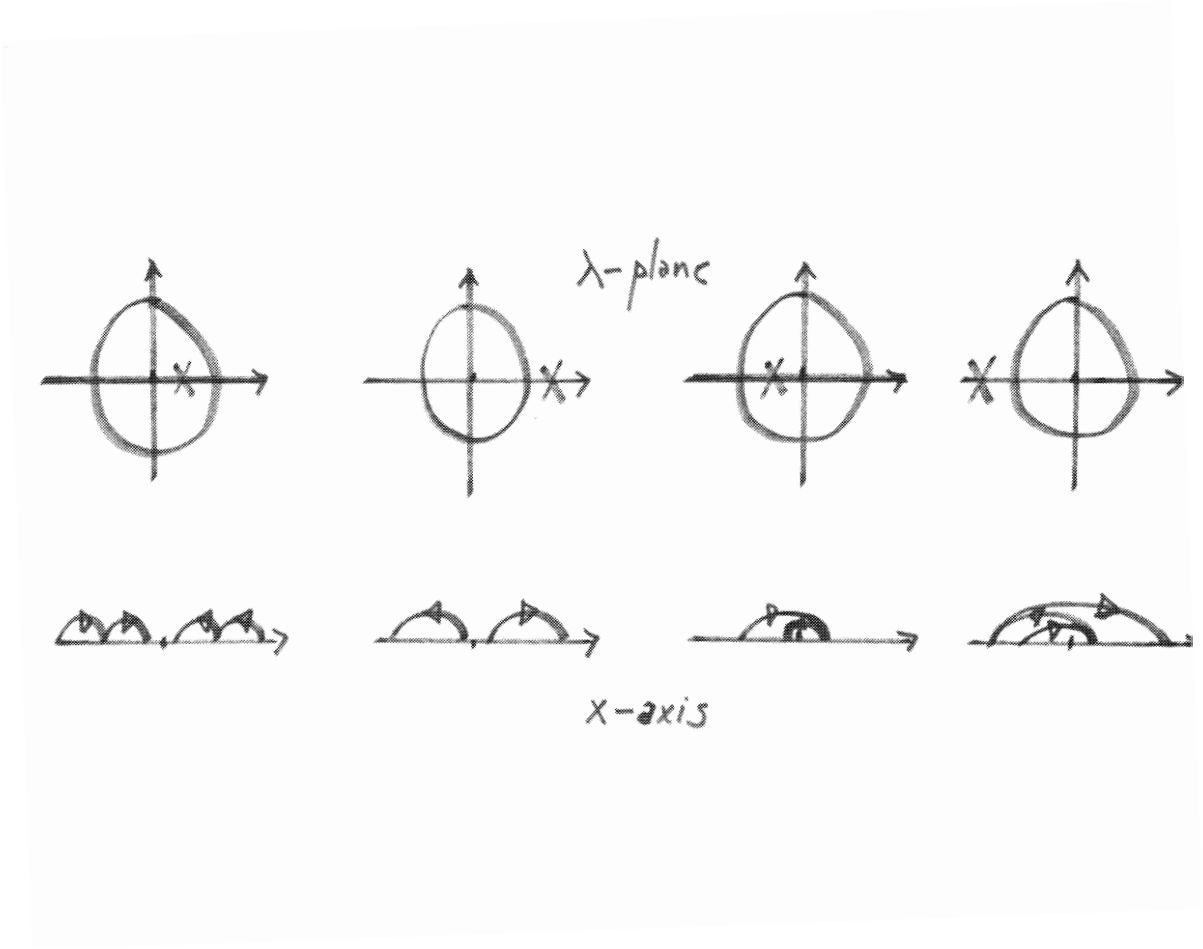

Figure 5.3: The positions of the eigenvalues and the corresponding motion of the iterates of a one-dimensional map in phase space. The first two maps are orientation preserving and the last two orientation reversing.

Exercise 5.1 *Draw the eigenvalue configurations and map phase portrait for the 8 two-dimensional cases.*

5.3 Horseshoe Maps and Symbolic Dynamics

The canonial example of a diffeomorphism with a complex invariant set is the horseshoe map invented by Steven Smale. Consider the square $S = \{(x,y)|\ |x|,|y| \leq 1\}$ and the map that consist of the following two acts:

1. Stretch S in the x- direction and compress it in the y- direction such as to map S onto the horizontal rectangle

$$R = \{(x,y)|\ |x| \leq 5,\ |y| \leq 1/5\}.$$

2. Bend R into a horseshoe and place it on top of S so that the intersection of S and the horseshoe consists of two horizontal rectangles H_0 and H_1, see Figure 2.

Heuristically, the stretching and compressing accounts for the hyperbolic part of the map and the bending makes it nonlinear. Notice that the preimages of H_0 and H_1 are vertical strips V_0 and V_1 and now we define the horseshoe map on S,

$$f(S) \cap S = H_0 \cup H_1$$

to be those two steps. In particular,

$$f(V_j) = H_j, \quad j = 0,1.$$

The precise form of the map on $S \setminus V_0 \cup V_1$ is not crucial, it is linear on $V_j,\ j = 0,1$. We take it to be as in Figure 2 and this becomes important when we embed the map later in the sphere. The image of $H_j,\ j = 0,1$, in S, consists of four horizontal strips $H_{jk},\ j,k = 0,1$, see Figure 5.3. In general, the image of $H^n = f(H^{n-1}) \cap S,\ H^0 = H_0 \cup H_1$ consists of 2^n horizontal strips which are contained in H_0 and H_1. The width of these strips is $\leq 1/5^n \longrightarrow 0$ as $n \longrightarrow \infty$. Thus the intersection of all of these strips $\bigcap_{n\in\mathbb{Z}^+} H^n$ is the product of the interval [0,1] and a Cantor set.

The inverse map similarly defines vertical strips, see Figure 5.3. f^{-1} is really only defined on the horizontal strips $H_0 \cup H_1$, but we define

$$V^0 = V_0 \cup V_1 = f^{-1}(H_0 \cup H_1)$$

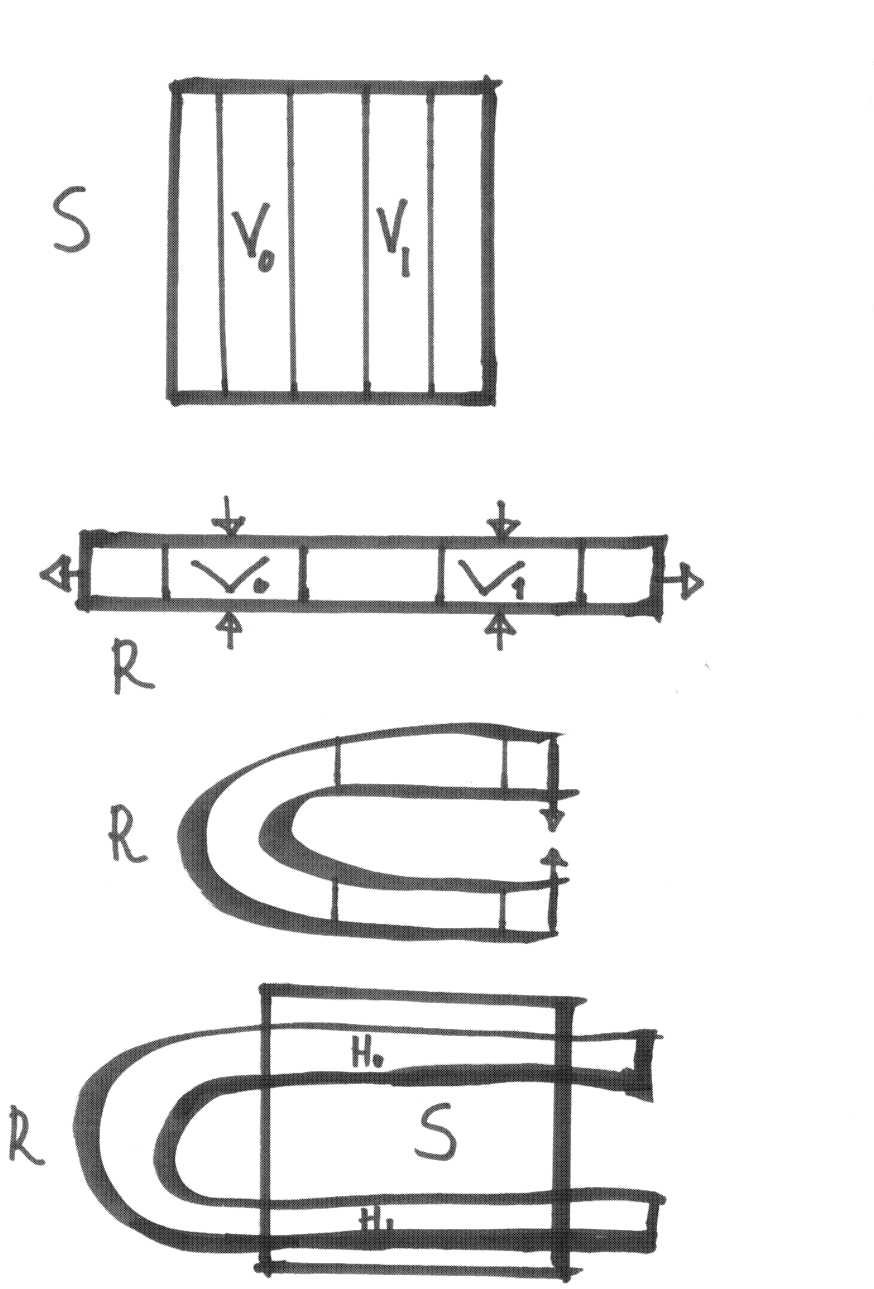

Figure 5.4: The Horseshoe Map consists of stretching the square in the x direction, compressing it in the y direction, bending the resulting rectangle into a horseshoe and intersecting the horseshoe with the original square

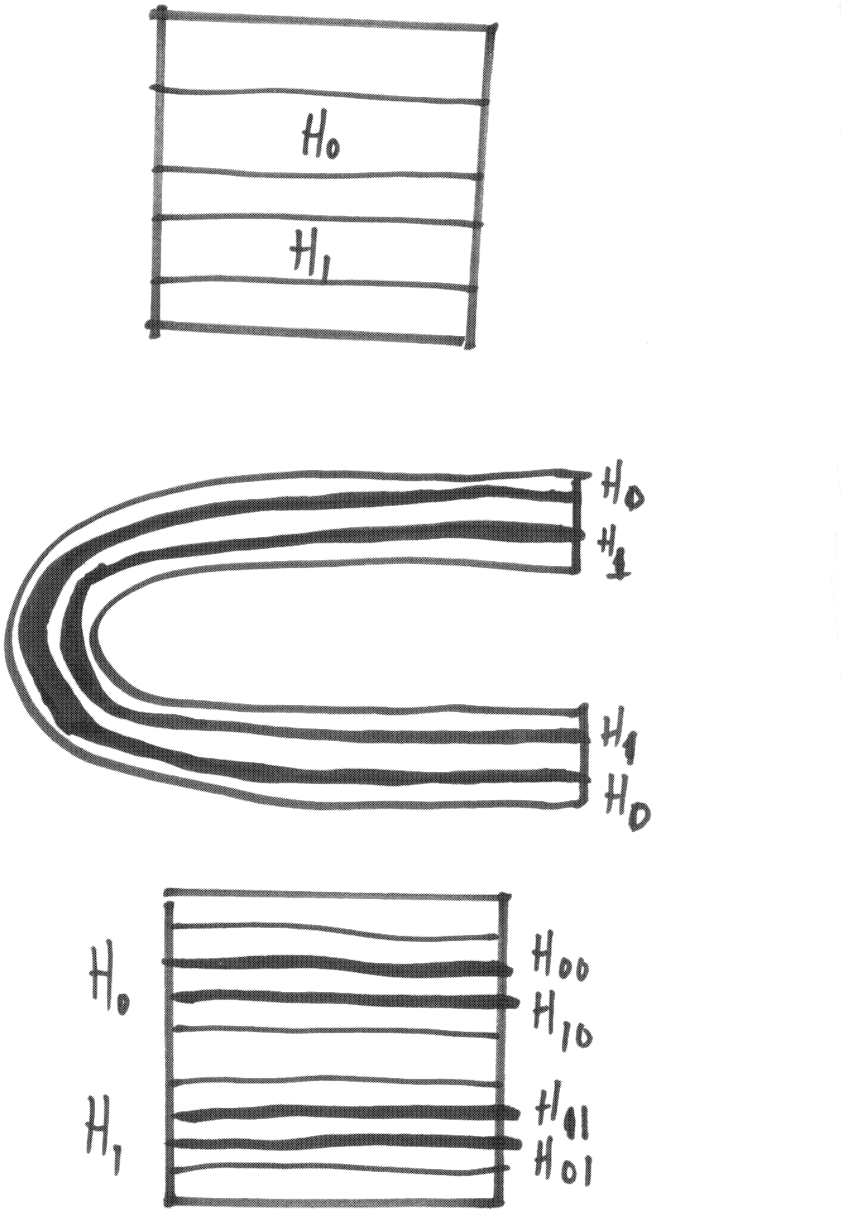

Figure 5.5: The map of the first two horizontal strips consists of four horizontal strips.

and then define

$$V^n = f^{-1}(V^{(n-1)}) \cap S, \quad n \in \mathbb{Z}^+,$$

so that f^{-1} stretches in the y direction and compresses in the x analogously to f, see Figure 5.3. This gives 2^n vertical strips of width $1/5^n$. $\bigcap_{n\in\mathbb{Z}^+} V^n$ is now a product of a Cantor set with the y-interval $[0,1]$ and we define the *Smale horseshoe* to be

$$\Lambda = \bigcap_{n\in\mathbb{Z}^+} H^n \cap \bigcap_{n\in\mathbb{Z}^+} V^n = \bigcap_{n\in\mathbb{Z}} f^n(H_0 \cup H_1).$$

The intersection of the first four vertical and horizontal strips in shown in Figure 5.3.

Lemma 5.3 *The Smale horseshoe is invariant with respect to f and f^{-1}.*

Proof: We show that $f(\Lambda) \subset \Lambda$, let $x \in f(\Lambda)$ then $x \in f(H^n)$ and $x \in f(V^n)$, for all n. Now $f(H^n) \cap f(V^n) \subset S$, compare Figure 5.3. Thus $x \in f(H^n) \cap S = H^{n+1}$ and $x \in f(V^n) \cap S = V^{n-1}$, for all n. This shows that $x \in \Lambda$. f^{-1} is similar. **QED**

We now establish the relationship of the horseshoe map and symbolic dynamics. Consider the space Σ of binfinite sequences of two symbols $\{0,1\}$. $\sigma \in \Sigma$ is a sequence of zeroes and ones infinite in both directions

$$\sigma = (\cdots, 1, 0, 1, 1, 1, 0, 0, 1, 0, \cdots).$$

We will denote $\sigma = (\sigma_j), \quad j \in \mathbb{Z}$, where $\sigma_j = 0, 1$, and we will be interested in two operations on Σ. The left shift $\alpha : \Sigma \longrightarrow \Sigma$, $\alpha\sigma = (\sigma_{j-1}), \quad j \in \mathbb{Z}$, and the right shift $\beta : \Sigma \longrightarrow \Sigma$, $\beta\sigma = (\sigma_{j+1}), \quad j \in \mathbb{Z}$. Now recall the construction of the horizontal strips in Figure 5.3. We denoted the upper strip H_0 and lower strip H_1. If a point x sits in upper strip we will let $\sigma_0 = 0$, if it sits in the lower strip we will let $\sigma_0 = 1$. Of course this does not give a very precise location of x. The second iterate gave four horizontal strips. The ones that originated with H_0 we gave the first subscript 0. If strips ended up in H_0 they got the second subscript 0, if they ended up in H_1, they got the second subscript 1. Accordingly, $\sigma_1 = 0$ if $x \in H_0$, $\sigma_1 = 1$ if $x \in H_1$, and we get the strips, $H_{\sigma_0\sigma_1}, \quad \sigma_j = 0, 1, \quad j = 0, 1$. Now the labelling is clear, the nth iterate of $H_0 \cup H_1$ gives $H_{\sigma_0\cdots\sigma_n}, \quad \sigma_j = 0, 1$, and $\sigma_j = 0$ indicates that x lies in the strip that ended up in H_0 under the jth iterate, whereas $\sigma_j = 1$ indicates that x lies in the strip that ended up in H_1 under the jth iterate, see Figure 5.3.

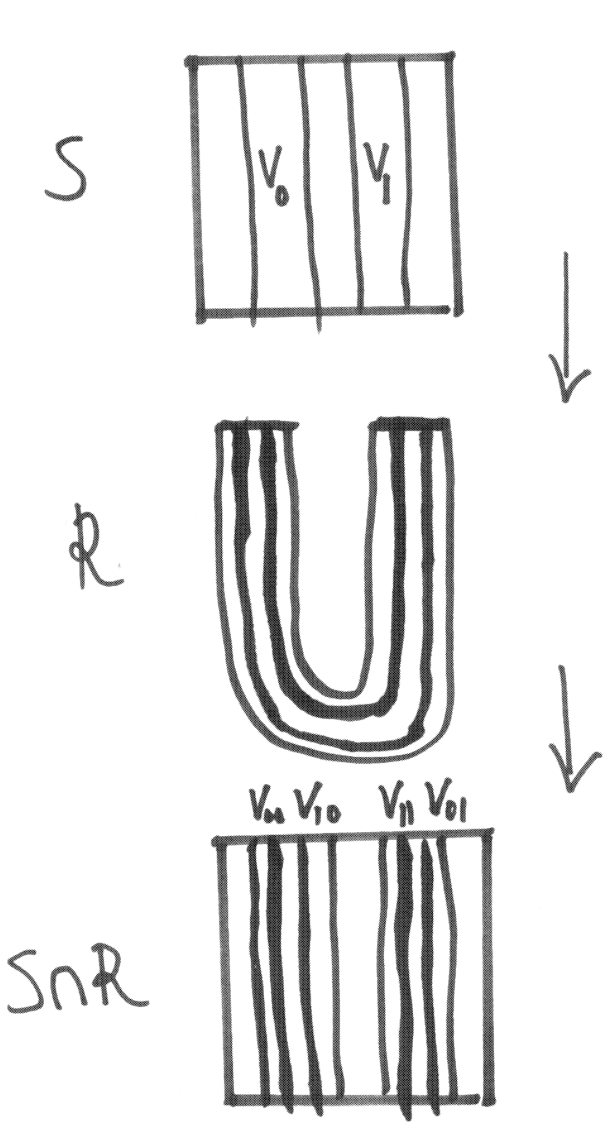

Figure 5.6: The map of the first two vertical strips consists of four vertical strips.

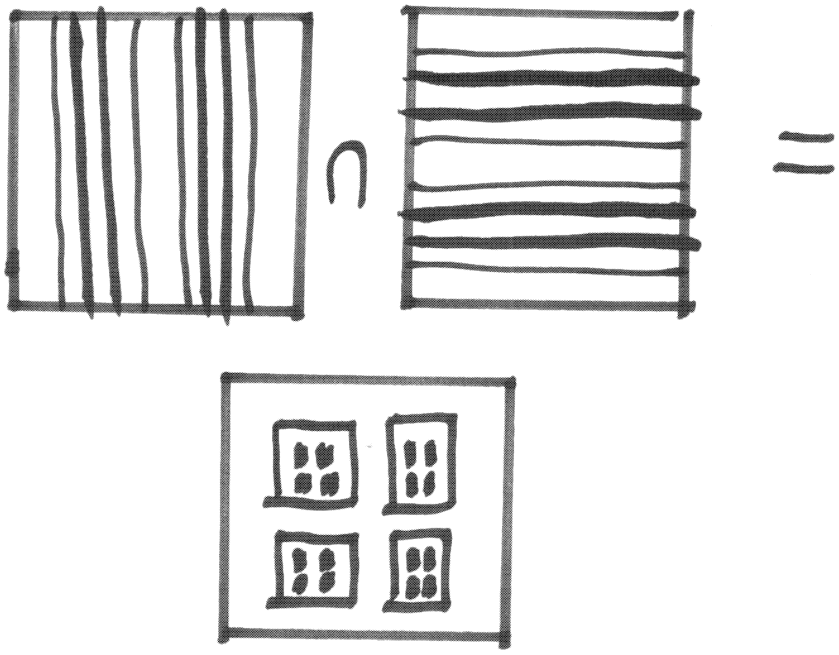

Figure 5.7: The horseshoe is the intersection of the vertical and horizontal strips.

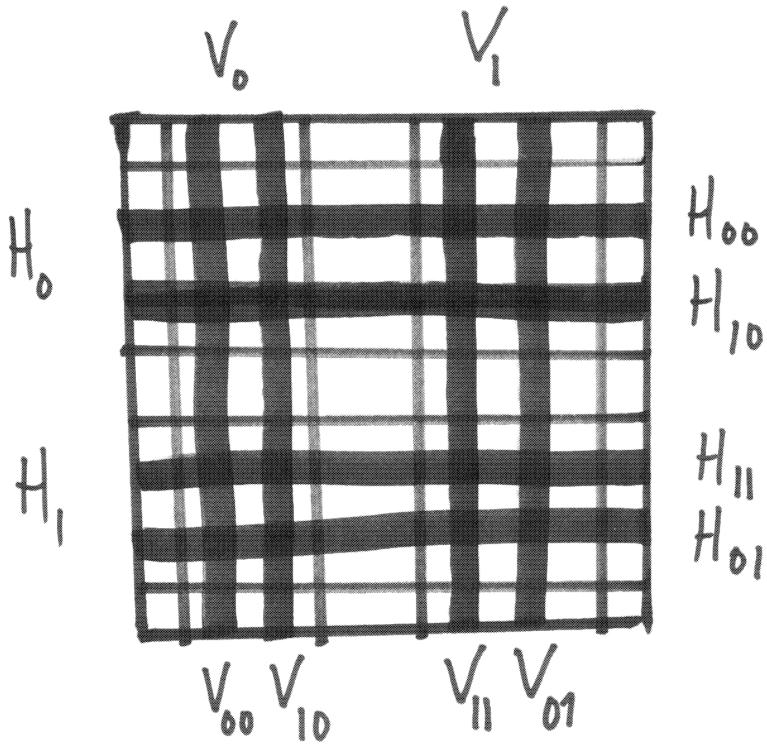

Figure 5.8: The Smale Horseshoe lies with in the 16 squares that are labeled according to which horizontal and vertical strips they came from.

But these strips are nested $H^0 \supset H^1 \supset \cdots \supset H^n$ and the forward symbol sequence

$$(\sigma_0, \sigma_1, \sigma_2, \cdots)$$

restricts x to lie in a unique line $H_{\sigma_0\sigma_1\cdots}$ of the horizontal Cartesian product of a line with a Cantor set. This is because a nested sequence of strips contains a unique line. Moreover, we can repeat this labelling with the backward sequence

$$(\cdots, \sigma_{-n}, \cdots, \sigma_{-2}, \sigma_{-1})$$

and the vertical strips $V_{\sigma_{-1}\cdots\sigma_{-j}}$. Then the sequence segment

$$(\sigma_{-(j+1)}, \cdots, \sigma_{-1}, \sigma_0, \cdots, \sigma_j)$$

restricts x to lie in the rectangle $V_{\sigma_{-1}\cdots\sigma_{-(j+1)}} \cap H_{\sigma_0\cdots\sigma_j}$ and since these rectangles are also nested and $V_{\sigma_{-1}\cdots} \cap H_{\sigma_0\cdots}$ contains only one point, there is a 1:1 correspondence between the points $x \in \Lambda$ and the biinfinite sequences $\sigma \in \Sigma$. This proves the following lemma.

Lemma 5.4 *The map* $h : \Lambda \longrightarrow \Sigma,\ h(x) = \sigma$ *is* $1:1$ *and onto.*

We will prove later on that this map is a homeomorphism, but if we take this to be the case for the time being we get,

Lemma 5.5 *The horseshoe map* $f : \Lambda \longrightarrow \Lambda$ *is topologically conjugate to shift on two symbols.*

Proof: Consider $\sigma = h(x)$ and suppose $x \in V_{\sigma_{-1}\cdots} \cap H_{\sigma_0\cdots}$. Then $f(x) \in V_{\sigma_{-2}\sigma_{-3}\cdots} \cap H_{\sigma_{-1}\sigma_0\sigma_1\cdots}$ or

$$\begin{aligned} h(f(x)) &= (\cdots \sigma_{-2}, \sigma_{-1}, \sigma_0, \cdots) \\ &= \alpha\sigma, \end{aligned}$$

where α is the left shift. This says that

$$h \circ f = \alpha \circ h.$$

QED

The dynamics on the sequence of two symbols can now be used to give a complete description of the dynamics on the horseshoe.

Fact 5.1 *There are infinitely many periodic orbits of all periods in* Λ.

Just consider the sequences $\sigma = (\sigma_j),\ \sigma_j = 0$ and $\sigma = (\sigma_j),\ \sigma_j = 1$. These correspond to fixed points of f on Λ, by the topological conjugacy, since $\alpha\sigma = \sigma$ where α is the left shift on Σ. Then consider $\sigma = (\sigma_j),\ \sigma_j = 0$, if j is even, $\sigma_j = 1$ if j is odd. This is a periodic orbit of period 1, $\alpha^2\sigma = \sigma$, and there is another one namely $\sigma_j = 1$, if j is even, $\sigma_j = 0$ if j is odd. Thus Λ has exactly two orbits of period 1 under f. Next we can make a periodic orbit out of a segment of length three say 011, it is

$$\sigma = (\cdots, 0, 1, 1, 0, 1, 1, 0, 1, 1, 0, 1, 1, \cdots)$$

and there are $8 = 2^3$ such because we have choice of two symbols for each σ_j, $j = 0, 1, 2$. However, this counts the fixed points (but not the periodic orbits) above so there are $6 = 8 - 2$ periodic orbits of genuine period 2. It is clear that by taking a segment of length 4 etc, we can construct periodic orbits of any period and count them all.

Fact 5.2 *There exist aperiodic orbits.*

This is an easy construction. Take a segment of lenght n add a segment of lenght $2n$ which is not two copies of the preceeding one then repeat this process in both forward and backward direction to get an aperiodic orbit.

A Metric

Now we define a *metric* on the space of sequences

$$\|\sigma_1 - \sigma_2\|^2 = \sum_{j=-\infty}^{\infty} (\sigma_j^1 - \sigma_j^2)^2 / 2^{|j|}.$$

Fact 5.3 *The periodic orbits are dense in* Σ.

Exercise 5.2 *Verify Fact 5.3.*

Fact 5.4 *The left shift has an orbit which is dense in* Λ.

We construct the dense orbit in the following manner. First consider all segments of lenght two. There are four such segments $(0,0)$, $(1,1)$, $(0,1)$ and $(1,0)$. We string these segments together and make them the first eights digits $\sigma_{-8} \cdots \sigma_{-1}$ in the negative direction in a sequence σ. σ can have any digits what so ever in

the positive direction. Then we take all segments of lenght three and string them together. They will make the next segment of σ in the negative direction and so on. Thus we get a sequence that contains arbitrarily large centrally located finite segments of any sequence σ_1. Now let $\varepsilon > 0$ then there exist integers N and m such that

$$\|\sigma_1 - \alpha^N \sigma\| = \sum_{|j|>m} (\sigma_j^1 - \sigma_{j-N}^2)^2/2^j \;\leq\; 1/2^{m-1} \;<\; \varepsilon,$$

because the centrally located, i.e. around the zeroth place, segments of σ_1 and $\alpha^N\sigma$, σ shifted left N times, of lenght $2m$ are identical.

Lemma 5.6 *The map $h : \Lambda \longrightarrow \Sigma$, $h(x) = \sigma$ is a homeomorphism.*

The Lemma is proven by the Contraction Mapping Principle, Theorem 2.10, in Moser [16].

Chaos

Fact 5.5 Λ *contains chaotic orbits topologically conjugate to random flips of a coin.*

In other words: Λ contains points the orbits of which under horseshoe map are topologically conjugate to a shift on a *random sequence* of two symbols.

We construct a sequence σ by flipping a unbiased coin, i.e. $\sigma_j = 0$ for heads, $\sigma_j = 1$ for tails, $j \in \mathbb{Z}$. Λ contains a sequence $\{f^n(x)\}$ $n \in \mathbb{Z}$, which is topologically conjugate to σ. This is the *precise mathematical meaning* of a chaotic orbit.

Fact 5.6 Λ *is uncountable and it contains uncountably many aperiodic orbits.*

The sequences σ in Σ are nothing but a binary representation of the real numbers and the real numbers are uncountable. The finite sequences that generate the periodic orbits (of the shifts) in Σ are a binary representation of the *rationals* that are countable. Their uncountable complement the *irrational numbers* are topologically conjugate to aperiodic orbits in Σ.

Example 5.2 *Examples of periodic orbits.*

a A sequence that terminates

$$00001110.1 \sim 1 + \frac{1}{2^2} + \frac{1}{2^3} + \frac{1}{2^4}$$

corresponds to a rational number.

b A sequence that repeats also corresponds to a rational number

$$\cdots 100100100.0 \sim \sum_{j=0} \frac{1}{2^{3j}} - 1 = \frac{1}{1-1/8} - 1 = \frac{8}{7} - 1 = \frac{1}{7}$$

Fact 5.7 *The inset and outset of Λ in the square S are the Cartesian product of the Cantor sets and lines,*

$$in\ (\Lambda) \cap S = \bigcap_{n\in\mathbb{Z}^+} V^n, \quad out\ (\Lambda) \cap S = \bigcap_{n\in\mathbb{Z}^+\cup\{0\}} H^n.$$

Proof: Let $x \in \bigcap_{n\in\mathbb{Z}^+} V^n \diagdown \Lambda$ and consider the contraction of the horizontal strips in Figure 5.3. The map f contracts the horizontal strips onto $\bigcap_{n\in\mathbb{Z}^+\cup\{0\}} H^n$ and since each vertical strip contains points in Λ, $f(x) \in \bigcap_{n\in\mathbb{Z}^+} V^n \cap H^0 \subset S$. This shows that

$$y = \lim_{m\to\infty} f^m(x) \in \bigcap_{n\in\mathbb{Z}^+} V^n \cap \bigcap_{n\in\mathbb{Z}^+\cup\{0\}} H^n = \Lambda$$

or $y \in \Lambda$. Similarly if

$$x \in \bigcap_{n\in\mathbb{Z}+\cup\{0\}} H^n \diagdown \Lambda, \quad \lim_{m\to\infty} f^{-m}(x) \in \Lambda.$$

QED

The points in in(Λ) can be thought of as semi-infinite sequences $\sigma_- = \{\cdots, \sigma_{-1}\}$ by the map h above, similarly points in out(Λ) can be mapped to semi-infinite sequences $\sigma_+ = \{\sigma_0, \sigma_1, \cdots\}$. These sequences get closer and closer (in the norm) to sequences in Σ under the left and right map respectively. Each point in Λ is the intersection of a unique inset and a unique outset line.

Exercise 5.3

1. The sixteen squares on Figure 5.3 that are the intersections of the four horizontal and the four vertical strips contain each an initial point of a periodic sequence of period three.

   (a) Find the symbolic sequence for each of these periodic orbit and show in which square it lies.

(b) How many of these are genuine orbits of period three? What are the others?

(c) Describe how each initial point of a period three orbit moves around some of the sixteen squares under the horseshoe map.

5.4 The Smale-Birkhoff Homoclinic Theorem

Suppose that the phase space of an ODE contains a hyperbolic stationary solution and we add small periodic forcing. Then if there is a correct balance of dissipation and forcing in the system, the associated Poincaré map contains a hyperbolic fixed point with unstable and stable manifolds that have formed a homoclinic tangle, see Figure 1.4. The homoclinic tangle was discovered by Poincaré in 1898 and he used it to prove that the three body problem is not integrable. Roughly speaking his argument was the familiar argument from complex analysis, that if an analytic function has the same values on a sequence in the complex plane converging to a point, then the function must be a constant. Poincaré noticed that the homoclinic tangle has many sequences of points converging to a point and his argument was that any integral that was an analytic function of the phase variables and constant on the sequence had to be trivial. That is to say, the integral had to be the same constant for all points in the phase space. He also pointed out that the dynamics in the homoclinic tangle had to be very complex due to the stretching and contracting close to the hyperbolic point and involved a nonlinear re-injection of the points into the homoclinic tangle.

During the first half of the nineteen century Birkhoff developed the theory further and he was the first one to relate the map to a symbolic sequence. Birkhoff's ideas were then taken up by Steven Smale in the 1950's and 60's. He formulated and studied the horseshoe map and the associated symbolic dynamics. There was however no proof that the horseshoe map could exist in the phase space of a Poincaré map of a flow. This was finally proven in the 1970's by Charles Conley and Jürgen Moser. They found a mathematically rigorous way of expressing Poincaré's observations of a contraction, expansion and nonlinear re-injection in the vicinity of a hyperbolic point of a Poincaré map. The conclusion of their proof was that orbits of real flows of ODEs can exhibit the chaotic behaviour formulated by Birkhoff and Smale.

Conley's and Moser's proof is the culmination of one of the major achivements of 19th century mathematics. It layed the foundation for modern dynamical systems theory along with the work of Birkhoff and Smale and their mathematical

formulation of Poincaré's ideas reappear in the proofs of most important results in dissapative dynamical systems during the last three decades.

Theorem 5.3 *The Birkhoff-Smale Homoclinic Theorem.*

Suppose that a diffeomorphism $P : M \to M$, where M is an n-dimensional manifold, has a hyperbolic fixed point $\bar{x}$, with a stable $W^s(\bar{x})$ and unstable $W^u(\bar{x})$ manifold that intersect transversely at some point $x_o \neq \bar{x}$,

$$W^s(\bar{x}) \perp W^u(\bar{x}), \tag{5.2}$$

where $dimW^s + dimW^u = n$, then M contains a hyperbolic set Λ, invariant under P, on which P is topologically conjugate to a shift on finitely many symbols.

The transverse intersection is shown in Figure 5.4. Notice that for the Theorem to make sense at least one of the manifolds W^s and W^u has to be globally defined. We will not prove this theorem here but the book by Moser, Stable and Random Motion in Dynamical Systems [16], contains a very readable proof.

5.5 The Melnikov Method

The hypothesis (5.2) in the Birkhoff-Smale Homoclinic Theorm 5.3 is most easily proven by use of the Melnikov method. This method consists of computing a function $M(t_o)$ called the Melnikov function which measures the distance between the stable and unstable manifolds. When $M(t_o)$ has simple zeroes then these manifolds cross transversely. Consider the first order system

$$\dot{x} = f(x) + \varepsilon g(x,t),\ x \in \mathbb{R}^2,\ t \in \mathbb{R} \tag{5.3}$$

and assume that the perturbation g is periodic in time, $g(x,t+T) = g(x,t)$, and that the unperturbed system

$$\dot{x} = f(x)$$

has a hyperbolic stationary solution $\bar{x}$. Also assume that the stable and unstable manifolds of $\bar{x}$ form a homoclinic (or a heteroclinic) loop $x_o(t)$, see Figure 5.5. The following lemma is proven in Guckenheimer and Holmes [11].

Lemma 5.7 *The stable and unstable manifolds of the Poincaré map of (5.3) intersect transversely if and only if the Melnikov function*

$$M(t_o) = \int_{-\infty}^{\infty} f(x_o(t-t_o)) \wedge g(x_o(t-t_o),t)dt \tag{5.4}$$

has simple zeroes.

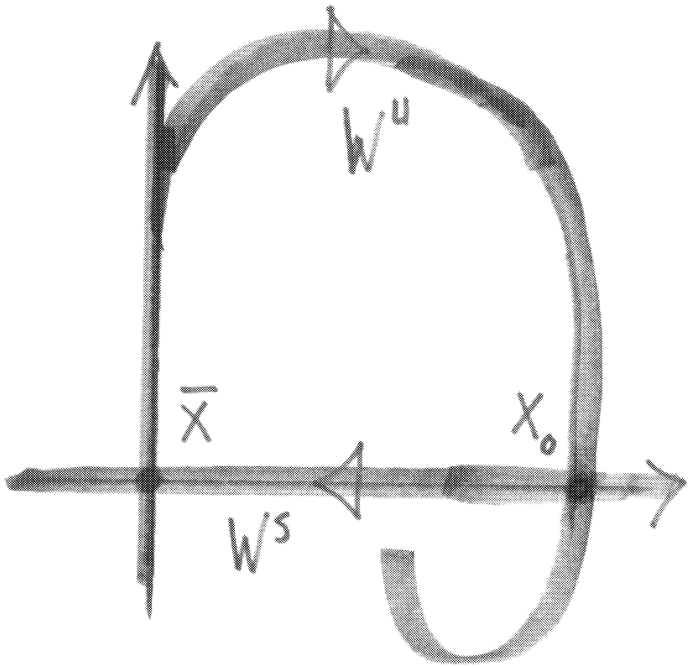

Figure 5.9: The unstable manifold must intersect the stable manifold transversely in a point $x_0 \neq \bar{x}$.

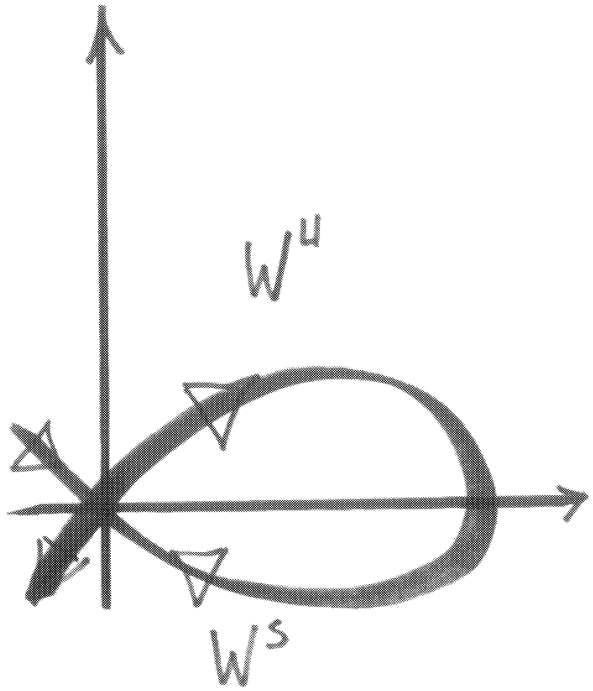

Figure 5.10: The homoclinic loop connect the stationary solution to itself $W^s = W^u$.

Exercise 5.4 *Show that the Poincaré Map of the damped and driven Duffing's Equation*

$$\ddot{x} + \delta\dot{x} - x + x^3 = \varepsilon\cos(t)$$

has a Smale Horseshoe in its phase space if

$$\frac{\varepsilon}{\delta} > \frac{4\cosh(\pi/2)}{32^{1/2}\pi}$$

5.6 Transient Dynamics

The horseshoe map is not a diffeomorphism of the square since $f(S) \nsubseteq S$, but we can extend it to a diffeomorphism on the two-sphere S^2. This is done in two steps. The first step is to extend the square into a soccer stadium so as to include the whole horseshoe on bottom portion on Figure 2. The results is shown on Figure 5.6. But then we must also extend the map to the portions of the stadium labelled A and E. This is most conveniently done by placing a sink p in E, outside the horseshoe, and by letting all the points on the outside perimeter of A be mapped into A. Then we extend the stadium to a disk so that the map is directed invard on the perimeter of the disk, see Figure 5.6. This concludes the first step. The second step is then to make the disk into a spherical cap, to cover the northern hemisphere and add another cap with a source q at the south pole, see Figure 5.6. It can be shown that the extended map F, $F|_S = f$ is a diffeomorphism of S^2.

Our main interest in the map F is to use it to figure out what happens to all the points of S, also those that get mapped outside S by f. The following theorem accounts for all points of S that do not lie on Λ. We let inΛ denote the inset of $\Lambda = \{x \in S^2 | \lim_{n\to\infty} F(x) \subset \Lambda\}$ and outΛ, the outset of $\Lambda = \{x \in S^2 | \lim_{n\to\infty} F^{-n}(x) \subset \Lambda\}$. These are not manifold because of the Cantor set structure mentioned above, however they generalize the notion of stable and unstable manifolds respectively, see Fact 5.7 in Section 5.3.

Theorem 5.4 *All points x of $S \setminus \bigcap_{n\in\mathbb{Z}^+} V^n$, where $\bigcap_{n\in\mathbb{Z}^+} V^n$ is the vertical Cartesian product of a Cantor set and the y-interval $[0,1]$, eventually approach the fixed point in E,*

$$\lim_{n\to\infty} F^n(x) = p.$$

Proof: Consider Figure 5.6. It shows that the regions A, B, D, and E are all mapped into E in one iteration. All points in E are attracted to p. C is mapped into A, but all of A gets mapped into E so C gets mapped into E in two iterations. Now

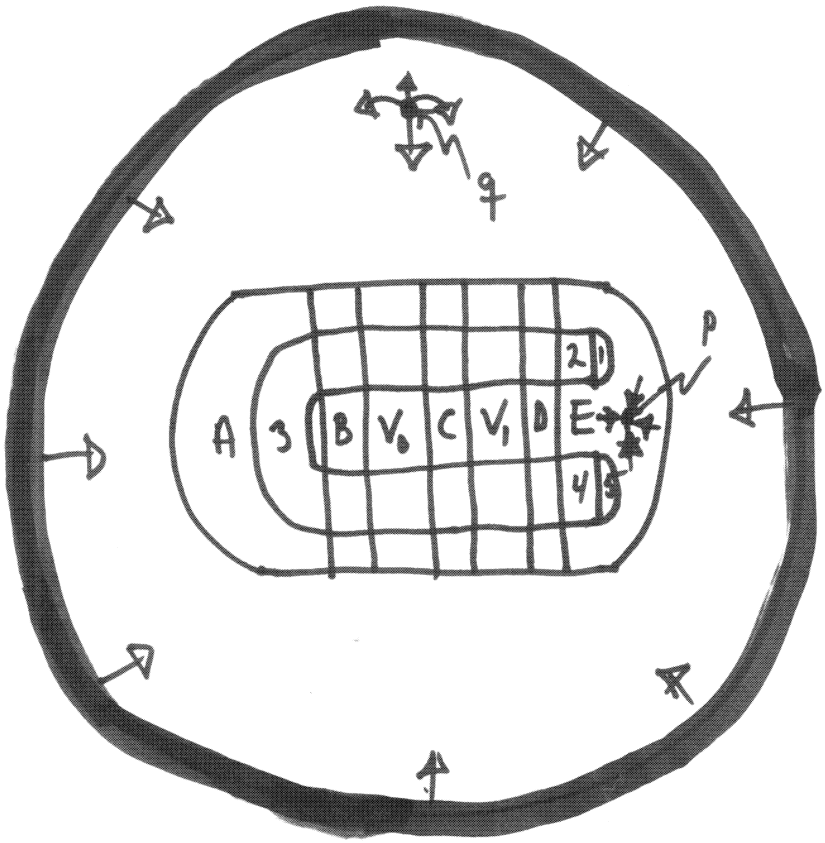

Figure 5.11: All points in a neighborhood, except the inset (stable manifold), of the horseshoe, are eventually mapped to the sink.

consider the two vertical strips V_0 and V_1. The strips $V^1 = V_{00} \cup V_{01} \cup V_{10} \cup V_{11}$ are mapped onto $V^0 = V_0 \cup V_1$ in one iteration. This means that the points in $V^0 \setminus V^1$ must be mapped into B, C or D and therefore into E in at most three iterations, by the above arguments. Similarly, $V^1 \setminus V^2$ is mapped into E in four iterations of F etc. The remainder that does not get mapped into E is the intersection of all the vertical strips $\bigcap_{n \in \mathbb{Z}^+} V^n$. **QED**

Chapter 6

Center Manifolds

Recall from Chapters 1 and 4 the linear stable and unstable manifolds E_s and E_u of a hyperbolic stationary solution. Now we will also consider stationary solution with pure imaginary eigenvalues and the linear center manifold E_c, spanned by the eigenvectors of these pure imaginary or zero eigenvalues. The following theorem give the existence of the nonlinear center manifold W^c tangent to E_c.

Theorem 6.1 The Center Manifold Theorem

Consider the systems of equations

$$\begin{aligned} \dot{x} &= Ax + f(x,y), \quad x \in \mathbb{R}^l,\ y \in \mathbb{R}^m, \\ \dot{y} &= By + g(x,y), \quad l+m=n, \end{aligned}$$

and assume that A has no pure imaginary (or zero) eigenvalues whereas B has only pure imaginary (or zero) eigenvalues. Moreover, assume that f and g are $C^k(\mathbb{R}^n)$ functions so that

$$\lim_{\|(x,y)\|\to 0} \frac{\|f(x,y)\|}{\|(x,y)\|} = 0 = \lim_{\|(x,y)\|\to 0} \frac{\|g(x,y)\|}{\|(x,y)\|}.$$

Then there exists a neighborhood U of the origin in $\mathbb{R}^n$ and a center manifold W^u which is tangent to E_c at the origin, or, in other words, there exists a C^k function,

$$h : \Pi^c(U) \longrightarrow E_s \times E_u,$$

$\Pi^c(U)$ being the projection of U onto E_c, whose graph is W^c and

$$h^c(0) = 0, \quad D_y h^c(0) = 0.$$

Corollary 6.1 *The Center manifold $x = h(y)$ is defined by the equation*

$$h'(y)\left[By + g(h(y), y)\right] = Ah(y) + f(h(y), y)$$

where $h' = D_y h$.

Proof: Substitute $x = h(y)$ into the equation for x and use the equation for y to eliminate $\dot{y}$. **QED**

Example 6.1 *Consider the system*

$$\begin{aligned} \dot{x} &= -x + x^2 - y^2 \\ \dot{y} &= \varepsilon y - y^3 + xy \end{aligned}$$

Here $A = -1$ and $B = \varepsilon$ so B only has a center manifold at $\varepsilon = 0$. However, if we write the equations in the form

$$\begin{aligned} \dot{x} &= -x + x^2 - y^2 \\ \dot{y} &= \varepsilon y - y^3 + xy \\ \dot{\varepsilon} &= 0 \end{aligned}$$

then there is a two dimensional center manifold. We let $x = h(y, \varepsilon)$ and substitute into the first equation

$$D_y h\dot{y} + D_\varepsilon h\dot{\varepsilon} = -h + h^2 - y^2$$

or

$$h'(y)\left(\varepsilon y - y^3 + xy\right) = -h + h^2 - y^2.$$

Now let

$$\begin{aligned} h(y,\varepsilon) &= ay^2 + by\varepsilon + c\varepsilon^2 + O\left((y,\varepsilon)^3\right) \\ D_y h &= 2ay + by + O\left((y,\varepsilon)^2\right) \\ \left(2ay + by + O(y,\varepsilon)^2\right)\left(\varepsilon y - y^3 + hy\right) &= -ay^2 - by\varepsilon - c\varepsilon^2 - y^2 + O(y,\varepsilon)^4 \\ O(y,\varepsilon)^3 &= y^2(a+1) + b\varepsilon + c\varepsilon^2 + O(y,\varepsilon)^3. \end{aligned}$$

This implies that $a = -1$ and $b = 0 = c$, or

$$h(y,\varepsilon) = -y^2 + O\left((y,\varepsilon)^3\right).$$

The higher order terms are computed by substituting in

$$h(y,\varepsilon) = -y^2 + ay^3 + by^2\varepsilon + cy\varepsilon^2 + d\varepsilon^3 + O(y,\varepsilon)^4$$

and solving for the coefficients a,b,c,d. Now the flow on the center manifold is determined by the equation

$$\begin{aligned} \dot{y} &= \varepsilon y - y^3 + hy = \varepsilon y - 2y^3 + O(y,\varepsilon)^4 \\ \dot{\varepsilon} &= 0 \end{aligned}$$

where we have substituted h into the center manifold (y) equation.

The example was taken from Carr [6].

Example 6.2

The Lorenz equation

$$\begin{aligned} \dot{x} &= \sigma(y-x) \\ \dot{y} &= \rho x - y - xz \\ \dot{z} &= xy - \beta z \end{aligned}$$

where σ, ρ and β are positive constants, have a stationary solution at the origin $(x,y,z) = (0,0,0)$. It was shown in Section 2.3 that this stationary solution is stable if $\rho \leq 0$ so we let $\rho = 1+\mu$, then μ is a bifurcation parameter. We will now compute the center manifold of the Lorenz equation. First write the system in the form

$$\begin{aligned} \dot{x} &= \sigma(y-x) \\ \dot{y} &= (1+\mu)x - y - xz \\ \dot{z} &= xy - \beta z \\ \dot{\mu} &= 0 \end{aligned}$$

where we have added μ as a variable. Now the equations can be written in the form

$$\dot{z} = Az + f(z) \tag{6.1}$$

where A is the matrix

$$A = \begin{pmatrix} -\sigma & \sigma & 0 & 0 \\ 1 & -1 & 0 & 0 \\ 0 & 0 & -\beta & 0 \\ 0 & 0 & 0 & 0 \end{pmatrix}$$

The eigenvalues of A are $0, -(\sigma+1), -\beta, 0$ and the corresponding eigenvectors are

$$\begin{pmatrix} 1 \\ 1 \\ 0 \\ 0 \end{pmatrix}, \begin{pmatrix} -\sigma \\ 1 \\ 0 \\ 0 \end{pmatrix}, \begin{pmatrix} 0 \\ 0 \\ 1 \\ 0 \end{pmatrix}, \begin{pmatrix} 0 \\ 0 \\ 0 \\ 1 \end{pmatrix}.$$

Now let $z = Sy$ where S is the transformation matrix whose columns are the eigenvectors, then

$$\begin{pmatrix} x \\ y \\ z \\ \mu \end{pmatrix} = \begin{pmatrix} 1 & -\sigma & 0 & 0 \\ 1 & -1 & 0 & 0 \\ 0 & 0 & 1 & 0 \\ 0 & 0 & 0 & 1 \end{pmatrix} \begin{pmatrix} y_1 \\ y_2 \\ y_3 \\ w \end{pmatrix} = \begin{pmatrix} y_1 - \sigma y_2 \\ y_1 + y_2 \\ y_3 \\ w \end{pmatrix}$$

and the equation (6.1) gets transformed into the equation

$$\dot{y} = By + S^{-1} f \begin{pmatrix} y_1 - \sigma y_2 \\ y_1 + y_2 \\ y_3 \\ w \end{pmatrix}$$

where

$$S^{-1} = \begin{pmatrix} \frac{1}{1+\sigma} & \frac{\sigma}{1+\sigma} & 0 & 0 \\ \frac{-1}{1+\sigma} & \frac{1}{1+\sigma} & 0 & 0 \\ 0 & 0 & 1 & 0 \\ 0 & 0 & 0 & 1 \end{pmatrix}$$

and

$$B = S^{-1}AS = \begin{pmatrix} 0 & 0 & 0 & 0 \\ 0 & -(\sigma+1) & 0 & 0 \\ 0 & 0 & -\beta & 0 \\ 0 & 0 & 0 & 0 \end{pmatrix}$$

Now

$$S^{-1} f \begin{pmatrix} y_1 - \sigma y_2 \\ y_1 + y_2 \\ y_3 \\ w \end{pmatrix} = \begin{pmatrix} \frac{\sigma}{1+\sigma}(y_1 - \sigma y_2)(w - y_3) \\ \frac{1}{1+\sigma}(y_1 - \sigma y_2)(w - y_3) \\ (y_1 - \sigma y_2)(y_1 + y_2) \\ 0 \end{pmatrix}$$

This gives the equation

$$\dot{y} = \begin{pmatrix} 0 & 0 & 0 & 0 \\ 0 & -(\sigma+1) & 0 & 0 \\ 0 & 0 & -\beta & 0 \\ 0 & 0 & 0 & 0 \end{pmatrix} y + \begin{pmatrix} \frac{\sigma}{1+\sigma}(y_1-\sigma y_2)(w-y_3) \\ \frac{1}{1+\sigma}(y_1-\sigma y_2)(w-y_3) \\ (y_1-\sigma y_2)(y_1+y_2) \\ 0 \end{pmatrix}$$

This equation shows that the Lorenz equations have a two-dimensional center manifold at the origin and a two dimensional stable manifold. By the Center Manifold Theorem there exists a $h^c \in C^k$ such that

$$h^c : \Pi(U) \to E^s$$

in a neighborhood U of the origin, with $h^c(0,0) = (0,0)$ and $Dh^c(0,0)$ vanishing. We let

$$\begin{pmatrix} y_2 \\ y_3 \end{pmatrix} = h(y_1, w) = \begin{pmatrix} h_2(y_1,w) \\ h_3(y_1,w) \end{pmatrix}$$

The equation determining the center manifold is

$$\begin{aligned} D_{(y_1,w)}h \begin{pmatrix} \frac{\sigma}{1+\sigma}(y_1-\sigma h_2)(w-h_3) \\ 0 \end{pmatrix} &= \begin{pmatrix} -(1+\sigma) & 0 \\ 0 & -\beta \end{pmatrix} \begin{pmatrix} y_2 \\ y_3 \end{pmatrix} \\ &+ \begin{pmatrix} \frac{1}{1+\sigma}(y_1-\sigma h_2)(w-h_3) \\ (y_1-\sigma h_2)(y_1+h_3) \end{pmatrix} \end{aligned}$$

We approximate h by a power series using that the constant and linear terms must vanish

$$\begin{aligned} h_2 &= a_2 y_1^2 + b_2 y_1 w + c_2 w^2 + d_2 y_1^3 + e_2 y_1^2 w + f_2 y_1 w^2 + g_2 w^3 + O(y_1, w)^4 \\ h_3 &= a_3 y_1^2 + b_3 y_1 w + c_3 w^2 + d_3 y_1^3 + e_3 y_1^2 w + f_3 y_1 w^2 + g_3 w^3 + O(y_1, w)^4 \end{aligned}$$

The above equation for the center manifold can be written as two equations

(6.2)
$$\frac{\sigma}{1+\sigma}\frac{\partial h_2}{\partial y_1}(y_1-\sigma h_2)(w-h_3) = -(1+\sigma)h_2 + \frac{1}{1+\sigma}(y_1-\sigma h_2)(w-h_3)$$

(6.3)
$$\frac{\sigma}{1+\sigma}\frac{\partial h_3}{\partial y_1}(y_1-\sigma h_2)(w-h_3) = -\beta h_3 + (y_1-\sigma h_2)(y_1+h_3)$$

We compute the derivatives of h using the approximation above and substitute the approximation of h_2 and h_3 into the equations (6.2) and (6.3). This gives the equations

$$\begin{aligned}
\frac{\sigma}{1+\sigma}(2a_2y_1^2w &+ b_2y_1w^2) + O(y_1,w)^4 \\
(6.4) \qquad &= -(1+\sigma)(a_2y_1^2 + b_2y_1w + c_2w^2 + d_2y_1^3 + e_2y_1^2w + f_2y_1w^2 + g_2w^3) \\
+\frac{1}{1+\sigma}(y_1w &- a_3y_1^3 - b_3y_1^2w - c_3y_1w^2 - \sigma a_2wy_1^2 - \sigma b_2y_1w^2 - \sigma c_2w^3)
\end{aligned}$$

$$\begin{aligned}
\frac{\sigma}{1+\sigma}(2a_3y_1^2w &+ b_3y_1w^2) + O(y_1,w)^4 \\
(6.5) \qquad &= -\beta(a_3y_1^2 + b_3y_1w + c_3w^2 + d_3y_1^3 + e_3y_1^2w + f_3y_1w^2 + g_3w^3) \\
+(y_1^2w &+ a_3y_1^3 + b_3y_1^2w + c_3y_1w^2 - \sigma a_2y_1^3 - \sigma b_2y_1^2w - \sigma c_2y_1w^2)
\end{aligned}$$

Equating coefficients of the powers of y_1 and w on both sides of these equations produces the values of the coefficients

$$\begin{aligned}
a_2 &= 0, a_3 = \frac{1}{\beta},\ b_2 = \frac{1}{(1+\sigma)^2}, b_3 = \frac{1}{\beta},\ c_2 = 0, c_3 = 0,\ d_2 = -\frac{1}{\beta(1+\sigma)^2}, \\
d_3 &= \frac{1}{\beta^2},\ e_2 = -\frac{1}{\beta(1+\sigma)^2}, e_3 = \frac{\sigma^2-\sigma\beta-1}{\beta(1+\sigma)^2},\ f_2 = -\frac{2\sigma}{(1+\sigma)^4}, \\
f_3 &= -\frac{\sigma}{\beta^3(1+\sigma)},\ g_2 = 0, g_3 = 0
\end{aligned}$$

Substituting these values into the approximation gives the center manifold

$$\begin{aligned}
h_2(y_1,w) &= \frac{1}{(1+\sigma)^2}y_1w - \frac{1}{\beta(1+\sigma)^2}y_1^3 - \frac{1}{\beta(1+\sigma)^2}y_1^2w - \frac{2\sigma}{(1+\sigma)^4}y_1w^2 \\
h_3(y_1,w) &= \frac{1}{\beta}y_1^2 + \frac{1}{\beta}y_1w + \frac{1}{\beta^2}y_1^3 + \frac{\sigma^2-\sigma\beta-1}{\beta(1+\sigma)^2}y_1^2w - \frac{\sigma}{\beta^3(1+\sigma)}y_1w^2
\end{aligned}$$

up to terms of order $(y_1,w)^4$. Substituting these expressions into the differential equation for y_1 then gives the flow on the center manifold

$$\dot{y}_1 = \frac{\sigma}{(1+\sigma)}(y_1w - \frac{1}{\beta}y_1^3 - \frac{1}{\beta}y_1^2w - \frac{\sigma}{(1+\sigma)^2}y_1w^2) + O(y_1,w)^4 \tag{6.6}$$

We will show below that this equation gives a pitchfork bifurcation as $\mu = w$ increases through zero.

Chapter 7

Bifurcation Theory

Consider the system

$$\dot{z} = Cz + r(z),$$

where $r \in C^k$ and C is a $n \times n$ matrix. If C has some eigenvalues on the pure imaginary axis then we can make a change of coordinates such that the system can be written

$$\begin{aligned} \dot{x} &= Ax + f(x,y) \\ \dot{y} &= By + g(x,y), \end{aligned} \tag{7.1}$$

$f, g \in C^k$ and $f, g = O(\|(x,y)\|^2)$, and the eigenvalues of A are pure imaginary, $\sigma(A) = \sigma^c(A)$, whereas B has no pure imaginary eigenvalues $\sigma^c(B) = \{0\}$. Here σ denotes the spectrum and notice that we have switched the x and y from the statement of the Center Manifold Theorem 6.1. Moreover, the Center Manifold Theorem says that there exists a center manifold W^c_{loc}, given by $y = h(x)$, tangent to the linear center subspace E_c at the origin where $h \subset C^k$. We compute $h(x)$ in a power series in x by recipe

$$D_x h\,[A + f(x,h)] = Bh + g(x,h),$$

given in Corollary 6.1, and then we can observe what bifurcations take place on W^c_{loc} as the coefficients of the h expansion vary. It turns out that if dim $x = 1$ or 2 one can tell the whole story, these are called the codimension 1 and 2 bifurcations respectively. The codimension 3, dim $x = 3$, case is much more complicated and is still unresolved. For higher dimensional cases, dim $x > 3$, there is not much that can be said in general unless symmetries are present so that the bifurcations take place on lower-dimensional subspaces.

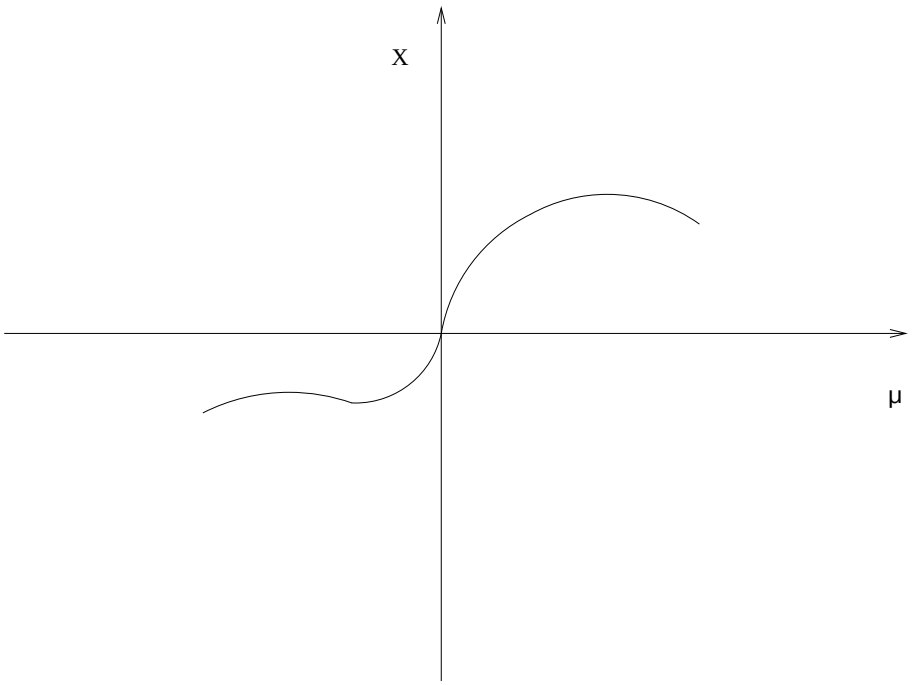

Figure 7.1: The curve of stationary solutions

7.1 Codimension One Bifurcations

We assume that A in (7.1) is a 1×1 matrix and that B has no pure imaginary eigenvalues, then by the Center Manifold Theorem there exists a center manifold W^c_{loc}, given by $y = h(x)$, such that the flow on W^c_{loc} is determined by the equation

$$\dot{x} = f(x, h(x)).$$

Namely, since A has only one eigenvalue it must be zero and this says that in the codimension one case the flow is given by a one-dimensional equation. We are interested in how the flow changes with parameters in the problem and therefore consider the one dimensional equation

$$\dot{x} = f(x, \mu) \tag{7.2}$$

where we have allowed f to depend on the parameter μ as well as x.

The point $x = 0,\ \mu = 0$ is a stationary solution of (7.2) if and only if

$$f(0,0) = 0,$$

and we assume that this is the case by translating, $x \to x - x_0$ and $\mu \to \mu - \mu_0$, if necessary. If

$$D_x f(0,0) \neq 0$$

then by the implicit function theorem there is a C^1 branch of stationary solutions (x,μ) through the origin, see Figure 7.1, such that

$$f(x,\mu) = 0.$$

A necessary condition for a bifurcation to take place is therefore

$$D_x f(0,0) = 0 \tag{7.3}$$

and we will now assume this is the case and that the two degeneracy conditions

$$D_\mu f(0,0) \neq 0, \quad D_x^2 f(0,0) \neq 0, \tag{7.4}$$

also hold.

7.1.1 The Saddle-Node Bifurcation

The two conditions (7.3) and (7.4) give the generic codimension one bifurcation. It is called the saddle-node bifurcation, see Figure 7.1.1 and Figure 7.1.1 and, and is the bifurcations that we should expect to see in the codimension one case unless there are some extra symmetries present. First we notice that the vector field will vanish

$$f(x,\mu) = 0$$

on a branch $x(\mu)$ of stationary solutions. A differentiation of $f(x,\mu) = 0$ with respect to x gives

$$D_x f(0,0) + D_\mu f(0,0)\frac{d\mu}{dx} = 0,$$

so

$$\frac{d\mu}{dx} = 0,$$

at the bifurcation point. A second differentiation gives

$$D_x^2 f(0,0) + 2D_{\mu x} f(0,0)\frac{d\mu}{dx} + D_\mu^2 f(0,0)\left(\frac{d\mu}{dx}\right)^2 + D_\mu f \frac{d^2\mu}{dx^2} = 0,$$

or

$$\frac{d^2\mu}{dx^2} = -\frac{D_x^2 f(0,0)}{D_\mu f(0,0)}.$$

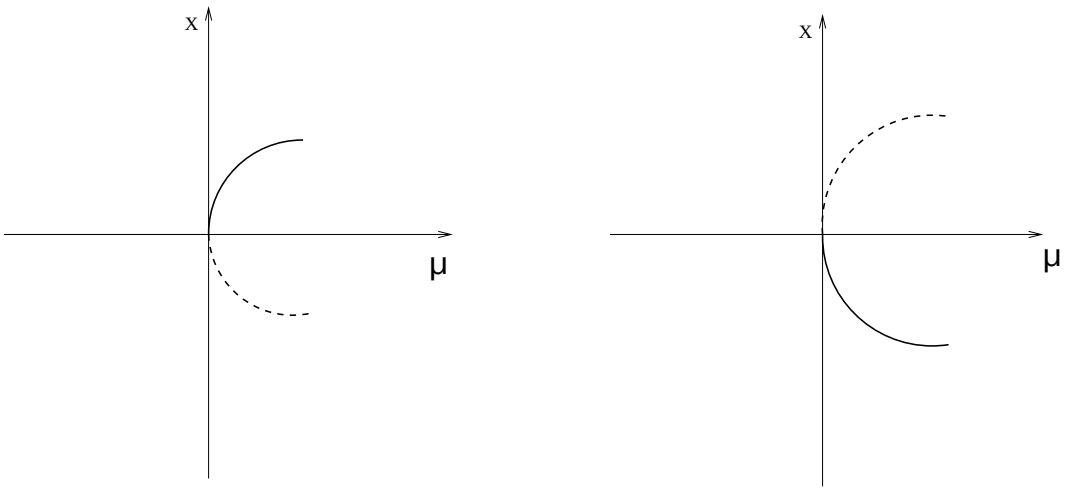

Figure 7.2: The supercritical saddle-node bifurcation, $\alpha = \beta = \pm 1$.

This says that locally the bifurcation curve is a parabola centered on the μ-axis. Moreover, since the stability of the bifurcating solutions (x,μ) are determined by the linearized equation (7.2),

$$\dot{y} = D_x f(x,\mu) y \tag{7.5}$$

and

$$D_x f(x,\mu) = -D_\mu f(x,\mu) \frac{d\mu}{dx}$$

we get the stability information in Table 7.1.1. Now there are 4 possible bifurcation diagrams which are illustrated on Figures 7.1.1 and 7.1.1.

Table III.1

	$D_\mu f > 0$	$D_\mu f < 0$
$\mu' > 0$	*Stable*	*Unstable*
$\mu' < 0$	*Unstable*	*Stable*

These bifurcations take place for the function

$$f(x,\mu) = \alpha\mu - \beta x^2, \quad \alpha,\beta = \pm 1 \tag{7.6}$$

and the supercritical cases on Figure 7.1.1 correspond to $\alpha = \beta = 1$ and $\alpha = \beta = -1$ respectively, whereas the subcritical cases on Figure 7.1.1 correspond to

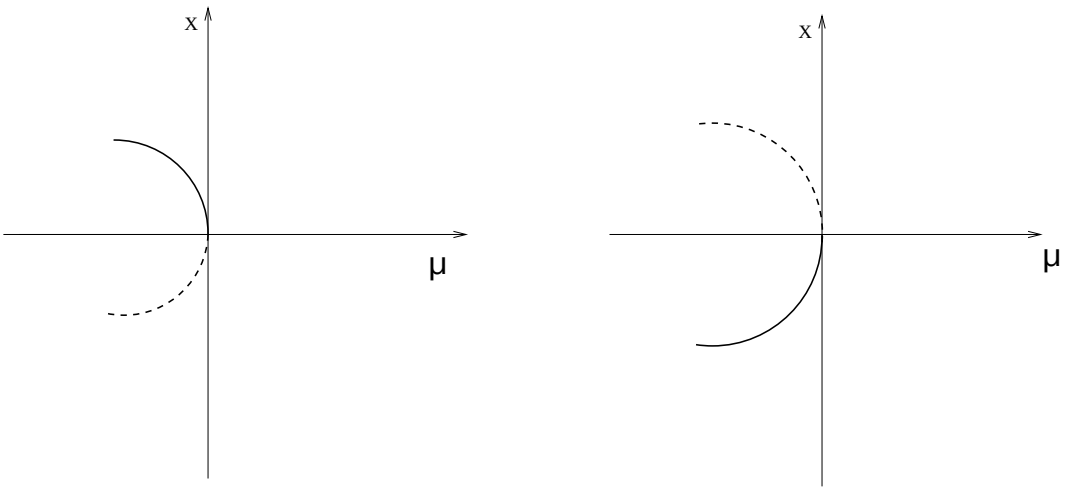

Figure 7.3: The subcritical saddle-node bifurcation, $\alpha = \pm 1$, $\beta = \mp 1$.

$\alpha = 1,\ \beta = -1$ and $\alpha = -1,\ \beta = 1$, respectively. In fact (7.6) is called the normal form of the saddle-node bifurcation because all codimension one flows exhibiting this bifurcation can be reduced to the form (7.6).

7.1.2 A Transcritical Bifurcation

Now suppose for a moment that $f(0,\mu) = 0$ so that $x = 0$ is a stationary solution of (7.2). This means that

$$D_\mu f(0,0) = 0 \tag{7.7}$$

and now we impose this condition along with the nondegeneracy condition

$$D_x^2 f(0,0) \neq 0. \tag{7.8}$$

We have to impose another condition in addition to (7.8), to get branches of stationary solutions. This condition says in the transcritical case that the origin $(0,0)$ is a saddle-point of $f(x,\mu)$. Notice that (7.3) and (7.8)

$$D_x f(0,0) = 0, \quad D_\mu f(0,0) = 0$$

state that $(0,0)$ is a critical point of f but this critical point cannot be a maximum, if we are to have branches of stationary solutions. We expand $f(x,\mu)$ in a Taylor series about the origin to make this explicit

$$f(x,\mu) = D_x^2 f(0,0)x^2 + 2D_{x\mu} f(0,0)x\mu + D_\mu^2 f(0,0)\mu^2 + O(x,\mu)^3.$$

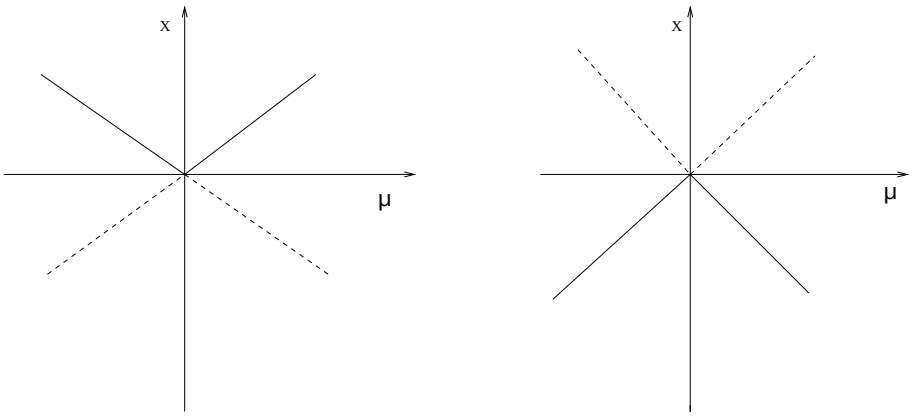

Figure 7.4: The transcritical bifurcations.

The origin is a saddle if and only if

$$D = \left(D_{x\mu}f(0,0)\right)^2 - D_x^2 f(0,0) D_\mu^2 f(0,0) > 0, \tag{7.9}$$

and then we get two branches of solutions of $f(x,\mu) = 0$, namely

$$x_\pm = \left(-D_{x\mu}f \pm \sqrt{D}\right) \frac{\mu}{D_x^2 f}$$

where D is the discriminant (7.9). Notice that in general $x = 0$ is not a branch of stationary solutions but it becomes one if

$$D_\mu^2 f(0,0) = 0. \tag{7.10}$$

However, the conditions (7.8) and (7.9) imply that there are two branches of stationary solutions going through the origin. The stability of those two branches is given by the linearization of the equation (7.2),

$$\begin{aligned} \dot{y} &= 2\left(D_x^2 f x + D_{x\mu} f \mu\right) y + O(x,\mu)^2 \\ &= \pm 2\sqrt{D}\mu y + O(x,\mu)^2. \end{aligned}$$

Thus the x_+ and x_- branch have opposite stability and since μ changes its stability at the origin, the two branches exchange stability at the origin.

The transcritical bifurcation is exhibited by the vector field

$$f(x,\mu) = x(\alpha\mu + \beta x), \quad \alpha,\beta = \pm 1$$

The two cases on Figure 7.1.2 correspond to $\alpha = -1$ and $\alpha = +1$ respectively. We get two bifurcation diagrams see Figure 7.1.2.

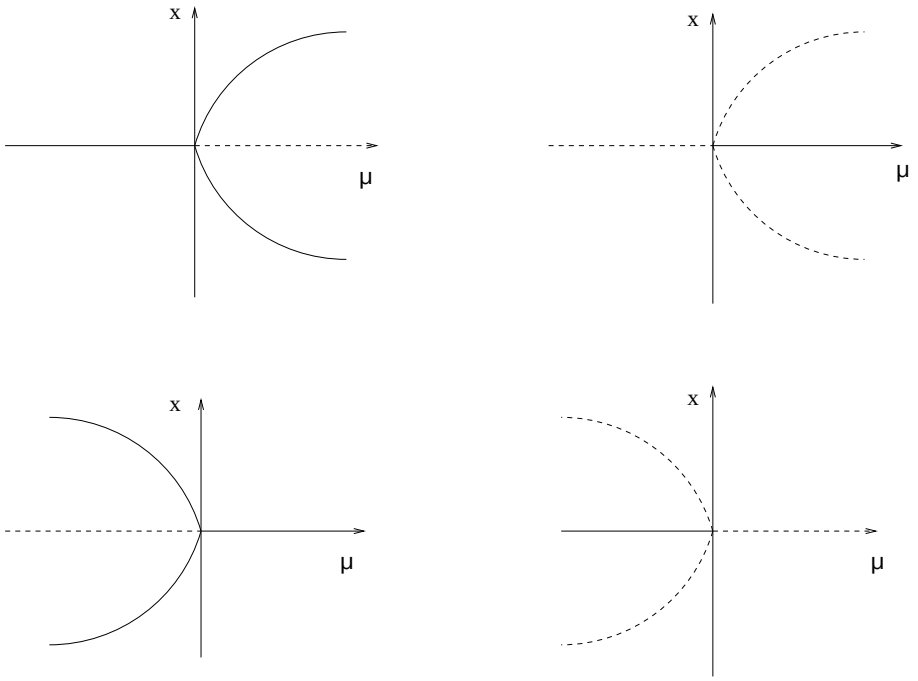

Figure 7.5: The pitchfork bifurcations.

7.1.3 A Pitchfork Bifurcation

We now let

$$D_x^2 f(0,0) = 0, \tag{7.11}$$

then the Taylor expansion of f around the origin becomes

$$\begin{aligned} f(x,\mu) &= 2D_{x\mu}f(0,0)x\mu + D_x^3 f(0,0)x^3 \\ &\quad +3D_x^2 D_\mu f(0,0)x^2\mu + O(\mu^2). \end{aligned}$$

This means that for μ small we can get 3 branches of stationary solutions. Namely,

$$f(x,\mu) = x\left(D_x^3 f x^2 + 3D_x^2 D_\mu f x\mu + 2D_{x\mu}f\mu\right) + O(\mu^2)$$

and we get the 3 solutions

$$x_0 = 0 \text{ and } x_\pm = \pm\sqrt{\frac{-2D_{x\mu}f(0,0)\mu}{D_x^3 f(0,0)}}. \tag{7.12}$$

This makes the second non-degeneracy condition

$$D_{x\mu}f(0,0) \neq 0 \tag{7.13}$$

clear. A differentiation of $f(x,\mu)/x$ similar to the one performed in the saddle-node case above also shows that

$$\frac{d\mu}{dx} = 0 \quad \text{and} \quad \frac{d^2\mu}{dx^2} = -\frac{D_x^3 f}{3D_x D_\mu f} \neq 0,$$

for the $x_\pm$ branches. This says that these branches form a parabola along the μ axis in the $\mu - x$ plane, see Figure 7.1.3.

The stability is determined by the linearization of (7.2) about these branches. For the $x = 0$ branch we get

$$\dot{y} = 2(D_{x\mu}f(0,0)\mu)y$$

and for the $x_\pm$ branches we get

$$\dot{y} = -4(D_{x\mu}f(0,0)\mu)y.$$

Thus the stability of the $x = 0$ is opposite to that of the $x_\pm$ branches and determined by the signature of $D_{x\mu}f(0,0)$, see Figure (7.1.3). The signatures of $D_x^3 f$ and $D_{x\mu}f$ determine in which μ half-plane we get three branches of stationary solutions,

$$\text{sign } D_x^3 f(0,0) \neq \text{ sign } D_{x\mu}f(0,0)$$

is called the supercritical and

$$\text{sign } D_x^3 f(0,0) = \text{ sign } D_{x\mu}f(0,0)$$

is called the subcritical case, see Figure 7.1.3. In the former case we get three branches for μ positive in the latter case we get three branches for μ negative.

Now the canonical example or normal form exhibiting pitchfork bifurcations is

$$f(x,\mu) = \alpha\mu x - \beta x^3, \quad \alpha,\beta = \pm 1.$$

The cases on Figure 7.1.3 correspond to $\alpha = 1 = \beta$, $\alpha = -1 = \beta$, $\alpha = -1$, $\beta = +1$ and $\alpha = +1$, $\beta = -1$, respectively.

Example 7.1

Recall the equation (6.6) describing the flow on the center manifold of the Lorenz equations

$$\dot{y} = \frac{\sigma}{(1+\sigma)}(y\mu - \frac{1}{\beta}y^3 - \frac{1}{\beta}y^2\mu - \frac{\sigma}{(1+\sigma)^2}y\mu^2) + O(y,\mu)^4 = f(y,\mu) \qquad (7.14)$$

We compute the derivatives give us the criteria for a bifurcation and the type of bifurcation of the stationary solution at the origin $(y,\mu) = (0,0)$.

$$\begin{aligned}
\frac{\partial f}{\partial y} &= \frac{\sigma}{1+\sigma}(\mu - \frac{3}{\beta}y^2 - \frac{2}{\beta}y\mu - \frac{\sigma}{(1+\sigma)^2}\mu^2) = 0, \text{ at } (0,0) \\
\frac{\partial f}{\partial \mu} &= \frac{\sigma}{1+\sigma}(y - \frac{1}{\beta}y^2 - \frac{2\sigma}{(1+\sigma)^2}y\mu) = 0, \text{ at } (0,0) \\
\frac{\partial^2 f}{\partial y^2} &= \frac{\sigma}{1+\sigma}(-\frac{6}{\beta}y - \frac{2}{\beta}\mu) = 0, \text{ at } (0,0)
\end{aligned}$$

The first line shows that there is a bifurcation point at the origin. The second line shows that it is not a saddle-node bifurcation. The third line shows that it is not a transcritical bifurcation. Next we show that the non-degeneracy conditions for a pitchfork bifurcation at the origin are satisfied.

$$\begin{aligned}
\frac{\partial^2 f}{\partial y \partial \mu} &= \frac{\sigma}{1+\sigma}(1 - \frac{2}{\beta}y - \frac{2\sigma}{(1+\sigma)^2}\mu) = \frac{\sigma}{1+\sigma} \neq 0, \\
\frac{\partial^3 f}{\partial y^3} &= -\frac{\sigma}{1+\sigma}\frac{6}{\beta} \neq 0
\end{aligned}$$

Thus the Lorenz equation have a pitchfork bifurcation at the origin and now we show that it is supercritcal, namely

$$\text{sign}\frac{\partial^2 f}{\partial y \partial \mu} \neq \text{sign}\frac{\partial^3 f}{\partial y^3}$$

More information on the bifurcation theory of ODEs and proofs can be found in Iooss and Joseph [13] and for PDEs in Chow and Hale [7]. The reduction to normal forms is performed in Arrowsmith and Place [3].

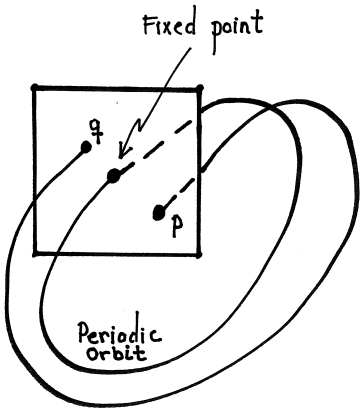

Figure 7.6: The Poincaré Map.

7.2 The Poincaré Map

We discussed in Definition 2.7 how one can produce a map from a flow by taking the time-T map. It is important to realize that not all such maps are equivalent or topologically conjugate see Arrowsmith and Place [3]. For example if the flow has a periodic orbit a of period T then the time-T map has a fixed point but the time-$\frac{T}{2}$ has a periodic orbit of period one. Consequently their topological type is different.

Poincaré constructed a map by taking a hyperplane transverse to a periodic orbit and defining the map to be the return map to the hyperplane. These maps are parametrized by the intersection point of the hyperplane and the periodic orbit and they are all topologically conjugate for a sufficiently small neighborhood of the periodic orbit, see Figure 7.2. Now we generalize Poincaré's construction slightly,

Definition 7.1 *Let $\{\{T(t)\},X\}$ be a flow, then we say that a codimension one hypersurface $\Gamma \subset X$ is a* transversal*, in a neighborhood U of $\overline{u} \in \Gamma$, if every orbit $u(t) = T(t)u_o$ meets Γ again and the vector field $\dot{u}$, at $\overline{u}$, is not tangent to Γ. Γ is*

a global transversal *if* $T(t)u_o$ *meets* Γ *for arbitrarily positive or negative* t.

Not every flow has a transversal but if it does we define the first return map in the following way:

Definition 7.2 *The Poincaré map of* $\Gamma \cap U$ *is defined to be*

$$P(w) = T(\tau)w, \;\; w \in \Gamma \cap U, \tag{7.15}$$

where $\tau(w)$ *is the first time that the orbit* $u(t) = T(t)w$ *returns to* $\Gamma \cap U$, U *being a neighborhood of* w *in* X.

7.3 The Period Doubling Bifurcation

Now consider a map

$$x_{m+1} = f(x_m, \mu), \quad x, \mu \in \mathbb{R}, \; m \in \mathbb{Z}, \tag{7.16}$$

and suppose

$$f(0,0) = 0 \;\text{ and }\; D_x f(0,0) = -1.$$

This gives rise to a bifurcation which is not possible for one-dimensional flows, namely a branch of fixed points bifurcates into a periodic orbit. The names comes from the fact that if the map is the Poincaré map of a flow and the fixed point of the map corresponds to the periodic orbit of the flow, of period one, then the periodic orbit of the map corresponds to a periodic orbit of the flow with period two. Now the implicit function theorem implies that there is a branch of fixed points going through the origin. We analyze the bifurcation by considering the second iteration of the map

$$x_{m+1} = f^2(x_m, \mu)$$

and consider the flow

$$\dot{x} = g(x, \mu) = f^2(x, \mu) - x.$$

The derivatives at the origin are

$$D_x g = \left(D_x f\right)^2 (0,0) - 1 = 0$$

by chain rule,

$$D_\mu g = \left(D_x f D_\mu f(0,0)\right) = 0,$$

if $D_x f = -1$, and $D_\mu f = 0$.
In addition

$$D_x^2 g = D_x^2 f D_x f (D_x f + 1) = 0,$$

but

$$D_{\mu x}^2 g = 2 D_x f D_{x\mu} f(0,0) + D_x^2 f D_\mu f = -2 D_{x\mu} f(0,0) \neq 0,$$

and

$$\begin{aligned} D_x^3 g &= D_x f D_x^3 f \left[1 + (D_x f(0,0))^2\right] + 3 \left[D_x^2 f\right]^2 D_x f(0,0) \\ &= -\left\{2 D_x^3 f(0,0) + 3 \left[D_x^2 f(0,0)\right]^2\right\} \neq 0 \end{aligned}$$

in general. Thus by the analysis of the pitchfork bifurcation in the previous section,

$$x_{m+1} = f^2(x_m, \mu)$$

has a pitchfork bifurcation at the origin. This means that if we denote by x_+ the top and x_- the bottom pitchfork branch, then

$$x_+ = f(x_-, \mu)$$

and

$$x_- = f(x_+, \mu).$$

The reasoning is that the second iterate must be a stable fixed point of f^2, but there are only two such fixed points. Moreover,

$$x_- = f(x_-, \mu)$$

is impossible because then f would have another branch of fixed points going through the origin. The following theorem holds,

Theorem 7.1 *Suppose that* $f \in C^3$

$$D_{x\mu} f(0,0) \neq 0$$

and

$$2 D_x^3 f(0,0) + 3 \left[D_x^2 f(0,0)\right]^2 \neq 0,$$

then the map (7.16) has a period-doubling (also called a flip) bifurcation at the origin. There exists a stable branch of fixed points for $\mu < 0$ *that becomes unstable for* $\mu > 0$*, at the origin, and there exists a branch of stable periodic orbits for* $\mu > 0$.

7.4 The Hopf Bifurcation

The Hopf bifurcation is the generic codimension two bifurcation from a stationary solutions. The stationary solution becomes unstable and bifurcates to a periodic orbit, see Figures 7.4 and 7.4.

Theorem 7.2 *Suppose that the system*

$$\dot{z} = F(z,\mu),\ z \in \mathbb{R}^2 \tag{7.17}$$

has two complex (conjugate) eigenvalues $\lambda = \alpha \pm i\beta$ *crossing the pure imaginary axis at* $\mu = 0$*, with positive speed,*

$$Re\lambda(0) = 0,\ \frac{Re\lambda}{d\mu} > 0, \tag{7.18}$$

Then if the origin is a stable stationary solution, (this is the case if the coefficient a below is negative) $\mu = 0$ *is a bifurcation point and the bifurcation is supercritical,* $x = 0$ *is a stable stationary solution for* $\mu < 0$*, and* $x = 0$ *is an unstable stationary solution, encircled by a stable periodic orbit, for* $\mu > 0$*.*

Using the theory of Poincaré-Birkhoff normal forms, see for example Arrowsmith and Place [3], the equation (7.17) can be reduced to an equation in polar coordinates,

$$\begin{aligned} \dot{r} &= \mu r + ar^3 + O(r^5,\mu) \\ \dot{\theta} &= \omega + br^2 + O(r^4,\mu). \end{aligned} \tag{7.19}$$

The bifurcation is controlled by the r equation and it is the pitchfork equation that we analyzed above. The quantity a is computed from the vector field $F = (f,g)$,

$$\begin{aligned} a &= \frac{1}{16}\left(f_{xxx} + f_{xyy} + g_{xxy} + g_{yyy}\right) \\ &+ \frac{1}{16}\left(f_{xy}(f_{xx} + f_{yy}) - g_{xy}(g_{xx} + g_{yy}) - f_{xx}g_{xx} + f_{yy}g_{yy}\right), \end{aligned} \tag{7.20}$$

see for example Guckenheimer and Holmes [11]. If $a < 0$ then the bifurcation is supercritical and we get a branch of stable stationary solution for $\mu < 0$, that becomes unstable at the origin and throws off a stable periodic orbit. These orbits form a paraboloid whose center is the branch of unstable stationary solutions for $\mu > 0$, see Figure 7.4. For $\mu > 0$, the origin in x-space is encircled by a unique stable periodic orbit whose size and period changes continuously with μ, see [3].

If $a > 0$ the bifurcation is subcritical and the stability reverses, the unstable periodic orbit encircles the origin, in x-space, see Figure 7.4, for $\mu < 0$.

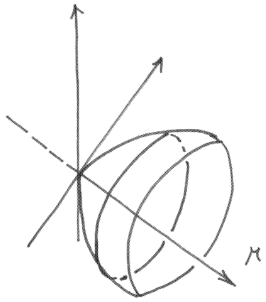

Figure 7.7: The Supercritical Hopf Bifurcation.

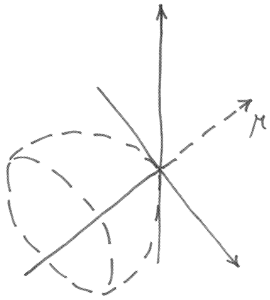

Figure 7.8: The Subcritical Hopf Bifurcation.

Chapter 8

The Period Doubling Cascade

8.1 The Quadradic Map

We consider the one-dimensional quadratic map

$$x_{m+1} = f(x_m, \mu), \quad x, \mu \in \mathbb{R},\ m \in \mathbb{Z},$$

where

$$f(x, \mu) = 1 - \mu x^2.$$

We will use this map to illustrate the phenomena that occur for a range of μ-values. These are in fact typical for a whole class of one-dimensional maps and this will be made precise below. The iterations are illustrated in Figure 8.1 . We consider the map in the interval $x \in [-1, 1]$ and f forms a hump in this interval. The fixed points $\bar{x}$ of f are the points where the line $y = x$ intersects the graph $y = f(x)$. These fixed points are stable if $|f'(\bar{x})| < 1$, unstable if $|f'(\bar{x})| > 1$, i.e. if the slope of f at the fixed point is less or greater than 45° respectively.

It turns out that there is a natural condition that the function f has a negative Schwartzian derivative which implies that if the map has a stable fixed point then it is unique. The Schwartzian derivative is

$$SD(f(x)) = \frac{f'''(s)}{f'(x)} - \left(\frac{3f''(s)}{2f'(x)}\right)^2$$

see [8], and the condition is that $SD(f(x)) < 0$. Moreover, then the set of points which is not attracted to the fixed point has Lebesgue measure zero. But we may ask if there are maps which have no stable fixed points, see Figure 8.1, and what happens then to the iterations of most points.

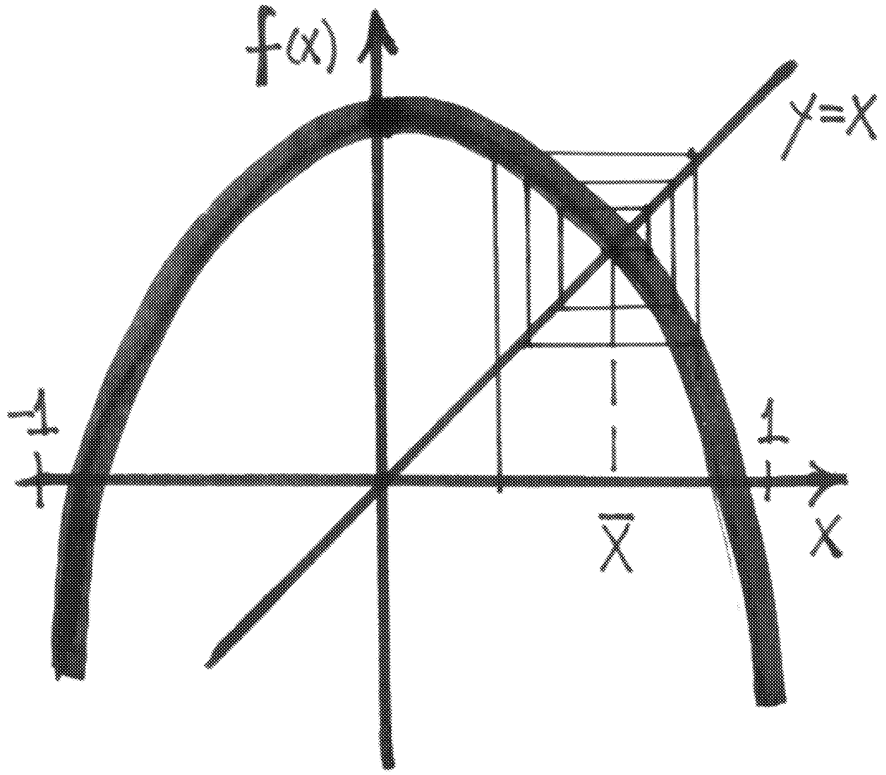

Figure 8.1: The Stable Quadradic Map.

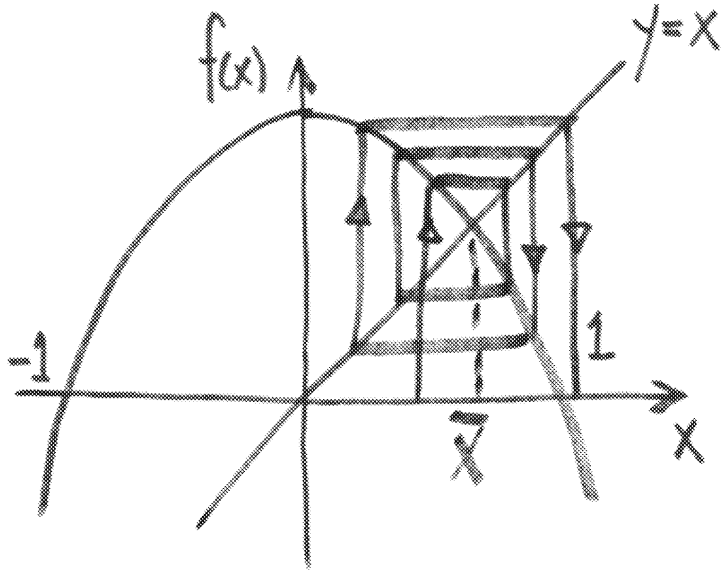

Figure 8.2: The Unstable Quadradic Map.

If we consider the bifurcation diagram of x, see Figure 8.1 as a function of μ then there is an initial interval where the attractor is a stable fixed point. Then a period doubling bifurcation occurs and we get an interval where the attractor is a stable periodic orbit of period one. Then another period doubling bifurcation takes place and we get a much shorter interval where the attractor is a stable periodic orbit of period two. This continues and we get a sequence of intervals where the attractors are stable periodic orbits of period 4, 8, 16 etc. These bifurcation points $\{\mu_n\}$ converge at μ_∞,

$$\lim_{n\to\infty} \mu_n = \mu_\infty,$$

see Figure 8.1, where the attractor becomes a *singularly supported strange attractor*, see Figure 8.1. Notice that in each interval the periodic orbit from the previous interval survives but becomes unstable. Thus each interval contains unstable periodic orbits of all the previous periods. Moreover, at the center of each interval lies a point where periodic orbit contains zero and the derivative $D_x f(0) = 0$. These orbits are called the *superstable* periodic orbits. What can we say about the region beyond μ_∞? It is known that the set of μ'_∞ for which there exists no stable periodic orbit has positive Lebesgue measure and the slightly smaller set for which there is sensitive dependance on initial conditions also has positive Lebesgue measure. It has been proven more recently that the still smaller set where there exists *absolutely continuous invariant measures*, see Figure 8.1, has positive Lebesgue measure. If a map has a density that is an absolutely continuous function ρ with respect to Lebesgue measure and the measure defined by this density

$$d\mu = \rho(x)dx$$

is invariant with respect to the map

$$d\mu(f^n(S)) = d\mu(S)$$

where $S \subset [-1,1]$ is any subset of the interval. Then we say that the map possesses an *absolutely continuous invariant measures*. We shall think about such maps as being *strongly chaotic* because they also possess positive Lyapunov exponents and the associated *sensitive dependance on initial conditions*.

Now we describe how to construct a map with sensitive dependance on initial conditions. The method is to let f fall on an unstable fixed point after a few iterations of the map. The reason is that $f'(0) = 0$ and this is the greatest stability one can achieve in any neighborhood. If that neighborhood falls on the neighborhood of an unstable fixed point after a few iterations, then the points in the

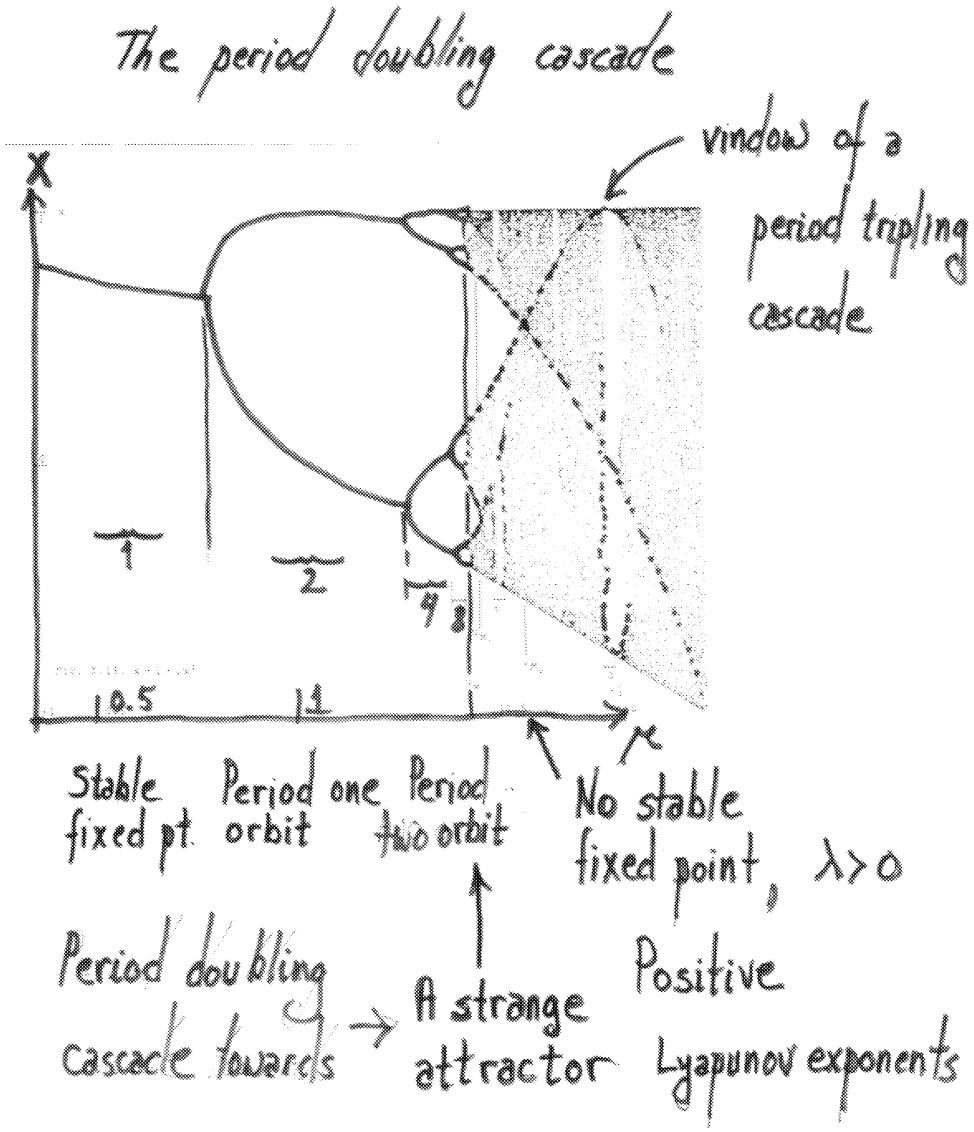

Figure 8.3: The Period Doubling Cascade.

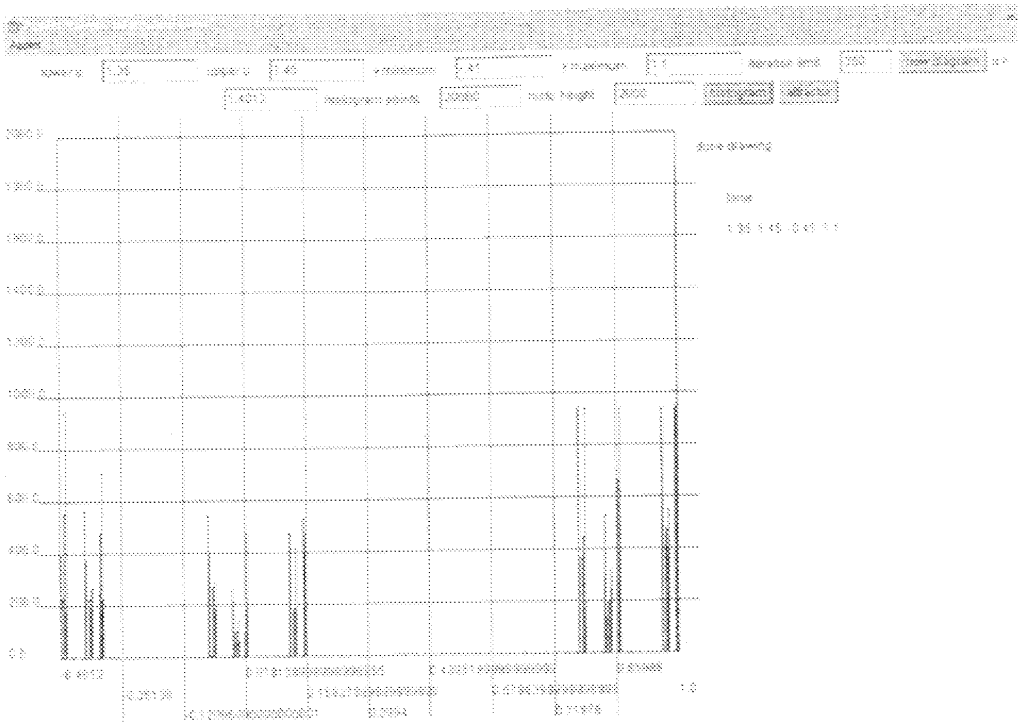

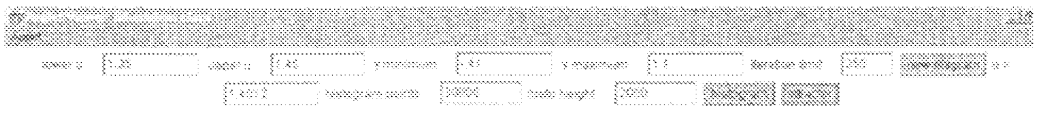

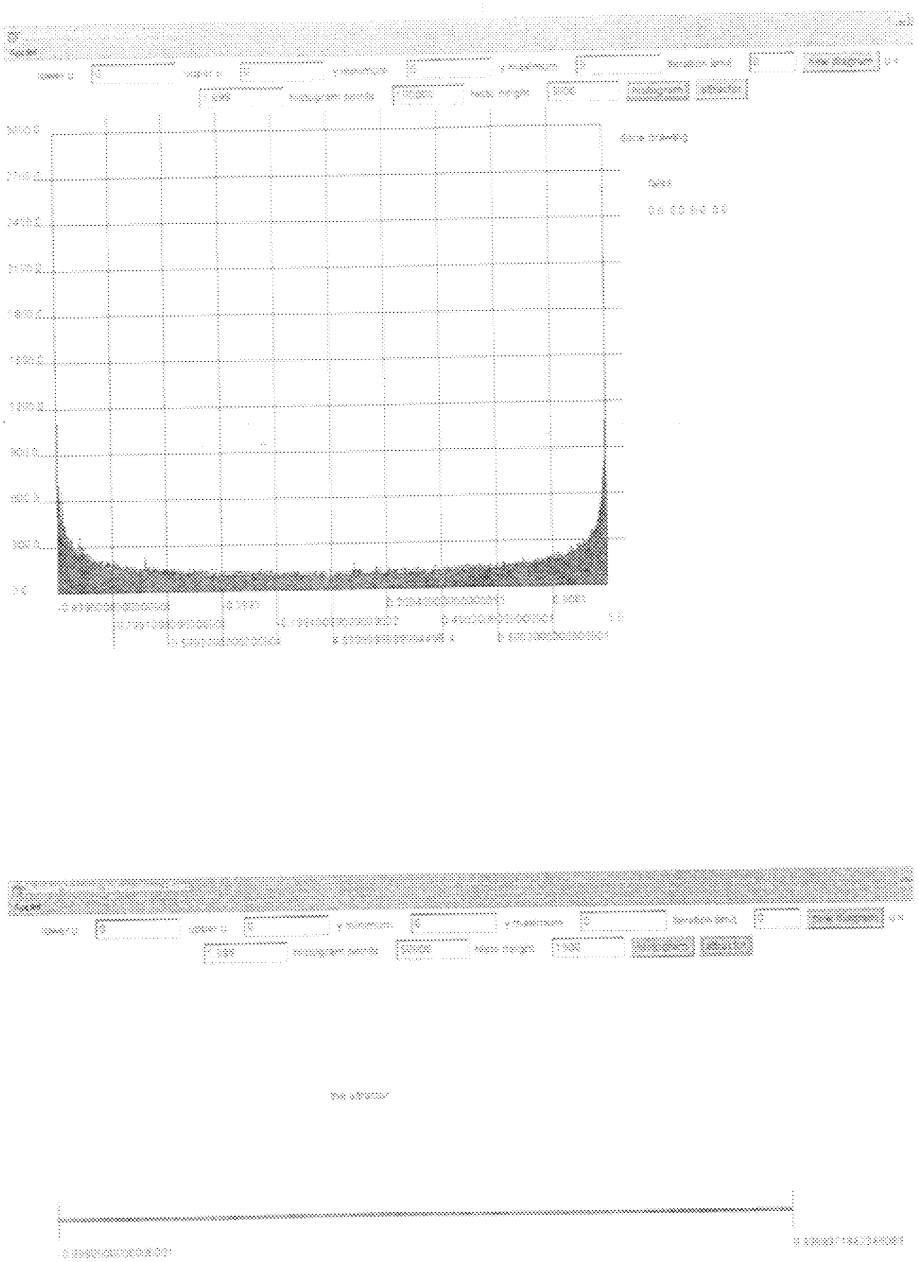

Figure 8.5: The histogram and support of the strange attractor with an absolutely continuous invariant measure at $\mu = 2$.

neighborhood must disperse. We illustrate this in Figure 8.1. where

$$f(x) = 1 - 1.544x^2.$$

The origin is mapped onto the unstable fixed point $\bar{x}$ in three iterations and nearby points must disperse. In Figure 8.1 we show the corresponding histogram and the support of the strange attractor.

8.2 Scaling Behaviour

We now consider a numerical observation made by Feigenbaum. Let 2^n denote the period and μ_n the μ-value where a bifurcation from the period 2^{n-1} to 2^n occurs. Then we list the μ_ns, the difference $\mu_n - \mu_{n-1}$ and the ratios $\frac{\mu_n - \mu_{n-1}}{\mu_{n+1} - \mu_n}$. The last column of the table shows a striking feature.

Table III.1

n	μ_n	$\mu_n - \mu_{n-1}$	$\frac{\mu_n - \mu_{n-1}}{\mu_{n+1} - \mu_n}$
0	.75	.5	
1	1.25	.1180989394	4.233738275
2	1.3680989394	.0259472172	4.551506949
3	1.3940461566	.0055850823	4.645807493
4	1.3996312389	.0011975035	4.663938185
5	1.4008287424	.0002565289	4.668103672
6	1.4010852713	.000054943399	4.668966942
7	1.401140214699	.000011767330	4.669147462
8	1.401151982029	.000002520208	4.669190003
9	1.401154502237	.000000539752	4.669196223
20	1.401155041989		

The first column shows that the μ_n values actually converge to a terminal point μ_∞. The second column shows that the windows of periodicity get smaller and smaller. The last column shows that the ratio converge to a constant

$$\delta = 4.66920\cdots.$$

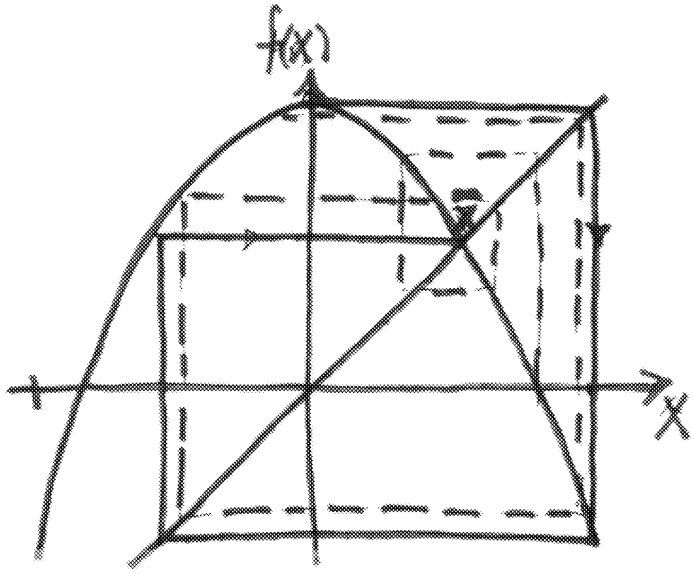

Figure 8.6: The Unstable Quadradic Map.

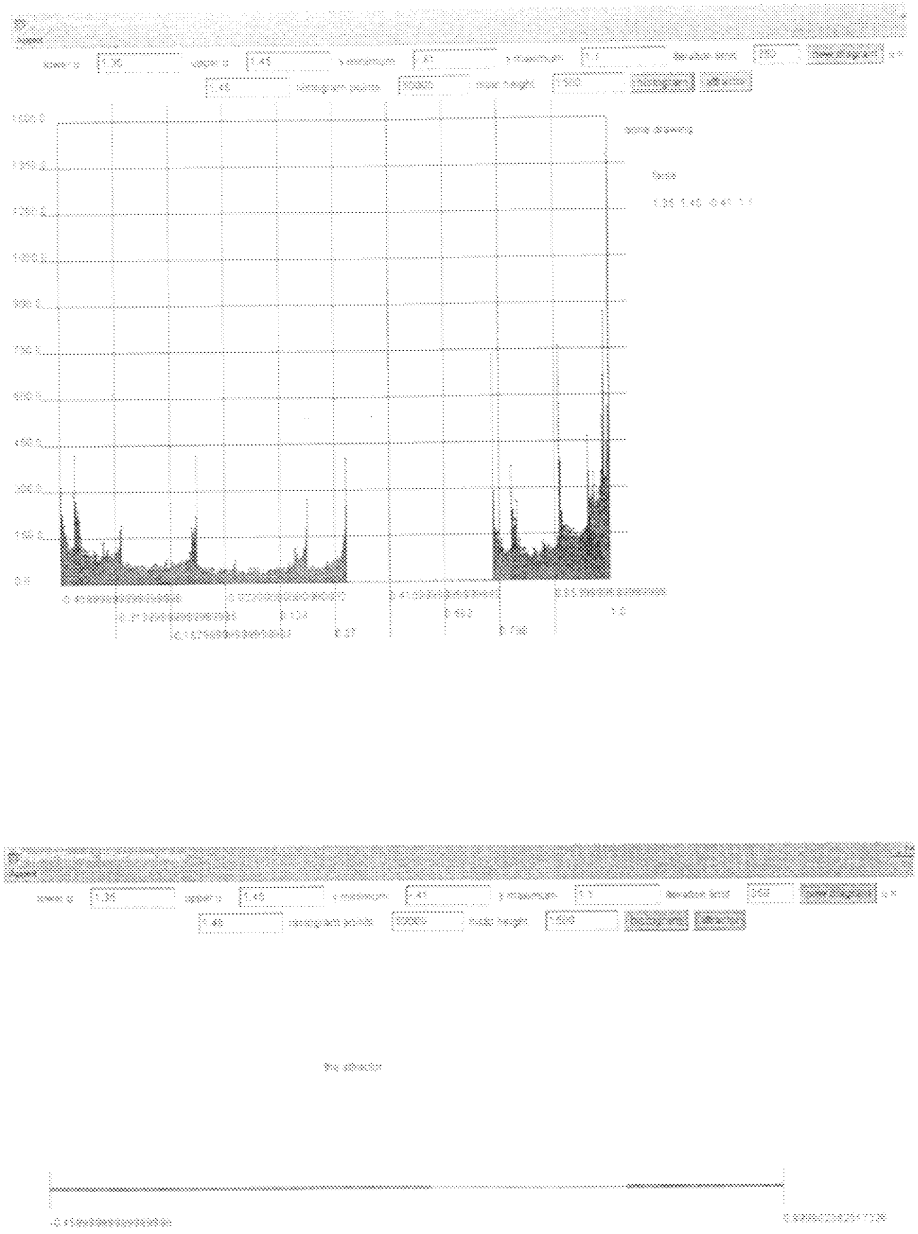

Figure 8.7: The histogram and support of the strange attractor with an absolutely continuous invariant measure, covering part of the interval, at $\mu = 1.544$.

The bifurcation points μ_n are given by the scaling formula

$$\mu_n = \frac{(\mu_0 - \mu_\infty)}{\delta^n} + \mu_\infty$$

The surprising fact that was discovered by Feigenbaum and proven by Collet-Eckmann-Lanford is that the constant δ does not depend on the particular map but is a universal constant for sufficiently smooth map of the interval to itself. In fact there are two universal constants associated to smooth maps from the interval to itself, the other being

$$\lambda = 0.3995\cdots$$

and some geometrical features of the bifurcation diagram in Figure 8.1 scale like λ^n.

Definition 8.1 *The periodic points μ'_n of period 2^n, whose periodic orbits contain zero, are called superstable.*

The name superstable comes from the fact that

$$D^{2^n} f(0) = 0,$$

which gives the strongest linear contraction possible for the period 2^n. The superstable points satisfy the scaling relationship

$$\mu'_n = \frac{(\mu'_0 - \mu_\infty)}{\delta^n} + \mu_\infty$$

We plot in Figure 8.2. the period doubling cascade with $-\log(\mu_\infty - \mu)$ on the vertical axis instead of μ. The result is periodic windows of period 2^n. An even more dramatic result is achieved if we scale the x-axis as well. Figure 8.2. shows the period doubling sequence with the vertical axis $x \cdot |\mu_\infty - \mu|^{-0.59367}$, where the exponent $\alpha = 0.59367$ is given by the relationship

$$\lambda = \delta^\alpha$$

between the two universal constants. This gives a periodic bifurcation diagram with a reflection (about the unstable pitchfork branch) symmetry.

Now we consider the other side of μ_∞. The point marked μ_{μ_0} is the point where $f^3(0)$ is an unstable fixed point and we get a sequence of values μ_{μ_n} such that at

$$\mu_{\mu_n} = \frac{(\mu_{\mu_0} - \mu_\infty)}{\delta^n} + \mu_\infty$$

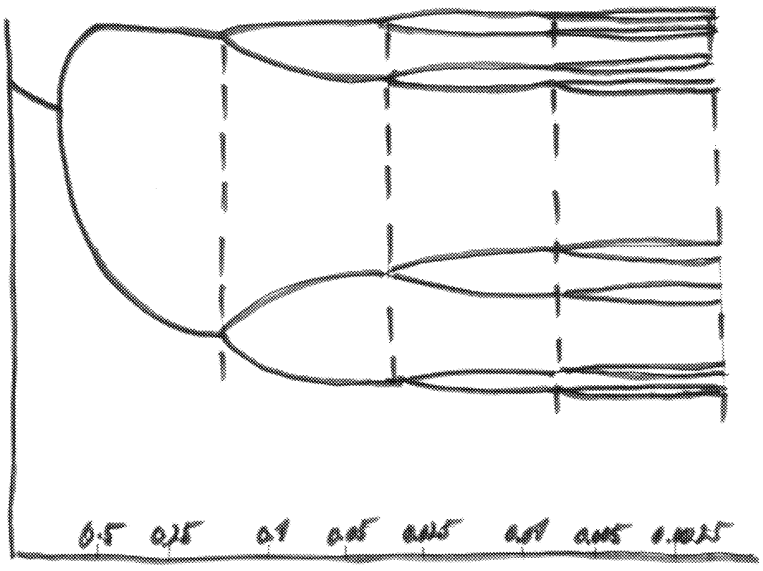

Figure 8.8: The rescaled Period Doubling Cascade.

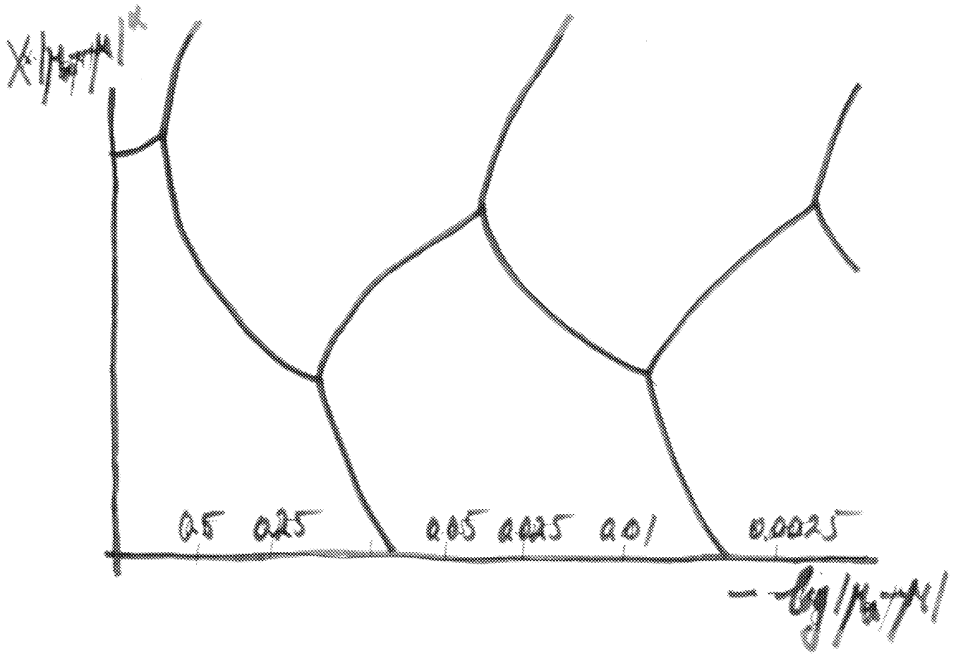

Figure 8.9: The rescaled Period Doubling Cascade.

$f^{3\cdot 2^n}(0)$ falls on an unstable periodic orbit of period 2^n. In the period 3 window f will have a periodic orbit of period $3\cdot 2^{n-1}$ at $\mu_n^{(3)}$, and

$$\mu_{3\cdot 2^n} = \frac{(\mu_3 - \mu'_\infty)}{\delta^n} + \mu'_\infty$$

for a new accumulation point μ'_∞. In other words, the scaling holds on both sides of μ_∞ and applies to period doubling of period two on one side and period three on the other side. Furthermore, the same analysis applies to period tripling, quadrapling etc. sequences, with new universal constants $\lambda(n)$ and $\delta(n), 3, 4, \cdots$.

Figure 8.2 illustrates the stable and unstable manifold of the renormalization map in the following theorem.

Theorem 8.1

$$\mathcal{F}g(x) = -\frac{1}{a}g\circ g(-ax),$$

where $g(0) = 1$ and a is a constant, denotes the period halving map acting on the space $G_\varepsilon = \{g(x) : [-1,1] \to \mathbb{R} \mid g(x) = f(|x|^{1+\varepsilon}),\ \varepsilon \le 1\}$, where f is a bounded analytic function on $[0,1]$ satisfying $f(0) = 1$, $\frac{df}{dy} < 0$ on $[0,1]$ and $f(1) > -1$; then for $\varepsilon \le 1$, $\mathcal{F}$ has a unique fixed point g_ε in G_ε, with a negative Schwartzian derivative. g_ε is hyperbolic and

$$dim W^u(g_\varepsilon) = 1 = codim W^s(g_\varepsilon),$$

where both W^u and W^s are smooth manifolds.

Corollary 8.1 *For each $a \in [-1,1]$ there exists a unique point $g_a \in W^u \subset G_\varepsilon$ such that $g_a(1) = -a$. W^u intersects the hypersurfaces*

$$\Sigma_1 = \{g \in G_\varepsilon \mid g(1) = 0\}$$

and

$$\widetilde{\Sigma}_1 = \{g \in G_\varepsilon \mid g^3(1) = -g(1)\}$$

transversely.

For a proof of the Theorem and the Corollary, see Collet and Eckmann [8].

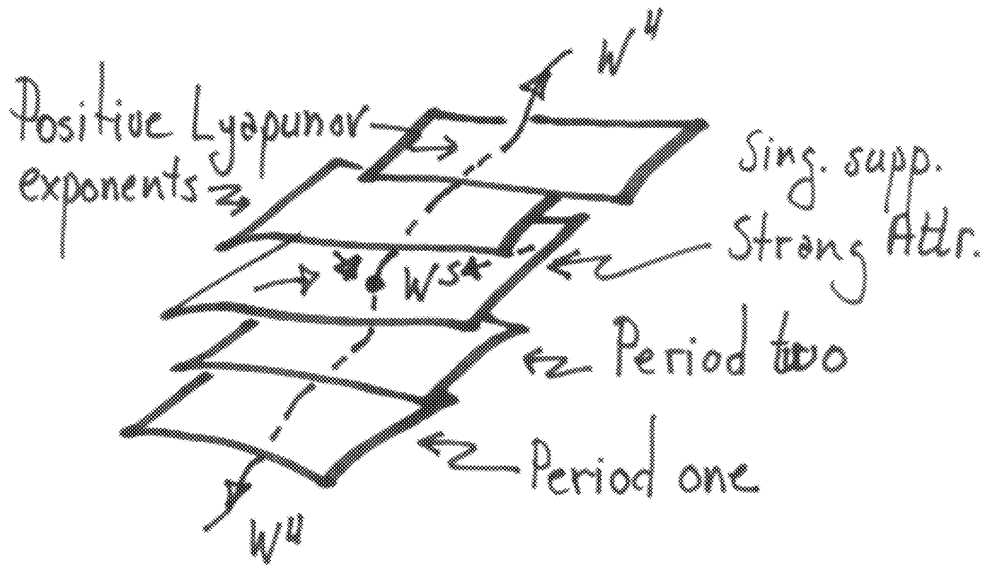

Figure 8.10: The stable and unstable manifolds of the period halving map.

Corollary 8.2 *Let $g_\mu \subset G_\varepsilon$ be a continously differentiable family parametrized by μ, and suppose that g_μ intersects W^s tranversally with non-zero velocity, at μ_∞. Then there exists sequence $\{\mu_j\}$ and $\{\widetilde{\mu}_j\}$ converging to μ_∞ from opposite sides of W^s such that the finite limits*

$$\lim_{j\to\infty} \delta^j(\mu_\infty - \mu_j) \quad \textit{and} \quad \lim_{j\to\infty} \delta^j(\mu_\infty - \widetilde{\mu}_j)$$

exists. The corresponding maps g_{μ_j} have a super-stable orbit of period 2^j, and $g_{\widetilde{\mu}_j}$ admits an absolutely continous invariant measure for j large enough.

Remark 8.1 *The ratio of the limits $\lim_{j\to\infty}\left(\frac{\mu_\infty-\mu_j}{\mu_\infty-\widetilde{\mu}_j}\right)$ is universal, i.e. does not depend on the particular family g_μ in question and we can for example choose the representative maps*

$$g_\mu(x) = 1 - \mu|x|^{1+\varepsilon}.$$

8.2.1 The Singularly Supported Strange Attractor

Theorem 8.1 and its Corollaries describe what happens on each side of the stable manifold $W^s \subset G_\varepsilon$, see Figure 8.2. Now we will describe what happens on the stable manifold W^s.

Definition 8.2 *Let $g \in G_\varepsilon$, then $J = \cap J_j$ is a* **g-invariant Cantor set** *if*

1. *The J_js form a nested sequence of closed subsets of $[-1,1]$*

   $$J_0 \supset J_1 \supset \cdots,$$

   $0 \in J_j$, for all j, and $g(J_j) \subset J_j$.

2. *J_{j+1} consists of 2^{j+1} closed intervals formed by deleting an open subinterval from all the closed intervals forming J_j.*

3. *g maps the subintervals of J_j onto one another, $J_j \subset g(J_j)$, such that the action of g on J_j is a cyclic permutation of order 2^j.*

4. *The map $g : J \to J$ is an isomorphism and every orbit of g in J is dense in J.*

We call J a **strange g-invariant Cantor set** *if in addition, g has a negative Schwartzian derivative and it satisfies two more conditions:*

5. *For each $j = 1,2,\cdots$, g has a unique repelling periodic orbit of period 2^j which does not belong to J_j.*

6. *Each orbit of g either,*

   (a) *lands after finitely many iterates on one of the periodic orbits in 5, (there are only countably many such orbits), or*

   (b) *converges to J, such that for each j it is eventually contained in J_j.*

Theorem 8.2 *Let $g \in W^u$, then g possesses a g-invariant Cantor set; if $g \in W^u$ has a negative Schwartzian derivative, then it possesses a strange g-invariant Cantor set. Moreover, if ν is a probability measure with support(ν)=J, such that each of the 2^j subintervals of J_j are assigned equal weight under ν, then ν is the only probability measure on J, invariant under g. The dynamical system (ν, g) is ergodic but not weakly mixing and consequently,*

$$\lim_{n\to\infty} \frac{1}{n} \sum_{j=0}^{n-1} \phi(g^n(x)) = \int_J \phi(x) d\nu,$$

where x is any point in $[-1,1]$ whose orbits converge to J and ϕ is any continuous function on $[-1,1]$.

For a proof of the Theorem see Collet and Eckmann [8].

We now define the tools we need for sensitive dependence on initial conditions.

Definition 8.3 *A Lyapunov exponent of a one-dimensional map $x_{m+1} = f(x_m, \mu)$, $m \in \mathbb{N}$, is the limit*

$$\lambda(x) = \lim_{n\to\infty} \frac{\log |D_x f(x)|}{n} \tag{8.1}$$

Notice that the Lyapunov exponent is defnined for any x in the phase space of the map not only for fixed points. At a fixed point the Lyapunov exponent equals the eigenvalue from Lemma 5.1.

A measure m is invariant under a map f if

$$m(I) = m(f^{-1}(I))$$

where I is a measurable set.

The following theorem was proven by Benedickts and Carleson [5].

Theorem 8.3 *Let $c < \log 2$ be given. Then there exists a set E of positive Lebesgue measure close to $\mu = 2$, for the map $f(x,\mu) = 1 - \mu x^2$, such that the Lyapunov exponent at $x = 1$ for $\mu \in E$ is greater than c.*

Corollary 8.3 *There exists a small positive number α such that*

$$|f^j(0)| \geq e^{-\alpha\sqrt{j}}, \text{ for all } j \geq 0 \tag{8.2}$$

The Corollary shows that the contraction rate of the map at the origin is bounded from below. This is exactly what one needs to prove Jacobson's Theorem [14]:

Theorem 8.4 *If $\mu \in E$ so that (8.2) holds, then the map $x \to f(x,\mu)$ has an invariant Borel probability measure that is absolutely continuous with respect to Lebesgue measure.*

The period doubling cascade has applications in all branches of science and engineering. For applications to superconductors see [4], to electrons in quantum wells driven by lasers see [10] and [1] and to earthquakes see [9].

Example 8.1 *The map $x \to 1 - 2x^2$ on $[-1,1]$ is mapped to the map $y \to 1 - 2|y|$ on $[-1,1]$ by the homeomorphism*

$$y = \frac{4}{\pi}\sin^{-1}(\sqrt{\frac{x+1}{2}}) - 1 \tag{8.3}$$

The Lyapunov exponent of the latter map is obviously $\lambda(y) = 2$ because $D_y f = \pm 2$ depending on whether y is positive or negative. The latter map has the invariant measure

$$dm = \frac{1}{\pi}\frac{1}{(1-y^2)^{1/2}}dy \tag{8.4}$$

This measure is obviously absolutely continuous with respect to Lebesgue measure, since

$$\frac{1}{\pi}\frac{1}{(1-y^2)^{1/2}} > 0$$

and m is a probability measure because

$$\frac{1}{\pi}\int_{-1}^{1}\frac{1}{(1-y^2)^{1/2}}dy = \frac{1}{\pi}\sin^{-1}(y)|_{-1}^{1} = 1$$

Exercise 8.1

1. Show that the map (8.3) maps $x \to 1 - \mu x^2$ to $y \to 1 - 2|y|$.
2. Show that the measure (8.4) is invariant under the map $y \to 1 - 2|y|$.

Appendix A

The Homoclinic Orbits of the Pendulum

We start with the energy of the pendulum

$$E = \frac{y^2}{2} + 1 - \cos(x)$$

where $y = \dot{x}$ and set it equal to the energy of the stationary solution $(x, y) = (\pi, 0)$,

$$\begin{aligned} E(\pi, 0) &= 1 - \cos(0) = 2, \\ \frac{y^2}{2} &+ 1 - \cos(x) = 2, \\ \frac{y^2}{2} &= 1 + \cos(x) = 2\cos^2\left(\frac{x}{2}\right), \end{aligned}$$

by the identity

$$\cos^2(z) = \frac{1}{2}(1 + \cos(2z))$$

from trigonometry. This gives the equation

$$\frac{\dot{x}^2}{2} = 2\cos^2\left(\frac{x}{2}\right)$$

or

$$\dot{x} = \pm 2\cos\left(\frac{x}{2}\right).$$

We let $z = \frac{\dot{x}}{2}$ to get

$$\dot{z} = \pm\cos(z).$$

This first order ODE is separable

$$\frac{dz}{\cos(z)} = dt$$

or

$$\int \sec(z)dz = \pm(t+t_0).$$

This integral is evaluated in calculus

$$\int \sec(z)dz = \ln|\sec(z)+\tan(z)|$$

or

$$\ln|\sec(z)+\tan(z)| = \pm(t+t_0)$$

so exponentiating both sides we get that

$$\sec(z)+\tan(z) = e^{\pm(t+t_0)}.$$

This is now an equation that we need to solve for z, to do that we use the trigonometry identity

$$1+\tan^2(z) = \sec^2(z)$$

or

$$\sec(z) = \sqrt{1+\tan^2 z}.$$

If we set $e^{\pm(t+t_0)} = q$ the equation becomes

$$\sqrt{1+\tan^2(z)}+\tan(z) = q.$$

We move $\tan(z)$ to the right hand side and square both sides

$$\sqrt{1+\tan^2(z)} = q-\tan(z)$$

so

$$1+\tan^2(z) = q^2-2q\tan(z)+\tan^2(z).$$

Thus

$$1 = q^2-2q\tan(z)$$

and solving for $\tan(z)$ gives

$$\tan(z) = \frac{1}{2}(q-q^{-1}).$$

However,

$$\frac{1}{2}(q-q^{-1}) = \frac{e^{\pm(t+t_0)} - e^{\mp(t+t_0)}}{2} = \pm\sinh(t+t_0).$$

Thus

$$\tan(z) = \pm\sinh(t+t_0)$$

and

$$x = 2z = \pm 2\tan^{-1}(\sinh(t+t_0))$$

since both sinh and tan are odd functions. Moreover,

$$\begin{aligned} \dot{x} &= \pm 2\frac{\cosh(t+t_0)}{1+\sinh^2(t+t_0)} \\ &= \pm 2\frac{1}{\cosh(t+t_0)} = \pm 2\ \mathrm{sech}(t+t_0) \end{aligned}$$

using the trigonometry identity

$$1+\sinh^2(t+t_0) = \cosh^2(t+t_0).$$

We have now shown that the homoclinic orbits are

$$(x,y) = \pm 2(\tan^{-1}(\sinh(t+t_0)),\ \mathrm{sech}(t+t_0)),$$

as $t \longrightarrow \pm\infty$, we get

$$(x,y) \longrightarrow (\pm\pi, 0).$$

Bibliography

[1] Batista A, B. Birnir, P. I. Tamborenea, and D. Citrin. Period-doubling and Hopf bifurcations in far-infrared driven quantum well intersubband transitions. *Phys. Rev. B.*, 68:035307, 2003.

[2] V. I. Arnold. *Ordinary Differential Equations*. MIT Press, Cambridge, MA, 1991. (Translated and Edited by R. A. Silverman).

[3] D.K. Arrowsmith and C. M. Place. *An Introduction to Dynamical Systems*. Cambridge University Press, Cambridge, UK, 1994.

[4] B.Birnir and R.Grauer. The global attractor of the damped and driven sine-Gordon equation. *Comm. Math. Phys.*, 162:539–590, 1994.

[5] M. Benedicks and L. Carleson. On iterations of $1-ax^2$ on $(-1,1)$. *Annals of Math.*, 122:1–25, 1985.

[6] J. Carr. *Applications of Centre Manifold Theory*. Springer, New York, 1981.

[7] S.-N. Chow and J. Hale. *Methods of Bifurcation Theory*. Springer, New York, 1982.

[8] P. Collet and J.-P. Eckmann. *Iterated Maps on the Interval as Dynamical Systems*. Birkhäuser, Boston, 1980. PPhI Progress in Physics.

[9] B. Erickson, B. Birnir, and I. Lavallée. A model for aperiodicity in earthquakes. *Nonlin. Processes Geophys*, 15:1–12, 2008. Available at http://repositories.cdlib.org/cnls/.

[10] B. Galdrikian and B.Birnir. Period doubling and strange attractors in quantum wells. *Phys. Rev. Lett.*., 76(18):3308–11, 1996.

[11] J. Guckenheimer and P. Holmes. *Nonlinear Oscillations, Dynamical Systems, and Bifurcations of Vector Fields*. Springer, 1983.

[12] P. Hartman. *Ordinary Differential Equations*. Wiley, New York, 1964.

[13] G. Iooss and D. D. Joseph. *Elementary Stability and Bifurcation Theory*. Springer, New York, 1980.

[14] M. Jakobson. Absolutely continuous invariant measures for a family of one-dimensional maps. *Comm. Math. Phys.*, 73:39–88, 1981.

[15] E. N. Lorenz. Deterministic non-periodic flow. *J. Atmos. Sci.*, 20:130–141, 1963.

[16] J. Moser. *Stable and Random Motions in Dynamical Systems*. Ann. Math. Studies 77. Princeton Univ. Press, Princeton NJ, 1973.

[17] L. Perko. *Differential Equations and Dynamical Systems*. Springer, New York, 1996.

About the author

Björn Birnir is a Professor of Mathematics at the University of California at Santa Barbara (UCSB). He obtained his PhD in Mathematics at the Courant Institute in 1981 and held positions at the University of Arizona Tucson, University of California Berkeley and University of Iceland before coming to UCSB. He served as the UCSB coordinator for nonlinear science from 1985-1990. He is currently the director of the Center for Complex and Nonlinear Science at UCSB. His current research interest are: Stochastic nonlinear partial differential equations and turbulence; dynamical systems theory of partial differential equations; mathematical seismology and geomorphology; nonlinear phenomena in quantum mechanical systems; complex and nonlinear models in biology and applications of the above. The papers from the Center for Complex and Nonlinear Science can be found at the website: http://repositories.cdlib.org/cnls/

Björn was the Chair of the UCSB Graduate Council 2004-2005 and he is currently (2008-2009) the Chair of the Council for Budget and Planning. He is an active member of AMS, SIAM and AAAS and chaired the AMS-IMS-SIAM Selection Committee for Summer Conference from 2004-2006. At UCSB he developed programs in Computational Science and in Applied Mathematics. Björn runs a very active research program at UCSB where he has advised 25 Ph.D. students and Postdoctoral Researchers and authored a large number of research papers and monographs.